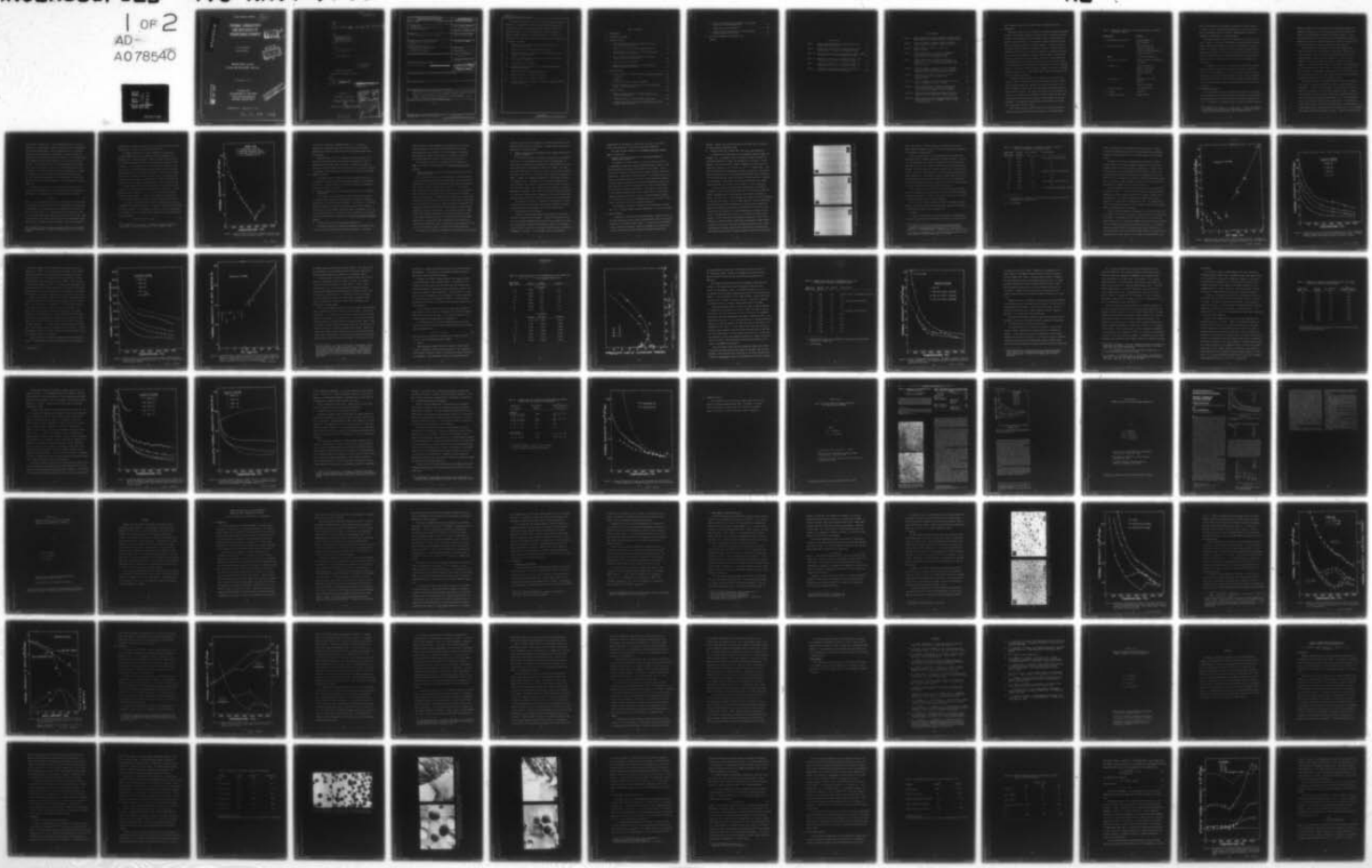
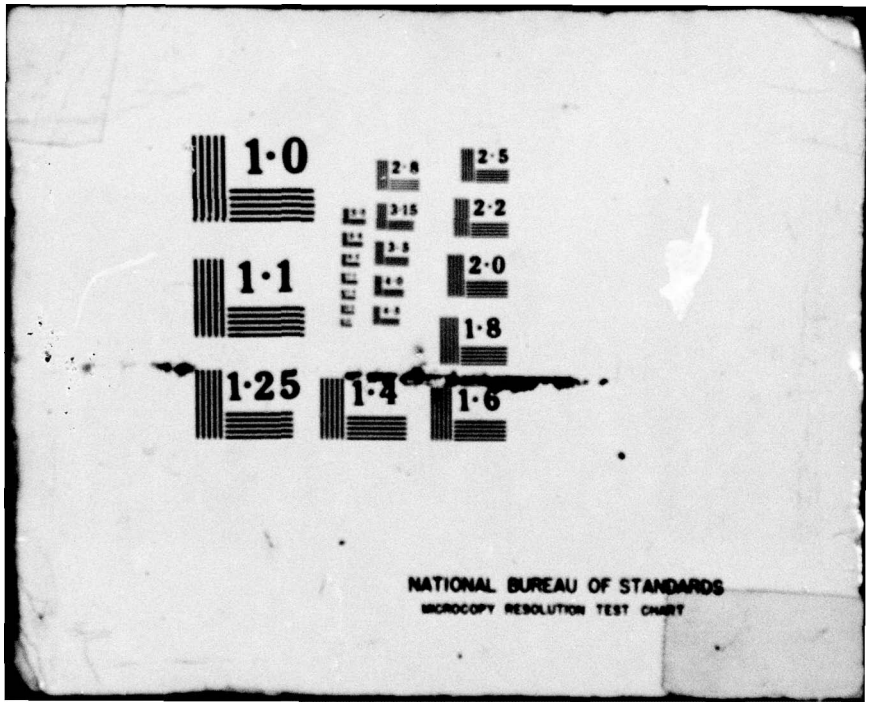
AD-A078 540 MONTANA ENERGY AND MHD RESEARCH AND DEVELOPMENT INST --ETC F/G 11/4
THERMAL CONDUCTIVITY AND DIFFUSIVITY OF ENGINEERING CERAMICS.(U)
NOV 79 G R YOUNGBLOOD , L D BENTSEN N00014-78-C-0726
UNCLASSIFIED 4TC-NAVY-F/79 NL

1 OF 2
AD-
A078540




1·0
1·1
1·25
1·4
1·6
1·8
2·0
2·2
2·5
NATIONAL BUREAU OF STANDARDS
MICROCOPY RESOLUTION TEST CHART

ADA078540

FINAL TECHNICAL REPORT

THERMAL CONDUCTIVITY AND DIFFUSIVITY OF ENGINEERING CERAMICS

LEVEL
A045527

G. E. YOUNGBLOOD

LARRY D. BENTSEN

DDC
DEC 14 1979
E

MONTANA ENERGY AND MHD
RESEARCH AND DEVELOPMENT INSTITUTE

NOVEMBER 15, 1979

DDC FILE COPY

This document has been approved for public release and sale; its distribution is unlimited.

Prepared for:
DEPARTMENT OF THE NAVY
Office of Naval Research
Arlington, Virginia 22217

AGREEMENT NO.: N00014-78-C-0726

79 11 26 154

(14) 4TC-NAVY-F/79

(9) FINAL TECHNICAL REPORT, 15 Sep 78 - 14 Sep 7[illegible]

(6) THERMAL CONDUCTIVITY AND DIFFUSIVITY OF ENGINEERING CERAMICS

(10) G. E. Youngblood

Larry D. Bentsen

@ 15 Nov 79

(12) 139

MONTANA ENERGY and MHD

RESEARCH AND DEVELOPMENT INSTITUTE

(11) 15 November 1979

DISTRIBUTION STATEMENT A
Approved for public release;
Distribution Unlimited

Prepared for:

DEPARTMENT OF THE NAVY

Office of Naval Research
Arlington, Virginia 22217

(15) Agreement No.: N00014-78-C-0726

Accession For
NTIS GRA&I
DDC TAB
Unannounced
Justification
Distribution/
Availability Codes
Dist | Avail and/or special
A

392916

SECURITY CLASSIFICATION OF THIS PAGE (When Data Entered)

REPORT DOCUMENTATION PAGE

READ INSTRUCTIONS BEFORE COMPLETING FORM

1. REPORT NUMBER

2. GOVT ACCESSION NO.

3. RECIPIENT'S CATALOG NUMBER

4. TITLE (and Subtitle)
THERMAL CONDUCTIVITY AND DIFFUSIVITY OF ENGINEERING CERAMICS

5. TYPE OF REPORT & PERIOD COVERED
Final Technical Report
Sept. 15, 1978-Sept. 14,1979

6. PERFORMING ORG. REPORT NUMBER

7. AUTHOR(s)
G. E. Youngblood and Larry D. Bentsen

8. CONTRACT OR GRANT NUMBER(s)
N00014-78-C-0726

9. PERFORMING ORGANIZATION NAME AND ADDRESS
Montana Energy and MHD R&D Inst.
Box 3809
Butte, Montana 59701

10. PROGRAM ELEMENT, PROJECT, TASK AREA & WORK UNIT NUMBERS

11. CONTROLLING OFFICE NAME AND ADDRESS
Department of the Navy
Office of Naval Research
Arlington, VA 22217

12. REPORT DATE
Nov. 15, 1979

13. NUMBER OF PAGES
130

14. MONITORING AGENCY NAME & ADDRESS(if different from Controlling Office)

15. SECURITY CLASS. (of this report)
Unclassified

15a. DECLASSIFICATION/DOWNGRADING SCHEDULE

16. DISTRIBUTION STATEMENT (of this Report)

See distribution list. [redacted]

DISTRIBUTION STATEMENT A
Approved for public release;
Distribution Unlimited

17. DISTRIBUTION STATEMENT (of the abstract entered in Block 20, if different from Report)

18. SUPPLEMENTARY NOTES

19. KEY WORDS (Continue on reverse side if necessary and identify by block number)
Thermal conductivity, thermal diffusivity, micro-cracking, alumina/zirconia composites, glass ceramics, thermal expansion mismatch, laser pulse calorimeter, glass-Ni composites, magnesia/magnesia-alumina spinel, Al_2O_3/SiC Composites, MgO/SiC Composites, Al_2O_3/TiC Composites, Yttrium chromites, electronic conducting ceramics.

20. ABSTRACT (Continue on reverse side if necessary and identify by block number)

-OVER-

DD FORM 1 JAN 73 1473 EDITION OF 1 NOV 65 IS OBSOLETE

Unclassified

SECURITY CLASSIFICATION OF THIS PAGE (When Data Entered)

This report summarizes the results of a one-year research program devoted to an investigation of the effect of compositional and microstructural variables on the thermal conductivity/diffusivity of engineering ceramics. Particular emphasis was placed on studies of thermal transport phenomena in composite materials. A total of six completed studies have resulted during this program, with another four in progress, as follows:

(1) Effect of Crystallization on the Thermal Diffusivity of a Cordierite Glass-Ceramic.

(2) Thermal Diffusivity of Ba-Mica/Alumina Composites.

(3) Thermal Diffusivity of Al_2O_3 with Dispersed Monoclinic and Tetragonal ZrO_2 particles.

(4) Effect of Thermal Expansion Mismatch on the Thermal Diffusivity of Glass-Ni Composites.

(5) Simple Laser Pulse Calorimeter.

(6) Thermal Diffusivity/Conductivity of Dense Magnesia/Magnesia-Alumina Spinel Ceramic.

(7) Thermal Diffusivity of Al_2O_3/SiC Composites.

(8) Thermal Diffusivity of MgO/SiC Composites.

(9) Thermal Diffusivity of Al_2O_3/TiC Composites.

(10) Thermal Diffusivity of a Partially Electronic Conducting Ceramic : Yttrium Chromites.

TABLE OF CONTENTS

I. INTRODUCTION 1

II. EXPERIMENTAL PROCEDURE 3

III. SUMMARY OF RESULTS 8

A. Effect of Crystallization on the Thermal Diffusivity of a Cordierite Glass-Ceramic. 8

B. Thermal Diffusivity of Ba-Mica/Alumina Composites. 8

C. Thermal Diffusivity of Al_2O_3 with Dispersed Monoclinic and Tetragonal ZrO_2 Particles. 9

D. Effect of Thermal Expansion Mismatch on the Thermal Diffusivity of Glass-Ni Composites 10

E. Simple Laser Pulse Calorimeter 10

F. Thermal Diffusivity/Conductivity of Dense Magnesia/ Magnesia-Alumina Spinel Ceramic. 11

IV. WORK IN PROGRESS 11

A. Thermal Diffusivity of MO/SiC (MO=BeO, Al_2O_3,MgO) Composites . 12

1. Al_2O_3/SiC 14

2. MgO/SiC 23

B. Thermal Diffusivity of Al_2O_3/TiC Composites. 29

C. Thermal Diffusivity of a Partially Electronic Conducting Ceramic: Yttrium Chromites. 36

V. TECHNICAL ARTICLES 40

A. "Effect of Crystallization on Thermal Diffusivity of a Cordierite Glass Ceramic". 41

B. "Thermal Diffusivity of Ba-Mica/Alumina Composites". 44

C. "Thermal Diffusivity of Al_2O_3 with Dispersed Monoclinic and Tetragonal ZrO_2 Particles" 47

D. "Effect of Thermal Expansion Mismatch on the Thermal Diffusivity of Glass-Ni Composites". 72

E. "Simple Laser Pulse Calorimeter". 98

F. "Thermal Diffusivity/Conductivity of Dense Magnesia/ Magnesia-Alumina Spinel Ceramic". 108

VI. BASIC AND SUPPLEMENTAL DISTRIBUTION LISTS 121

APPENDIX

LIST OF TABLES

Table I. Cooperating organizations and ceramic materials for thermal diffusivity studies 2

Table II. Compositions, densities, calculated porosities, and microstructural information for Al_2O_3/SiC system. 15

Table III. Coefficients A and B and rms deviations for least squares fit to α^{-1} or $\lambda^{-1} = A + BT$ for Al_2O_3/SiC system 24

Table IV. Compositions, densities, calculated porosities, and microstructural information for MgO/SiC system. 27

Table V. Compositions, densities, calculated porosities, and thermal diffusivity at RT for Al_2O_3/TiC system. 32

Table VI. Compositions, bulk densities, and RT thermal diffusivities for selected yttria-chromites. 38

LIST OF FIGURES

Figure 1. Measured thermal diffusivity of Armco iron by the laser flash diffusivity technique compared to reference values. . 7

Figure 2. Optical micrographs comparing composite structures of (A) Al_2O_3/SiC, (B) MgO/SiC, and (C) Al_2O_3/TiC. 13

Figure 3. Measured thermal diffusivity at 23°C for Al_2O_3/SiC system 17

Figure 4. Thermal diffusivity as a function of temperature for several hot-pressed Al_2O_3/SiC composites compared to that of hot-pressed α-Al_2O_3 18

Figure 5. Thermal conductivity calculated from measured thermal diffusivity and density and calculated heat capacity by $\lambda = \alpha\rho c$ for several compositions in the Al_2O_3/SiC system. 20

Figure 6. Calculated thermal conductivity at 23°C for several Al_2O_3/SiC composites compared to values predicted by Maxwell-Eucken Dispersed Phase Composite Theory. 21

Figure 7. Comparison of RT thermal diffusivity values for various compositions in the MgO/SiC and Al_2O_3/SiC systems 25

Figure 8. Effect of temperature cycling on thermal diffusivity values of MgO/30% SiC from RT to 1400°C 28

Figure 9. Temperature dependence of thermal diffusivity for 1, 30, and 40% TiC/Al_2O_3 composites compared to values for pure Al_2O_3 and TiC from RT to 1400°C 34

Figure 10. Calculated thermal conductivity values from RT to 1400°C for TiC, and 40 and 30% TiC/Al_2O_3 composites 35

Figure 11. Thermal diffusivity of $Y_{.95}Ca_{.05}CrO_3$ on heating and cooling from RT to 1400°C compared to similar values for $La_{.95}Mg_{.05}CrO_3$. 39

TITLE: Thermal Conductivity and Diffusivity of Engineering Ceramics

I. INTRODUCTION

The general objective of this program is to develop a quantitative understanding of the thermal conductivity and diffusivity of engineering ceramics in terms of phase composition, stoichiometry, purity, and microstructural features such as porosity, grain size, texture, phase distribution and geometry, and interphase bonding. Particular emphasis is placed on studies of thermal transport phenomena in composite materials. Depending upon the fabrication techniques utilized, physical properties of composite materials such as mechanical strength and elastic properties, thermal shock/fatigue resistance, erosion/corrosion resistance, resistance to creep deformation at high temperatures and electrical conductance as well as thermal conductivity/diffusivity may be adjusted over a wide range of values for optimized end uses. Correlation of these properties together with analysis of thermal transport properties aid in understanding some of the unique properties observed in composite materials.

To promote maximum productivity, the program is being carried out through a number of cooperative efforts with scientists at other organizations who supply appropriate specimens and other technical data. The effort at MERDI is concentrated on the measurement and interpretation of thermal diffusivity data. The program thus benefits from a combination of expertise. In addition, the cooperating scientists obtain data and characterization for their materials without a large investment in time and equipment. The cooperating organizations and the materials which they have supplied are listed in Table I.

The ceramic materials listed in Table I have current or future potential structural application at low, moderate, or high temperatures.

TABLE I.--Cooperating organizations and ceramic materials for thermal diffusivity studies.

Organizations	Materials
1. Naval Research Laboratory	Al_2O_3/BN composites B_4C/C composites
2. Max Planck Institute	Al_2O_3/ZrO_2 composites Si_3N_4/ZrO_2 composites Al_2O_3/ZrO_2 textured composites Al_2O_3/TiC composites
3. AMMRC	Al_2O_3/Ba-mica composites
4. University of California	Glass/Ni composites (bonded and non-bonded)
5. Ceradyne, Inc.	Al_2O_3/SiC composites Al_2O_3/TiC composites MgO/SiC composites BeO/SiC composites MgO
6. Trans-Tech, Inc.	$MgO/MgAl_2O_4$ composites $MgAl_2O_4$ $YCaCrO_3$ (with NBS)
7. Harwell (England)	Ni/Al_2O_3 composites
8. Fansteel	Al_2O_3/TiC
9. Corning Glass Works	Glass-ceramics

Many of the composites are intended for electronic or optical purposes in industrial and/or defense-related applications; some of the other materials included are used to investigate fundamental heat conduction phenomena in heterogeneous or textured systems.

This report presents the results of the past year's research activities. Section II reviews the experimental procedure employed including several modifications adopted to upgrade or expand analytic capability; Section III summarizes the results for the six studies completed during the past year; Section IV contains the preliminary results and analyses for four studies which are in progress; and Section V contains complete reprints or drafts of papers describing the six studies summarized in Section III.

For reference, a list of 17 technical articles which have resulted from this program during a previous three year contract (5/15/74 to 7/1/77) is given in Appendix A. Also listed are two articles for which the work was in progress during the previous contract and was completed during the current contract year (8/15/78 to 8/14/79) and four articles for which the experimental work has been completed and the articles are in review.

II. EXPERIMENTAL PROCEDURE

The laser-flash diffusivity technique[1] was selected as the primary method of determination of thermal transport properties. This method has been demonstrated to be rapid, convenient, and to give reproducible results. Furthermore, this technique uses a very small and simple specimen

[1] W. J. Parker, R. J. Jenkins, C. P. Butler and G. L. Abbot, "Flash Method of Determining Thermal Diffusivity, Heat Capacity, and Thermal Conductivity," Journal of Applied Physics, 32 (9), 1679-81 (1961).

geometry. Emphasis has been to obtain well-characterized samples from cooperating researchers so that the major effort could be devoted principally to the measurement and analysis of thermal properties. Since microstructure plays such an important role in determining the physical properties of ceramics, in-house facilities for optical and scanning electron microscopy analysis have been added during this past year.

The laser used for this program is of the glass-neodymium type (Korad #K-1) which fires a single pulse (pulse width of ≈800 nsec) of 1.06 μm radiation. The laser flash is directed at one face of a disc-shaped specimen, measuring 1/2 inch diameter by <0.1 inch thick and mounted in a suitable specimen holder within a cylindrical graphite chamber. In turn, the graphite chamber is contained in a high-temperature furnace (Astro Industries #1000) capable of attaining a temperature in excess of 2500°C. Specimens are coated with a thin layer of carbon in order to make them opaque to the laser radiation and to make the emittance/absorptance characteristics of all specimens the same.

During the past year the transient temperature detection system has been upgraded to extend the temperature range for thermal diffusivity measurements. An infrared (InSb) detector (Barnes Engineering #IT-7B) is capable of measurements in the 200-1200°C temperature range. A thermocouple detector to cover the RT-400°C range and a photodiode detector to cover the 1000-2000°C range were designed and built. For low temperature work the laser beam is deflected onto a sample held in a machined brass sample holder inside a split-tube wire-wound furnace. The thermocouple is a spring-loaded intrinsic type which has a fast response time. This arrangement facilitates rapid sample placement and removal. Thermal diffusivity values

can be quickly surveyed over a limited temperature range, at one temperature for a large number of samples in one day, or even simultaneously with another sample mounted in the high temperature rig. For measurements at very high temperatures (1000-2000°C), a silicon-diffused pin photodiode with associated electronics was mounted in a holder that swings into alignment using the same alignment pins as used for the infrared detector. In this manner thermal diffusivity measurements can be made over a 200°C overlap region to ensure all three detector systems are in coincidence. The transient signal from any of the detectors is recorded on a storage oscilloscope (Tektronix #511 with appropriate plug-ins). All high temperature measurements (T>200°C) were made in an inert atmosphere of dry nitrogen and measurements in the low temperature rig were made in air.

The thermal diffusivity (α) is calculated from the time ($t_{\frac{1}{2}}$) required for the temperature rise (ΔT) of the back-face of the specimen to reach half of its maximum value (also the steady-state value) from

$$\alpha = A\ell^2/t_{\frac{1}{2}} \qquad (1)$$

where ℓ is the specimen thickness and A is a dimensionless constant whose value depends on the rate of heat loss from the specimen during the time of measurement. Glass plates were used to attenuate the laser pulse so that ΔT was kept below $\sim$ 3°C. Assuming linear heat flow normal to the face of the heated disc and no heat losses, A has a value of 0.1388. Heat loss corrections, estimated to be less than 5% for all measurements below 1400°C, made in a manner described by Heckman.[2] The normal procedure for

[2] R. C. Heckman, "Finite Pulse-Time and Heat-Loss Effects in Pulse Thermal Diffusivity Measurements," Journal of Applied Physics, 44 (4), 1455-60 (1973).

determining $\alpha(T)$ consists of firing the laser at least three times at each temperature (T) in order to get an average value for α.

The thermal diffusivity of reference samples of a glass-ceramic (Corning #C9606), Armco iron, or high-purity MgO is periodically redetermined for calibration purposes. Values of thermal diffusivity from RT to 1000°C determined for Armco iron are compared to reference values[3] in Figure 1. It is noted that the Curie point at 769°C and the α-γ transition at 910°C are well-defined by the experimental data in both temperature and magnitude of the thermal diffusivity. As pointed out by Shanks, et al,[3] values of thermal diffusivity, specific heat, and thermal conductivity can vary by as much as ±10% above the α-γ transition depending on thermal history thus explaining the discrepancy in this temperature range.

At lower temperatures, where radiation effects can be neglected, the thermal diffusivity depends only on the elastic wave velocity [$v = (E/\rho)^{\frac{1}{2}}$] and phonon mean free path (L) by $\alpha = 1/3\ vL$ and is the more fundamental thermal transport property. Generally the temperature dependence of α can be explained in terms of various scattering mechanisms which affect L.

For purposes of engineering design requiring steady-state heat flow or temperature distribution calculations in components, the thermal conductivity (λ) must be obtained. For "homogeneous" materials λ can be calculated from α, the density (ρ), and the specific heat capacity at constant pressure (C_p) using the equation

$$\lambda(T) = \alpha(T) \cdot \rho(T) \cdot C_p(T) \qquad (2)$$

---

[3] H. R. Shanks, A. H. Klein, and G. C. Danielson, "Thermal Properties of Armco Iron," Journal of Applied Physics, 38 (7), 2885-92 (1967).

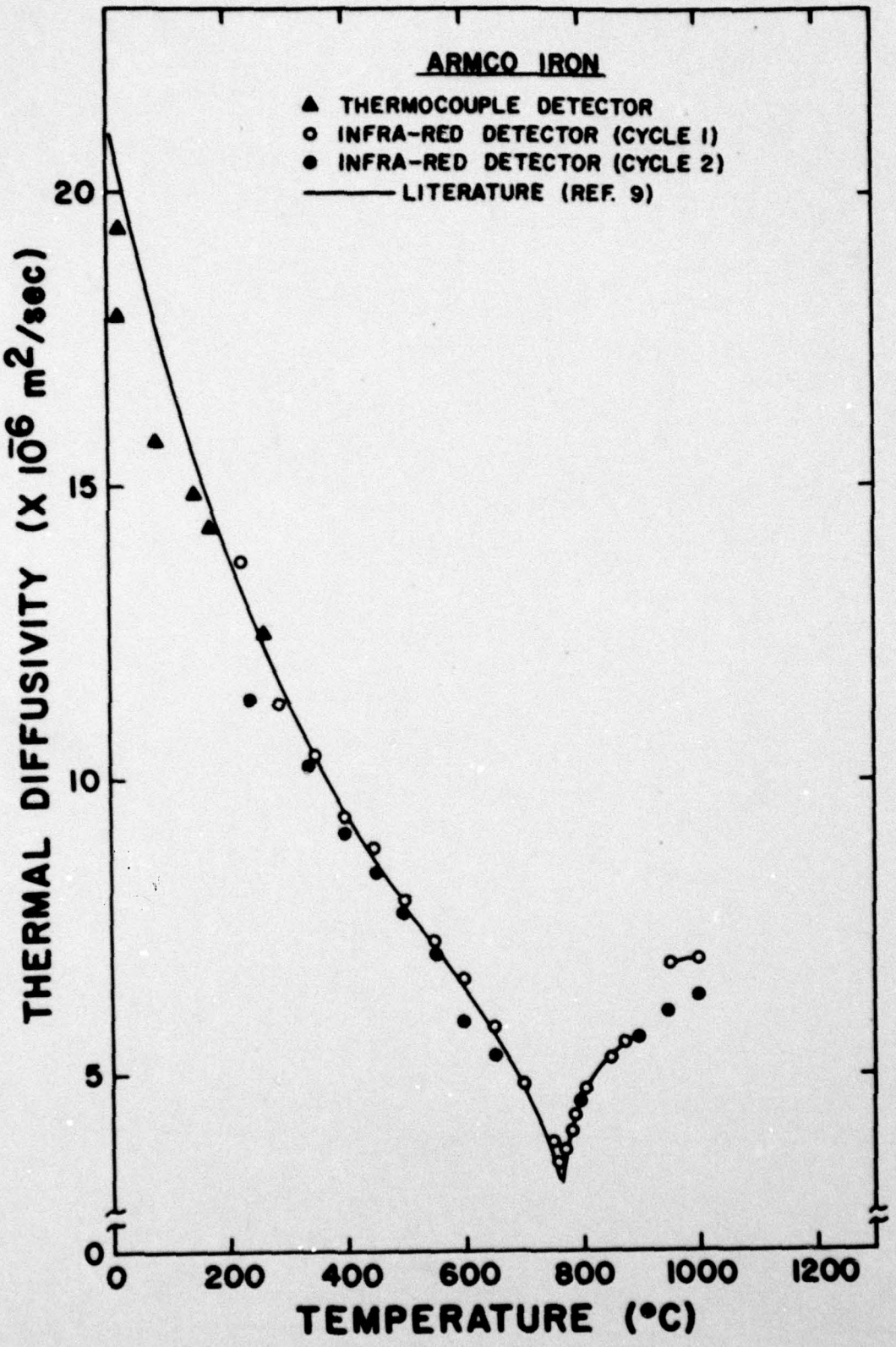


Figure 1.--Measured thermal diffusivity of Armco iron by the laser flash diffusivity technique compared to reference values.

In the case of composites, homogeneous means α, ρ, λ, and C_p are equivalent bulk properties that yield correct heat flux and boundary temperatures in materials when inserted into the standard thermal transport equations.

Calculated values of $\lambda(T)$ for composites then are analyzed by comparison to appropriate models and deviations are explained in terms of microstructural or compositional variables. Corroboration is generally obtained by analyzing other physical properties such as mechanical strength or toughness, thermal expansion, elastic moduli, and electrical conductance.

III. SUMMARY OF RESULTS

The following are brief summaries of the six technical articles resulting from this research; these articles are presented in their entirety in Section V. Complete reprints of the other 17 articles are appended in previous final reports for 1975-77.

A. "Effect of Crystallization on the Thermal Diffusivity of a Cordierite Glass-Ceramic."

This research relates the amount of thermal diffusivity increase to the relative amount and type of crystallization obtained in a commercial glass-ceramic after different heat treatments. The increases in the thermal diffusivity obtained for the cordierite glass-ceramic were far greater than for the mica glass-ceramic studied previously (see Appendix A, No. 15). This study was carried out in cooperation with researchers at Corning Glass Works; the technical article appeared in the Journal of the American Ceramic Society.

B. "Thermal Diffusivity of Ba-Mica/Alumina Composites."

The research analyzes the temperature dependence of the thermal diffusivity of several hot-pressed Ba-mica/alumina composites. The Ba-mica

phase consisted of flakes dispersed in an alumina matrix with preferential orientation of their basal planes perpendicular to the hot-pressing and heat flow directions. With this geometry, the Ba-mica flakes acted as effective thermal barriers; the thermal diffusivity was reduced dramatically parallel to the hot-pressing direction.

This study was carried out in cooperation with researchers at AMMRC; the technical article appeared in the American Ceramic Society Bulletin.

C. "Thermal Diffusivity of Al_2O_3 with Dispersed Monoclinic and Tetragonal ZrO_2 Particles."

In this study the variation in the magnitude of the thermal diffusivity values and hysteresis effects were related to the microcracking characteristics for two types of hot-pressed alumina/zirconia composites with a range of zirconia content from 0 to 24 vol. %. In one type many of the ZrO_2 particles exceed the critical size ($\simeq$ 3 μm) for tetragonal to monoclinic transformation and in the other most of the ZrO_2 particles are subcritical. A high density of microcracks, induced in the alumina matrix during fabrication only in the former type, is responsible for a large reduction in values of thermal diffusivity (conductivity) at temperatures below the zirconia phase transformation (in the 900-1000°C temperature range in these materials). For successive cycles to temperatures above the phase transformation, reproducible hysteresis occurs in the thermal diffusivity values. This indicates that the microcracks themselves close and partially heal on heating; on cooling below the transformation temperature (which is lower than on the heating part of the cycle), the microcracks reopen, restoring their original morphology.

This study was carried out in cooperation with researchers at Max Planck

Institute; the results were presented at the 80th annual meeting of the American Ceramic Society in Cincinnati. A technical paper has been prepared and is in the review stage.

D. "Effect of Thermal Expansion Mismatch on the Thermal Diffusivity of Glass-Ni Composites."

In this study the effect of interfacial de-cohesion on the thermal diffusivity of a hot-pressed glass matrix with a dispersed phase of nickel (due to thermal expansion mismatch) was investigated by the laser-flash technique over the temperature range of 25 to 600°C. The interfacial gap formed upon cooling acts as a barrier to heat flow and lowers the thermal diffusivity to values below those predicted from composite theory. However, the temperature dependence of the thermal diffusivity is strongly positive. Preoxidation of the Ni spheres promotes interfacial bonding to yield values of thermal diffusivity higher than those for non-oxidized spheres, and a thermal diffusivity which is relatively temperature independent. The concept of an effective thermal diffusivity for composites is demonstrated at temperatures near the fabrication temperature, where effects due to thermal expansion mismatch are negligible.

This study was carried out in cooperation with researchers at the University of California (Berkeley) and Virginia Polytechnic Institute. A technical paper has been prepared and is in the review stage.

E. "Simple Laser Pulse Calorimeter."

A technical paper has been prepared which describes a simple and sensitive relative energy calorimeter. The design incorporates the use of a silicon diode thermometer on the back face of a graphite disc infrared absorber which increases the calorimeter's sensitivity from about 100 μV/J, which is typical for a standard calorimeter based on thermopile thermometry, to 10 mV/J. This instrument allows the simultaneous

determination of the energy of a short laser pulse and, in this application, the operation of a laser-flash diffusivity experiment.

This paper has been submitted to the Review of Scientific Instruments for publication.

F. "Thermal Diffusivity/Conductivity of Dense Magnesia/Magnesia-Alumina Spinel Ceramics."

The thermal diffusivity values for a series of dense, polcrystalline $MgO/MgAl_2O_4$ compositions ranging in MgO concentration from 0 to 100% were determined during heating and cooling from RT to 1400°C. Binary mixtures were expected to microcrack due to thermal expansion mismatch between phases. No hysteresis effects (evidence of microcracking) were observed in the thermal diffusivity for any of these compositions; however, calculated thermal conductivity values for the intermediate compositions were lower than could be explained by thermal transport models based on rule of mixtures, especially below 600°C. These results indicate that 1) microcracks are present which do not thermally heal or extend during subsequent heating-cooling cycles, thus not causing hysteresis effects, or 2) solid-solution alloying of the $MgAl_2O_4$ phase is responsible for the overall lowering of the effective thermal conductivity.

This study was carried out in cooperation with researchers at Trans-Tech, Inc. A technical paper has been prepared and is in the review stage.

IV. WORK IN PROGRESS

In addition to the previously described research, thermal diffusivity data were obtained for other systems including MO/SiC composites, Al_2O_3/TiC composites, and yttrium chromite ceramics. At the end of the contractural period, further microstructural analysis was needed in most cases before a final interpretation could be reported and technical publications

prepared. However, some conclusions based on available date are reported for these partially completed studies.

A. "Thermal Diffusivity of MO/SiC (MO - BEO, Al_2O_3, MgO) Composites."

In cooperation with researchers at Naval Research Laboratory (NRL) and Ceradyne, Inc., a systematic study of the thermal transport properties of hot-pressed composites of Al_2O_3, BeO and MgO/SiC was initiated. The components in this series exhibit a range of mismatch of the coefficients of thermal expansion (8.0, 9.0, 13.6 and 4.5×10^{-6} $°C^{-1}$, respectively). Upon cooling from fabrication temperatures, residual stresses due to the thermal expansion mismatch may cause microcracking between phase (grain) boundaries or in the phase with the larger coefficient of thermal expansion. Reportedly microcracking in these materials also may be responsible for enhanced fracture toughness (or fracture surface energy) of various compositions.

In Figure 2 typical microstructures are depicted for (A) Al_2O_3/SiC, (B) MgO/SiC, and (C) Al_2O_3/TiC (See Subsection IV-B) where the carbide component, represented by the lighter phase in each optical micrograph, is 30 wgt. % for each case. The carbide phase was observed to be well-dispersed in the metal oxide matrix for all of these composites. When the composites are cooled from fabrication temperature (or from the minimum temperature where stress-relaxation can occur), the carbide particles will be in compression and the oxide matrix in tension immediately surrounding the particles. The magnitude of the stress at any location will depend on the degree of cooling below the stress-relaxation temperature as well as the difference in thermal expansion coefficients and respective Young's moduli. According to theory the stress does not depend upon particle size. Microcracking occurs, however, when the strain energy density integrated over the strained volume exceeds the energy required to create new crack surface

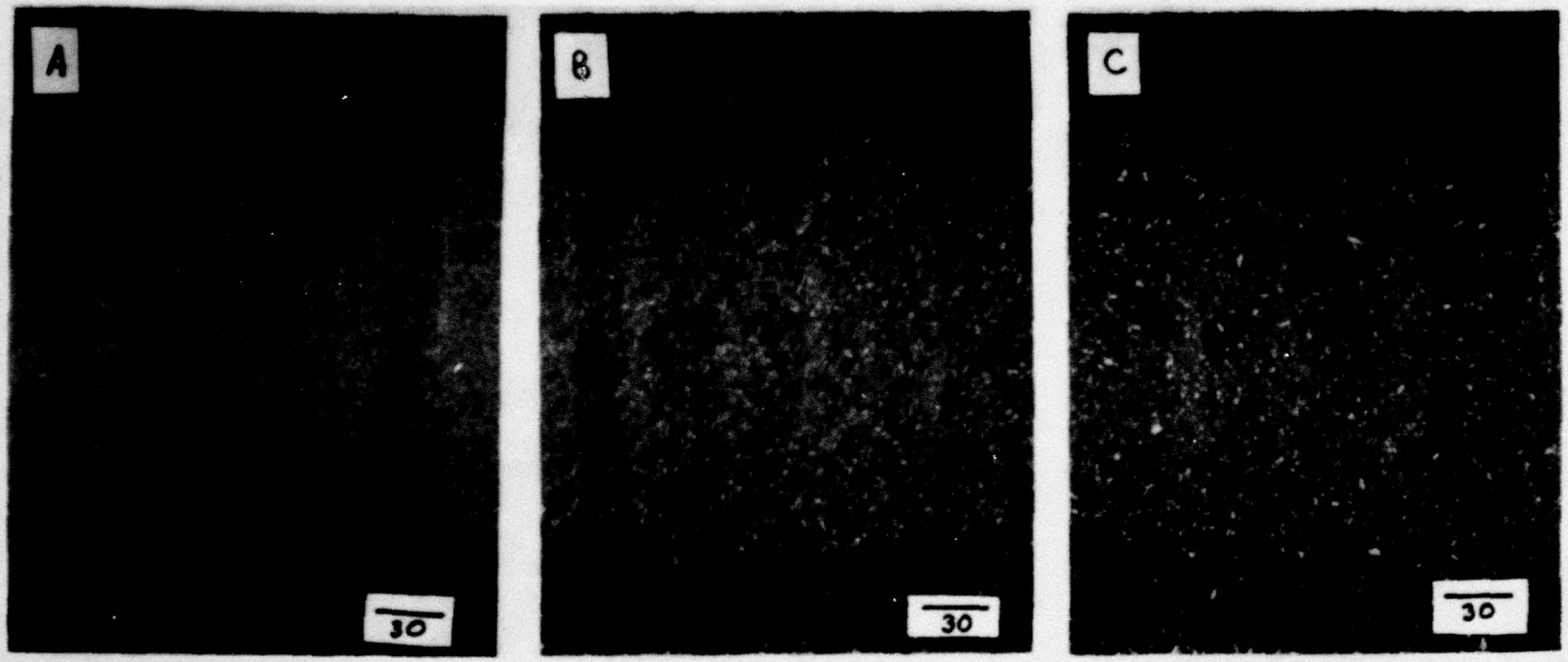


Figure 2.--Optical micrographs comparing composite structures of (A) Al_2O_3/SiC, (b) MgO/SiC, and (C) Al_2O_3/TiC. The carbide phase (light colored) is 30 wgt. % for each case. The bar = 30 μm.

area. Thus there is a critical particle size (modified by stress intensity factors dependent on particle shape) and concentration dependence for the onset of microcracking.[4,5]

It also is noted that SiC is a semi-conductor with a significant electronic as well as phonon contribution to thermal transport. In fact, it is the moderately high electrical conductance of the SiC composites that leads to one of their commercial applications as microwave absorbing ceramics. Similarly, the overall thermal conductivity of composites with SiC will reflect the high conductivity of the SiC component, especially at higher temperatures. Unfortunately, enhanced thermal conductivity due to SiC addition may be offset by microcracking in some of the compositions. The trade-off between the degree of these effects will have important bearing on the thermal shock resistance of MO/SiC composites.

This study examines the microstructure and compositional variables affecting the degree of microcracking and the resulting effect on thermal diffusivity/conductivity. Special attention will be given in this study to effects of temperature cycling and atmosphere.

At this time no results have been obtained for the BeO/SiC system. However, some thermal diffusivity data have been analyzed for the Al_2O_3/SiC and MgO/SiC systems and are presented below.

1. Al_2O_3/SiC

In Table II the compositions, measured densities, calculated porosities, and some pertinent microstructural information are given for this

---

[4] F. F. Lange, "Criteria for Crack Extension and Arrest in Residual Localized Stress Fields Associated with Second Phase Particles," pp 599-609 in Fracture Mechanics of Ceramics, Vol. 2 edited by R. C. Bradt, D. P. H. Hasselman, and F. F. Lange, Plenum Press, New York (1973).

[5] A. G. Evans, "Microfracture from Thermal Expansion Anisotropy-I, Single Phase Systems," Acta Metallurgica, 26, 1545-53 (1978).

TABLE II.---Compositions, densities, calculated porosities, and microstructural information for Al_2O_3/SiC system.

Composition (Wgt % SiC)	Density (gm/cm^3)	Calc. Porosity* %	Microstructure
0.0	3.981	< 0.5	2.5 μm grains, mixed fracture
0.5	3.977	< 0.5	n.c.
1.0	3.914	1.4	n.c.
1.5	3.952	0.5	n.c.
2.0	3.897	1.4	textured, transgranular fracture
3.0	3.899	1.4	n.c.
5.0	3.953	-	n.c.
30	3.636	2.9	5-10 μm grains, mixed fracture
40	3.41	7.1	n.c.
60	3.380	4.0	2-5 μm grains, intergranular fracture

* Calculated using 3.986 and 3.210 gm/cm^3 for the zero porosity densities of Al_2O_3 and SiC, respectively.

n.c. not completed

system. The densities were determined by liquid immersion. Assuming no interaction between Al_2O_3 and SiC, the calculated porosity represents the density deviation from the rule of mixtures density for each composition.

Preliminary microstructural examination was carried out by SEM on fracture surfaces for a few representative compositions. The porosity exceeded 5% only for the 40% SiC samples, therefore, no porosity corrections were made in any of the measured thermal diffusivity values. The porosity and phase distributions appeared very homogeneous with the exception of the 2% SiC sample which retained a definite texture not noticed in any of the other samples examined; this may in part be responsible for the difference in appearance of the fracture surface.

The room temperature thermal diffusivity values for each composition are shown in Figure 3. The data points represent the average and the bar represents the range of values measured for the number of samples (shown in parenthesis). No significant dependence of thermal diffusivity on composition is observed for SiC compositions of $\leq$3%. For compositions of $\geq$30% SiC, the thermal diffusivity (at RT) rapidly increases with an approximate linear dependence on SiC addition.

Figure 4 shows the temperature dependence of the thermal diffusivity for the 30%, 40%, and 60% SiC composites compared to that of pure Al_2O_3 from RT to 1400°C. The thermal diffusivity values of the 1%, 2%, and 3% SiC compositions were only a few percent higher than the values for pure alumina over this temperature range, and are omitted for clarity. In the higher temperature range (T>400°C) the extremely high thermal conductivity of SiC is responsible for the high overall thermal diffusivity values for the composites with at least 30% SiC. For instance, the thermal diffusivity

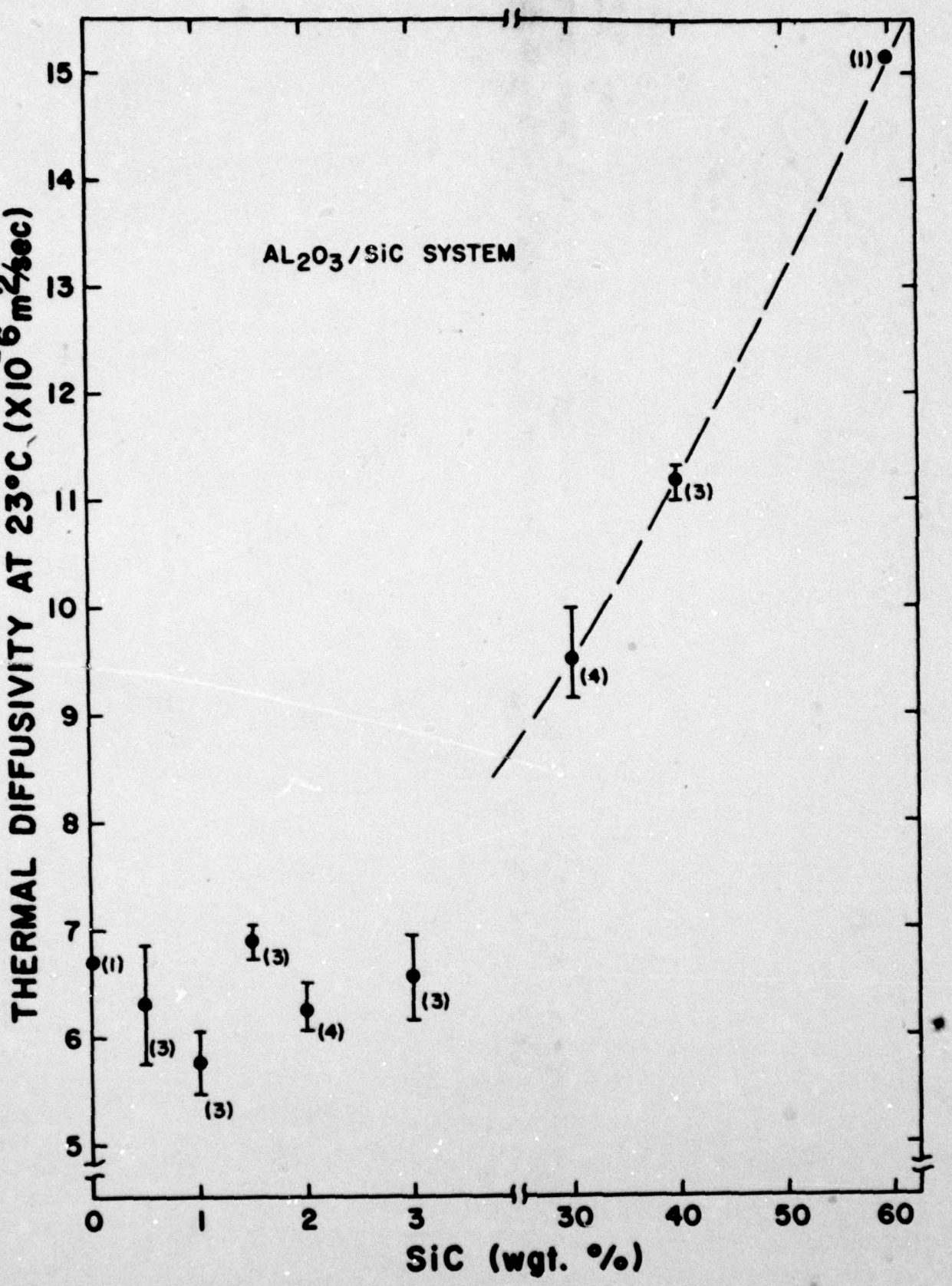


Figure 3.--Measured thermal diffusivity at 23°C for Al_2O_3/SiC system. The number of diffusivity samples tested is indicated in parenthesis for each composition.

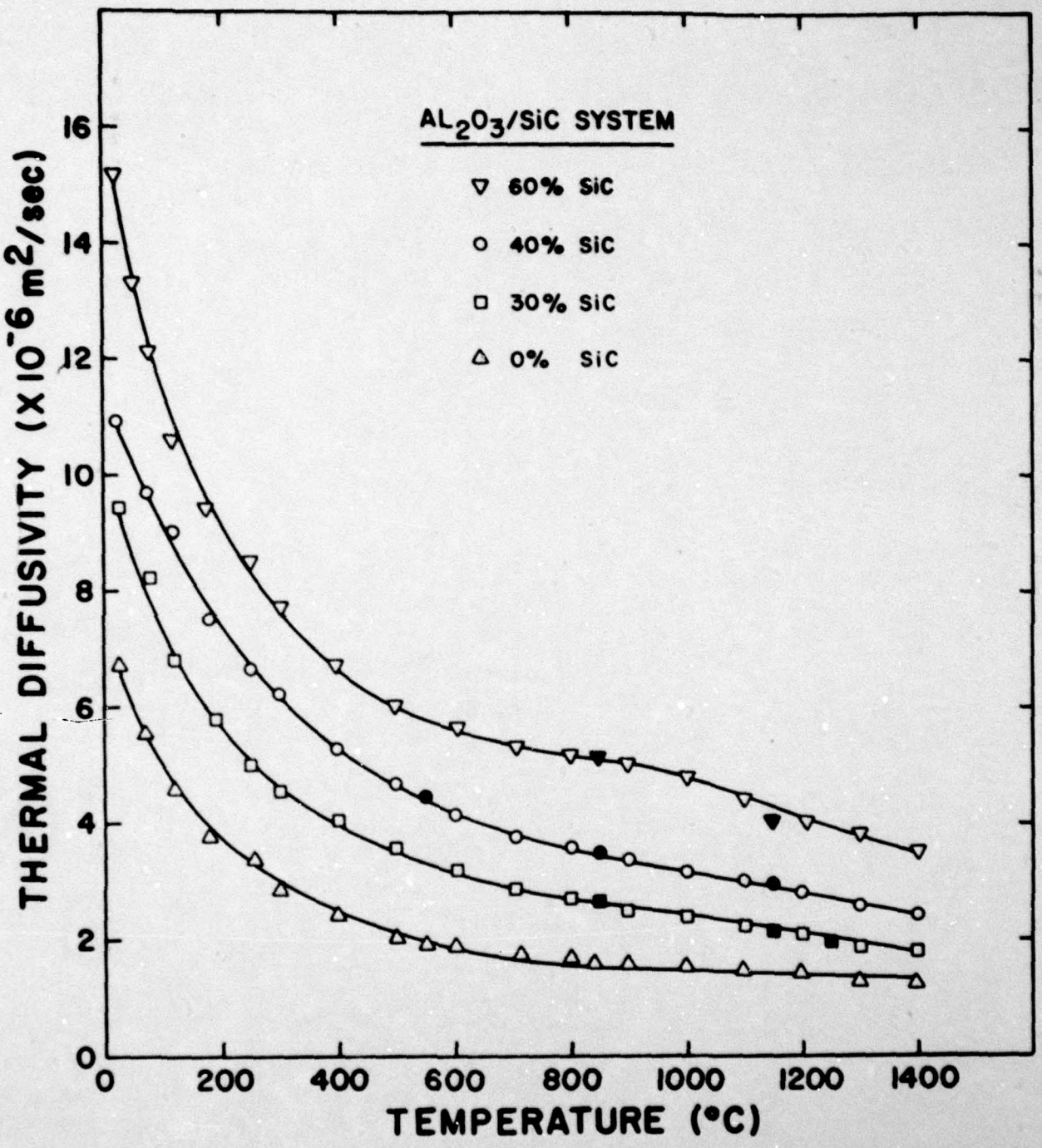


Figure 4.--Thermal diffusivity as a function of temperature for several hot-pressed Al_2O_3/SiC composites compared to that of hot-pressed α-Al_2O_3. The open (closed) symbols indicate data taken during heating (cooling).

of the 60% SiC sample at RT is slightly more than twice that of pure alumina; at T = 1000°C it is more than three times that of pure alumina. The thermal diffusivity values, measured during heating and cooling, were reproducible; i.e., no hysteresis effects were observed. Unfortunately data were taken only during cooling to ~500°C. Since the degree of microcracking depends on $(\Delta T)^2$*, it is possible that measurements were discontinued before a low enough temperature for the onset of microcracking was reached. The fact that hysteresis in the thermal diffusivity was not observed in the Al_2O_3/SiC composites must be qualified at this time.

Figure 5 shows thermal conductivity calculated from measured thermal diffusivity and density, and calculated heat capacity using Eq. (2) for the 0%, 30%, 40%, and 60% SiC compositions. These values are compared to the thermal conductivity of Norton Crystar SiC (81% dense). It is obvious that the magnitude and temperature dependence of the thermal conductivity of the composites are strongly influenced by the SiC phase. The high values of thermal diffusivity/conductivity, especially at high temperatures, should significantly enhance the thermal shock resistance for these composites. It is noted that the thermal conductivity of high-purity iron decreases from 80 to 30 watts/mK from RT to 1400°C. Over this same temperature range, the thermal conductivity of the Al_2O_3/60% SiC composite ranges from 40 to 16 watts/mK.

Figure 6 shows the calculated room temperature thermal conductivity values for several Al_2O_3/SiC composites compared to values predicted by

---

* See reference 4.

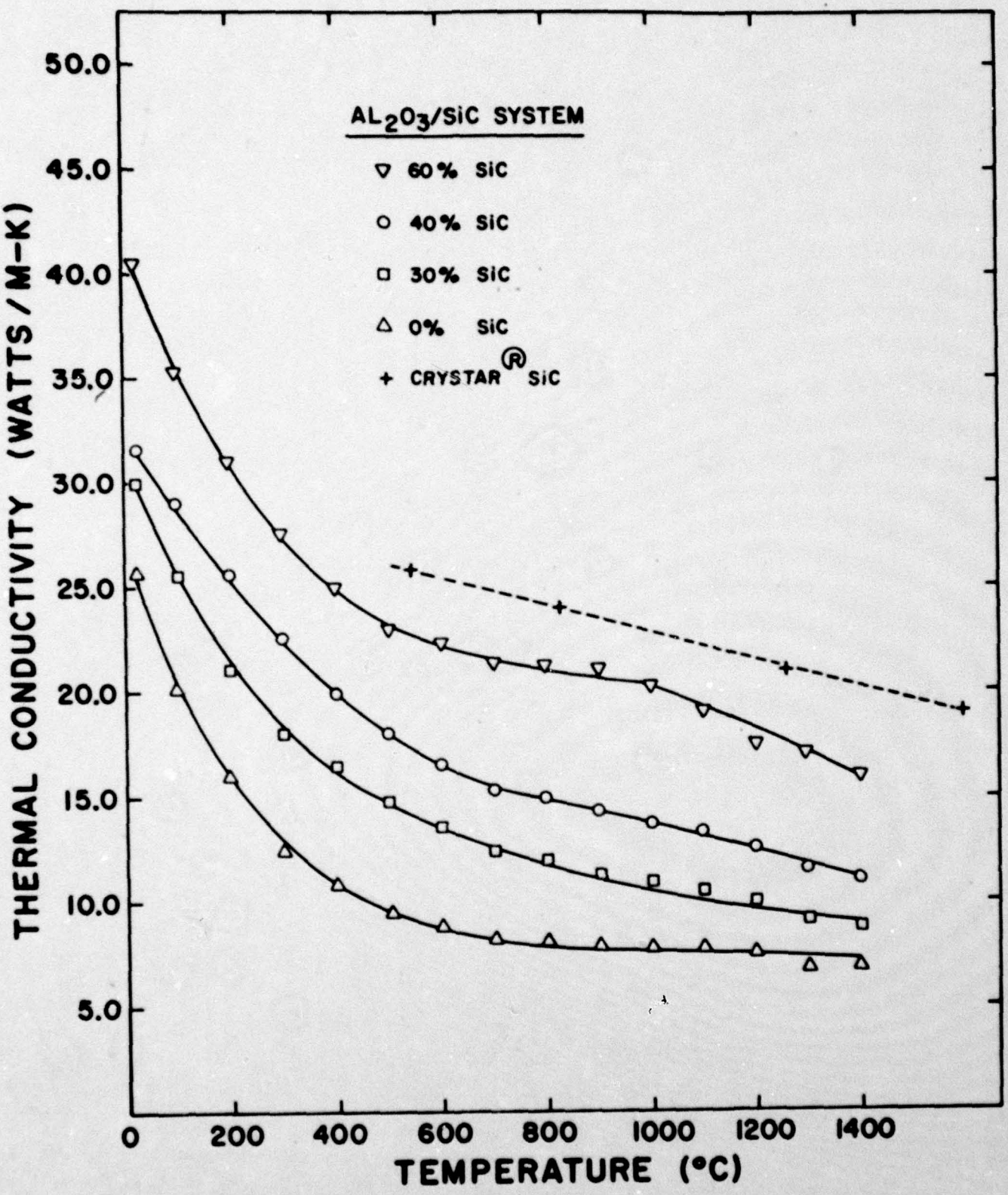


Figure 5.--Thermal conductivity calculated from measured thermal diffusivity and density and calculated heat capacity by $\lambda = \alpha\rho c$ for several compositionns in the Al_2O_3/SiC system.

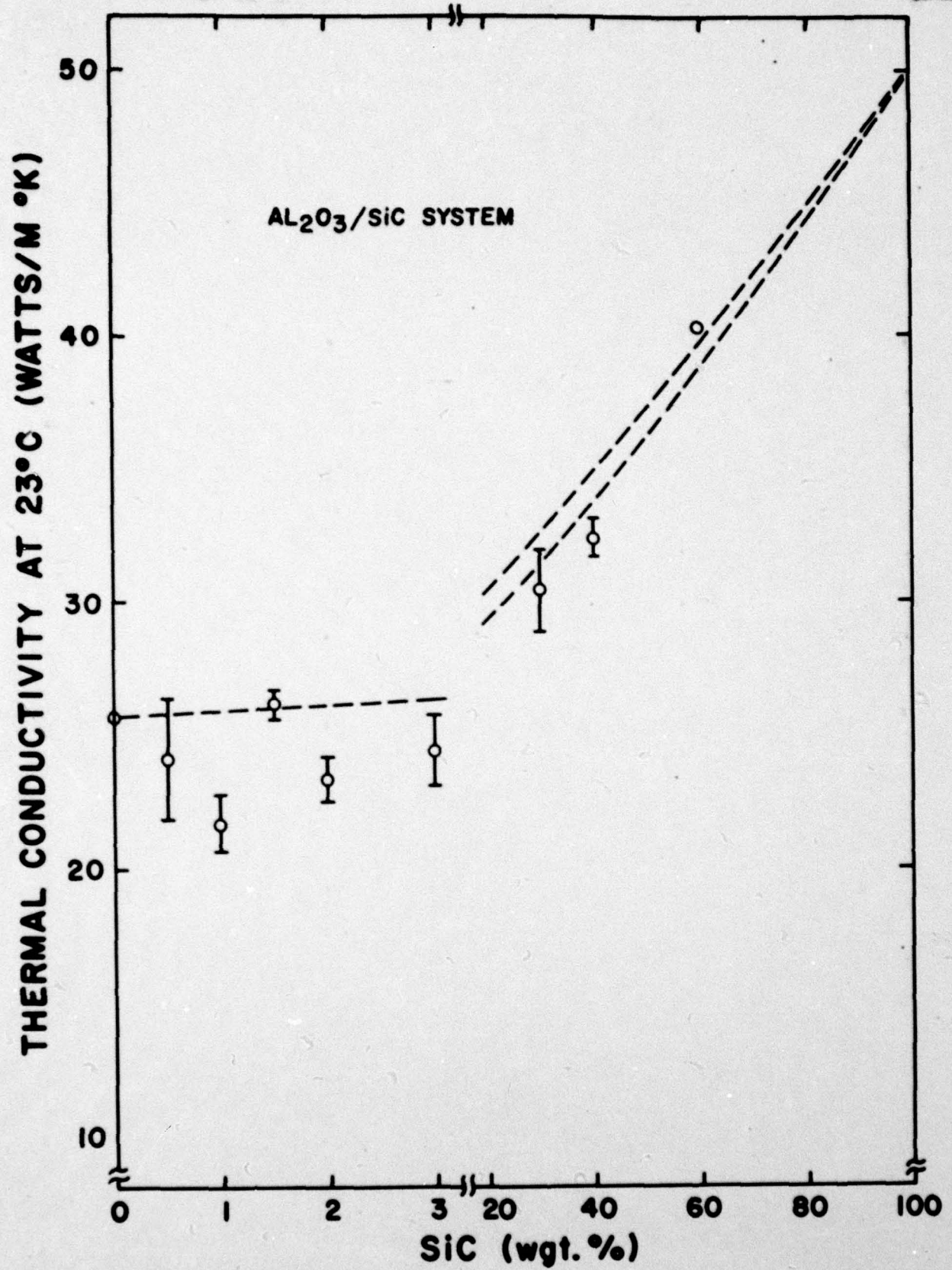


Figure 6.--Calculated thermal conductivity at 23°C for several Al_2O_3/SiC composites compared to values predicted by Maxwell-Eucken Dispersed Phase Composite Theory. For compositions with SiC > 30%, the upper (lower) dashed lines represent theory for SiC (Al_2O_3) as the dispersed phase.

10/24/79 0-000-000-A

the Maxwell-Eucken dispersed phase composite theory.* Both Al_2O_3 and SiC were considered to be the dispersed phase for SiC greater than 20 wgt. %, thus the spread between the two dashed lines representing theory.

A literature study revealed that the thermal conductivity of fairly dense SiC is extremely sensitive to impurity content. For instance, values from 50 to 490 watts/mK at RT were quoted. The lower value (50 watts/mK) for SiC was arbitrarily picked for modeling purposes, therefore the agreement between experimental and predicted values could be fortuitous. Nevertheless, it is interesting to note the apparent cross-over between the 40% and 60% compositions. Agreement with predicted λ depends upon exchanging the roles of SiC and Al_2O_3 as the dispersed or continuous phase.

Preliminary examination by SEM and optical microscope indicated homogeneous distribution of the SiC particles and the porosity. The SiC particles were $\sim$ 1-5 μm and the 1-3 μm pores were located primarily at grain boundary triple points. It is noted that it is very difficult to differentiate between SiC and Al_2O_3 phases by secondary electron imaging. There is sufficient contrast between these phases when using reflected light optical microscopy, but resolution is magnification limited. However, enhanced atomic number contrast obtainable by use of back-scatter electron imaging should reveal details of the SiC/Al_2O_3 morphology at higher magnifications than possible with optical microscopy. This analysis will be

---

* See, for instance, A. E. Powers, "Conductivity in Aggregates," Knolls Atomic Power Report KAPL 2145, General Electric Co. (March 6, 1961) for a review of several composite transport models. A computer program was developed to routinely compare calculated thermal conductivity values to values predicted by Bruggeman variable dispersion and mixture models as well as the simpler Maxwell-Eucken dispersed phase model.

carried out in a newly acquired Robinson back-scatter electron detector SEM attachment. Final analysis of the thermal transport data awaits completion of the microstructural analysis.

In general, the thermal transport data for this Al_2O_3/SiC system are well-explained by simple composite theory. No evidence for pre-existing microcracks which would effectively lower the thermal conductivity) was observed, although the presence of hysteresis effects still needs to be checked at lower temperatures. The SiC particles, in compression at most temperatures, are well-bonded or at least minimum thermal resistance occurs at the Al_2O_3-SiC interface. The SiC particles contribute significantly to the relatively high thermal conductivity of these composites.

The only unusual effect observed is the rather abrupt change in shape that occurs at $\sim$ 1000°C in the thermal diffusivity versus temperature curve for the 60% SiC sample. This effect was observed in two different samples, thus appearing to be reproducible.

For engineering use the reciprocal thermal diffusivity and conductivity values were fitted by least squares approximation to the temperature dependent forms

$$\alpha^{-1} \text{ or } \lambda^{-1} = A + BT \qquad (3)$$

The coefficients A and B and rms deviations are listed in Table III for a fit over the temperature range RT-1400°C.

2. MgO/SiC

Room temperature thermal diffusivity values for several compositions in the MgO/SiC system are shown in Figure 7. For comparison, the RT thermal diffusivity values for the Al_2O_3/SiC system from Figure 3 are reproduced. The compositions, densities, estimated porosities,

TABLE III.--Coefficients A and B and rms deviations for least squares fit to α^{-1} or $\lambda^{-1} = A + BT$ for Al_2O_3/SiC compositions.

Composition (wgt % SiC)	A (sec/cm^2)	B (sec/cm^2K)	σ (sec/cm^2)
		α^{-1} (sec/cm^2)	
0.0	0.0453	7.78	4.22
1.0	0.0546	2.84	2.79
1.5	0.0566	- 1.18	1.84
2.0	0.0541	3.28	2.03
30	0.0319	2.59	1.14
40	0.0228	3.07	0.75
60	0.0143	4.06	0.97
		λ^{-1} (mK/watt)	
	(mK/watt)	(m/watt)	(mK/watt)
0.0	0.729×10^{-4}	0.0353	0.0110
1.0	0.915 "	0.0270	0.0081
1.5	0.956 "	0.0175	0.0055
2.0	0.904 "	0.0283	0.0066
30	0.558 "	0.0217	0.0032
40	0.413 "	0.0212	0.0021
60	0.242 "	0.0212	0.0022

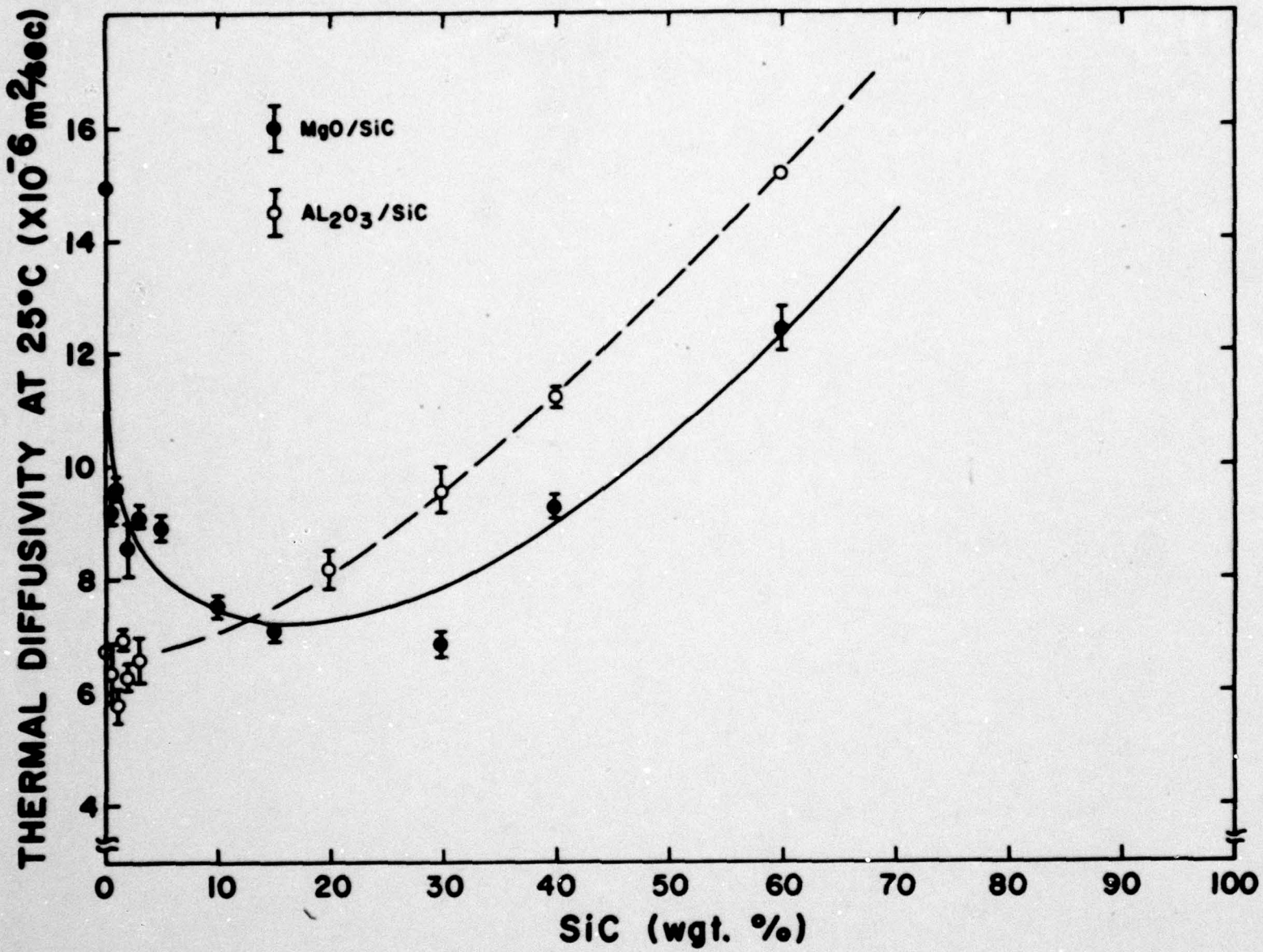


Figure 7.--Comparison of room temperature thermal diffusivity values for various compositions in the MgO/SiC and Al_2O_3/SiC systems.

and some pertinent microstructural information are listed in Table IV for the samples tested. An optical micrograph (Figure 2B) of the composite with 30% SiC shows that the SiC particles are dispersed in a MgO matrix.

Even though the thermal diffusivity of the MgO/SiC composites with ≤5% SiC is ∿ 50% higher than that of the Al_2O_3/SiC composites with similar SiC concentration, there is a dramatic decrease (by ∿ 1/2) in the thermal diffusivity when compared to the value for the high-purity MgO sample. As the concentration of SiC in MgO increases, thermal diffusivity decreases until a minimum is reached at 30% SiC. Above 30% SiC addition the thermal diffusivity increases proportionately with SiC content.

Temperature dependent thermal diffusivity values for MgO and MgO/30% SiC determined during heating and cooling to 1400°C are shown in Figure 8. At the end of the first heating-cooling cycle, the 30% SiC was remounted and thermal diffusivity measurements were made on reheating to 500°C. Two observations were made. First, it was observed that the thermal diffusivity values for the 30% SiC composite are lower than those for pure MgO for all temperatures up to 1400°C. In fact, they are much lower than values predicted by simple composite theory which would be above those for pure MgO due to the contribution of the high thermal diffusivity SiC. Second, during temperature cycling non-reproducible hysteresis in thermal diffusivity values is observed. Both observations indicate the existence of microcracks in the MgO/30% SiC composite.

After the thermal diffusivity runs the MgO/SiC samples and billets from which the samples were cut were stored in containers open to the atmosphere. About one month later inspection of the billets revealed that a network of macrocracks visible to the unaided eye had formed, especially

TABLE IV.--Compositions, densities, calculated porosities, and microstructural information for MgO/SiC system.

Composition (Wgt % SiC)	Density (gm/cm^3)	Calc. Porosity* %	Microstructure
0.0	3.580	0.0	30-60 μm grains, intergranular fracture
0.5	3.576	0.1	n.c.
1.0	3.557	0.6	2-5 μm grains, mixed fracture
2.0	3.544	0.8	n.c.
3.0	3.570	0.1	n.c.
5.0	3.544	0.5	1-3 μm grains, mixed fracture
10	3.502	1.3	n.c.
15	3.459	1.9	n.c.
20	3.408	2.9	n.c.
30	3.399	2.1	n.c.
40	3.352	2.5	n.c.
60	3.306	1.7	n.c.

* Calculated using 3.580 and 3.210 gm/cm^3 for the zero porosity densities of MgO and SiC, respectively.

n.c. not completed

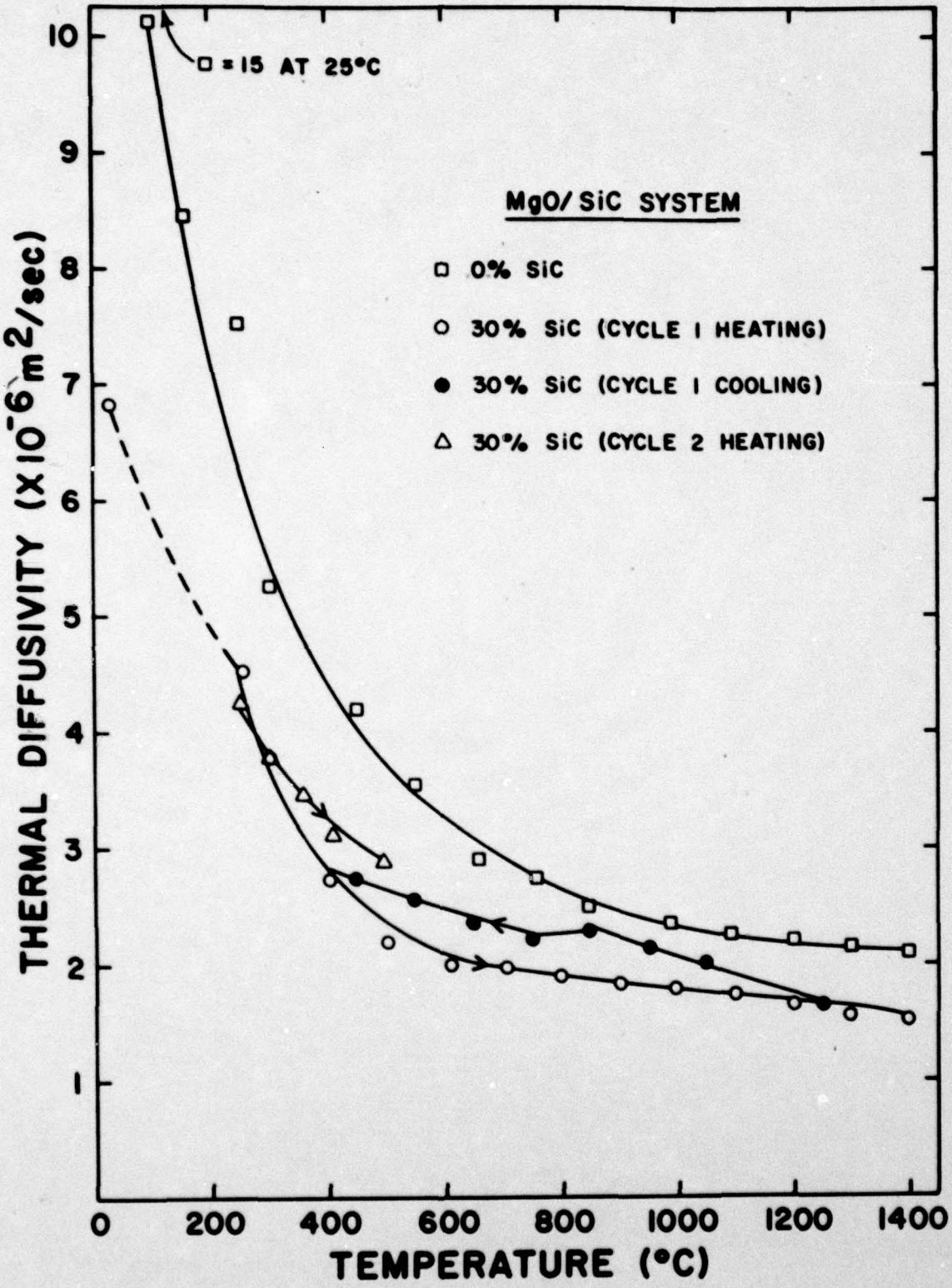


Figure 8.--Effect of temperature cycling from RT to 1400°C on thermal diffusivity values of MgO/30% SiC. For reference the thermal diffusivity values for pure MgO are also shown.

for samples with ≥15% SiC content. Apparently, the combination of residual stresses in the MgO/SiC composites and the affinity for MgO to react with water vapor leads to stress-corrosion cracking.* Although the cracks were not visible in the smaller diffusivity discs, it cannot be determined whether or not the measured thermal diffusivity values were influenced by nonvisible stress-corrosion macrocracks as well as microcracks. Perhaps the microcracks serve as nucleation sites for further stress-corrosion cracking when the MgO/SiC composites are stored in air.

Additional samples in the MgO/SiC system have recently been obtained and are being stored in a desicator prior to testing. At this time it is unclear whether the minimum in thermal diffusivity values ∿ 30% SiC is caused by microcracking due to thermal expansion mismatch between the MgO and SiC or by stress-corrosion macrocracking.

Obviously careful sample preparation and storage procedures must be followed to avoid similar problems with other consubstantial composites.

B. "Thermal Diffusivity of Al_2O_3/TiC Composites."

The thermal conductivity of solids is controlled in part by the specific carriers responsible for heat transfer such as phonons and photons. In some ceramics the electronic contribution to the thermal conductivity also may be significant. In the case of Al_2O_3/TiC composites scattering mechanisms such as phonon-phonon, phonon-electron, phonon-defect, and electron-defect may be used to describe the overall conductivity.

---

* An SEM examination of a MgO/1% SiC fracture surface that had hydrolized (stored in the open atmosphere for about a month) revealed severe macrocracking. Courtesy of Paul Becher, Naval Research Laboratory.

TiC is normally carbon-deficient with the primary defects being carbon-atom vacancies. The vacancies effectively scatter phonons which leads to a rather low, temperature independent lattice thermal conductivity contribution (λ_l) rather than a λ_l that varies T^{-1} as in normal crystalline solids. On the other hand, the electronic contribution (λ_e), which is quite large in TiC, increases proportionately with T. Since the overall conductivity (λ) is basically the sum of λ_l and λ_e, it also increases proportionately with T and becomes quite large. For instance, when T = 1400°C, $\lambda \simeq 50$ watts/mK.[6] At RT, however, TiC has a relatively low thermal conductivity for a carbide, e.g. at RT $\lambda \simeq 30$ watts/mK for TiC while $\lambda \simeq 450$ watts/mK for pure and dense SiC.[7]

The unusual thermal transport properties of TiC make it possible to fabricate a composite material with a high, approximately temperature independent thermal conductivity, at least at higher temperatures. As shown by Ganguly, et al[8], temperature dependent thermal conductivity can lead to large tensile stresses in a ceramic with a temperature gradient. In a high-purity oxide ceramic such as Al_2O_3 or MgO the thermal conductivity is extremely temperature dependent, decreasing by a factor of 5 or 6 between 100 and 1000°C. Normally the only way to attain a temperature independent λ for high-purity, high conductivity ceramics is to induce a large amount of porosity or solid-solution alloying elements. Unfortunately, both of these techniques also reduce the overall thermal conductivity, perhaps by an order

---

[6] James Bethin and Wendell S. Williams, "Ambipolar Diffusion Contribution to High-Temperature Thermal Conductivity of Titanium Carbide," Jour. Amer. Ceram. Soc., 60 (9-10), 424-427 (1977).

[7] G. A. Slack, "Nonmetallic Crystals with High Thermal Conductivity," J. Phys. Chemical Solids, 34, 321-35 (1973).

[8] B. K. Ganguly, K. R. McKinney, and D. P. H. Hasselman, "Thermal-Stress Analysis of Flat Plate with Temperature-Dependent Thermal Conductivity," Jour. Amer. Ceram. Soc. 58, (9-10), 455-567 (1975).

of magnitude.

In an effort to design a ceramic material with high, temperature independent thermal conductivity, a systematic study of the thermal diffusivity properties of the Al_2O_3/TiC system was initiated. In addition to the characteristic hardness of TiC, it may be that the unusual thermal transport properties of this composite contribute to making it an outstanding material for ceramic tool bits. This research effort is being carried out in cooperation with researchers at Fansteel and Ceradyne.

In Table V the compositions, densities, calculated porosities, and the thermal diffusivity at RT are given for samples tested in the Al_2O_3/TiC system. The samples, prepared by hot-pressing, all have generally theoretical densities. A typical optical micrograph (Figure 2C) indicates homogeneous distribution of TiC particles in an alumina matrix. It is observed that the TiC particles are somewhat smaller than the SiC particles in the Al_2O_3 or MgO composites.

None of the RT thermal diffusivity values for the composites fell between pure Al_2O_3 or TiC values. However, low temperature thermal conductivity (diffusivity) of TiC is particularly sensitive to the defect structure (deviation from stoichiometry) and may vary over an order of magnitude depending on fabrication conditions. At this time there is no explanation for the lower than expected values of RT thermal diffusivity observed for the composites other than suspecting that the values depend on the specific properties of TiC in each composite. Therefore modeling thermal transport properties using component values is difficult and probably meaningless for this system. However, microcracking is not expected in these composites since the degree of thermal expansion mismatch is rather small, i.e., the thermal expansion coefficients for Al_2O_3 and TiC between 20 and 1000°C are 8.0 and 7.2 x 10^{-6} $°C^{-1}$, respectively.

TABLE V.---Compositions, densities, calculated porosities, and thermal diffusivity at RT for Al_2O_3/TiC system.

Composition (Wgt. % Tic)	Density (gm/cm^3)	Calc. Porosity* (%)	RT Thermal Diffusivity ($x10^{-6}$ m^2/sec)
0.0	3.947	1.0	7.75
1.0	4.014	~ 0	6.00
3.0	4.025	~ 0	5.60
5.0	4.030	~ 0	5.85
15	4.141	~ 0	5.20
30	4.310	~ 0	5.60
40	4.485	~ 0	6.55
50	4.462	~ 0	6.35
100	4.782	2.8	9.45

* Calculated using 3.986 and 4.920 gm/cm^3 for the zero porosity densities of Al_2O_3 and TiC, respectively.

Correlation of thermal with electrical transport properties of TiC should be possible. A simple ohmmeter check of the composites indicated that those with ≤ 15% TiC had essentially infinite resistance which would indicate a very low amount of TiC to TiC contact. The resistance dropped abruptly for ≥ 30% TiC, indicating a significant amount of continuity through the TiC phase.

In Figure 9 the thermal diffusivity values from RT to 1400°C for the 1 , 30 , and 40% TiC composites are compared to values for pure Al_2O_3 and TiC. The influence of the TiC phase is obvious at the higher temperatures for the 30% and 40% TiC samples. For example, at 1400°C the thermal diffusivity of the Al_2O_3/40% TiC sample is twice that for pure Al_2O_3. Values of thermal diffusivity for the 1% TiC composite are similar to that of Al_2O_3. Preliminary measurements to 300°C (not shown here) for the 3 , 5 , and 15% TiC samples also have a temperature dependence that is similar to that of alumina. Not until the TiC concentration reaches 30% is the influence of the TiC phase on the temperature dependence of the thermal diffusivity noticed above ≈300°C. Apparently partial continuity of the TiC phase in the Al_2O_3/TiC composites is necessary before the contribution of the TiC to thermal transport in the composite becomes significant. It also is noted that there is no hysteresis for any of the composites; values of thermal diffusivity determined on heating to 1400°C and cooling to 350°C are reproducible.

The thermal conductivity values calculated from measured thermal diffusivities, densities, and reference values of heat capacities for TiC, 30% and 40% TiC/Al_2O_3 composite, and Al_2O_3 are given in Figure 10. The influence of TiC, which has a thermal conductivity that is both high in magnitude and

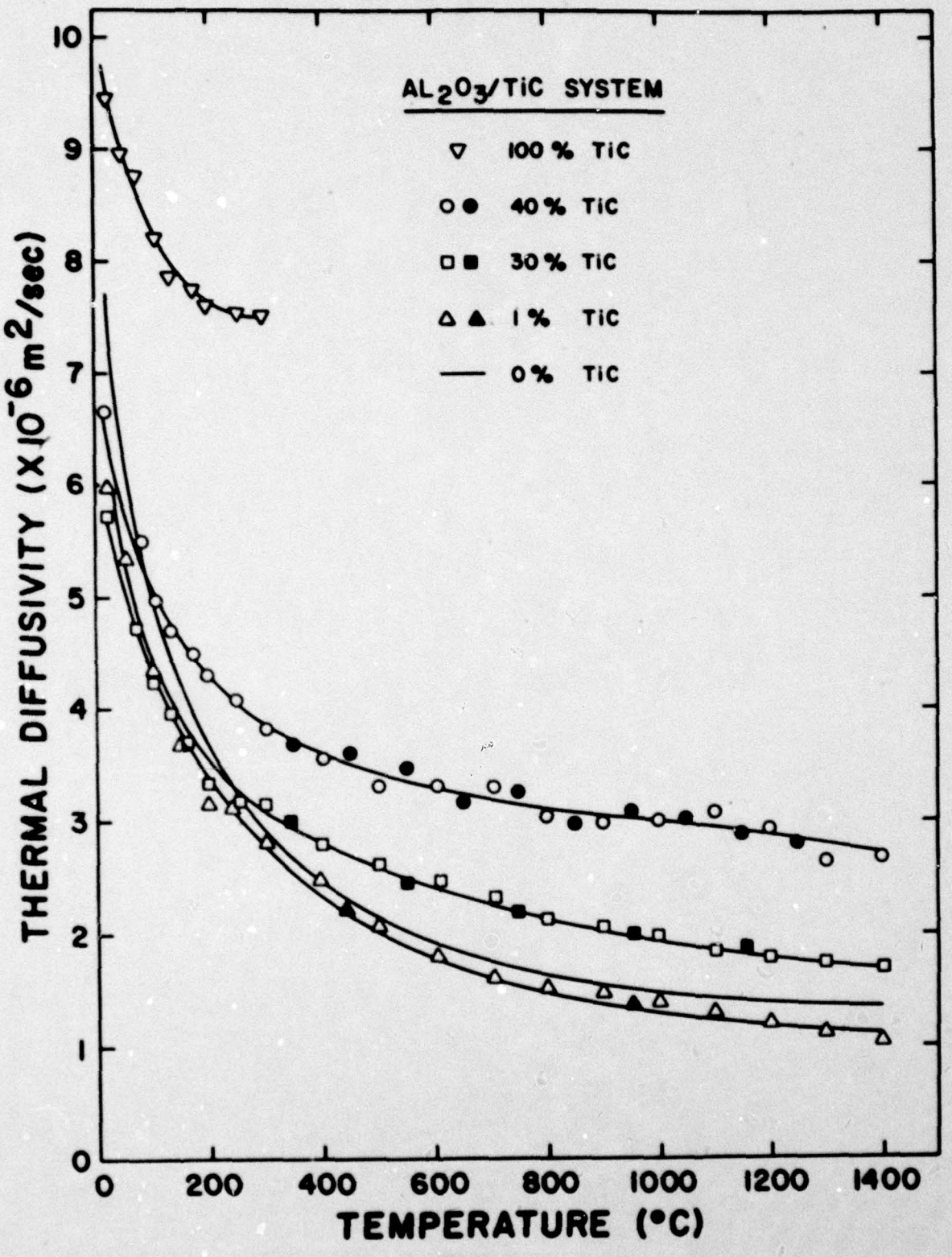


Figure 9.--Temperature dependence of thermal diffusivity from RT to 1400°C for 1, 30, and 40% TiC/Al_2O_3 composites compared to similar values for Al_2O_3 and TiC. The open (closed) symbols indicate data determined during heating (cooling).

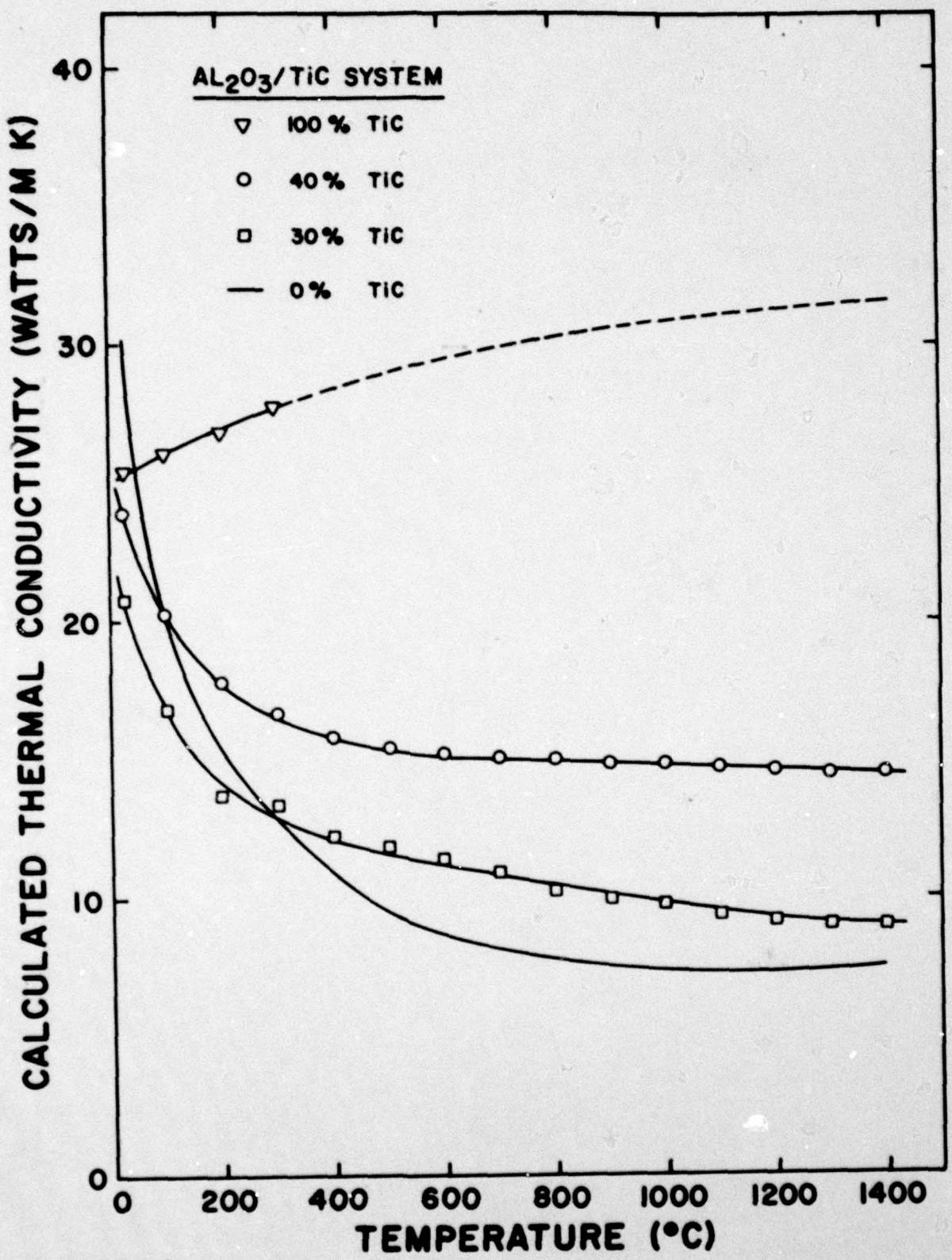


Figure 10.--Calculated thermal conductivity values from RT to 1400°C for TiC, 40 and 30% TiC/Al_2O_3 composites, and Al_2O_3. Thermal conductivity values above 300°C are estimated from reference values for TiC.

positive temperature dependence, is even more dramatically shown by these curves. In fact, for T >400°C, the thermal conductivity of the 40% TiC composite is approximately temperature independent while at the same time the magnitude is twice the value for dense, pure Al_2O_3.

Work is continuing for this system. Samples with similar concentrations but different TiC particle sizes have been obtained.

C. "Thermal Diffusivity of Yttrium Chromite Ceramics."

Perovskites, because of their refractoriness and unusual electrical and catalytic properties, are being considered as candidate materials for use as electrodes in magnetohydrodynamic (MHD) power generation, as oxide leadouts for high temperature fuel cells, and as catalysts for high temperature catalytic combustion. Yttria-based perovskites are particularly promising as they are not as susceptible as lanthanum-based perovskites to destructive hydration (even at room temperature) or critical compositional problems.[9]

This study seeks to examine the thermal transport properties for a series of yttrium chromite ceramics in the families $Y_{1-x}M_xCrO_3$ (M=Ca,Mg) and $YCr_{1-x}Mg_xO_3$ prepared by thermal sintering and hot pressing methods. The materials are fabricated to nearly full density in the reduced condition. Reduced materials, as prepared, are highly resistive (electrically) until oxidized at elevated temperatures. Under oxidizing conditions, $YCrO_3$ incorporates Ca^{2+} to X= 0.10, but Mg solubility appears very low. Phase changes and microcracking occur depending on thermal and atmospheric

---

[9] T. Negas, W. R. Hosler, and L. P. Domingues, "Preparation and Properties of Yttrium Chromite Ceramics," Proceedings of the 4th International Meeting on Modern Ceramics Technologies, Saint Vincent, Italy, May 28-31 (1979).

treatment. Correlations will be made among processing parameters and the resulting electrical, thermal, and microstructural properties. This work is being carried out in cooperation with researchers at Trans-Tech, Inc. and the National Bureau of Standards.

Table VI lists the compositions, bulk densities, and room temperature thermal diffusivity values for selected hot-pressed and thermal sintered yttria-chromites. The room temperature thermal diffusivity was remeasured for the two thermal sintered samples with X(Ca) = 0.02 and 0.05 after each had been given an oxidation treatment consisting of air heat and held at 1200°C for 6 hours. A slight decrease (≈10%) in the RT thermal diffusivity was observed after this treatment.

The thermal diffusivity values were then determined for the hot-pressed X(Ca) = 0.05 sample as a function of temperature during a single heating-cooling cycle to 1400°C. These data are presented in Figure 11 where they are compared to equivalent data for a lanthanum-based perovskite of similar composition.[10] On heating the thermal diffusivity values of the yttria-based perovskite are lower than those for the lanthanum-based perovskite, but on cooling the reverse is true. The hysteresis in the thermal diffusivity for the lanthanum material probably indicates severe microcracking, while the reproducibility in thermal diffusivity values on heating and cooling for the yttria material indicates a mechanically stable microstructure for the same conditions.

Further testing will examine the effects of high temperatures and of changing atmospheres (P_{O_2}) on the thermal diffusivity values for various compositions.

---

[10] J. Lambert Bates, "Development and Characterization of Materials for Open Cycle MHD, Quarterly Report, April-June, 1976," BNWL-2004-3 (1976).

TABLE VI.---Compositions, bulk densities, and room temperature thermal diffusivities for selected yttria-chromites.

Composition ($Y_{1-x}M_xCrO_3$)	Bulk density (gm/cm^3)	RT Thermal Diffusivity ($x10^{-6}m^2/sec$)
(Sintered)		
M = Ca, X = 0.02	5.666	1.93 ± 0.07 (2)
(after oxidation)+	-	1.80
M = Ca, X = 0.05	5.571	1.77 ± 0.10 (2)
(after oxidation)+	5.510	1.58
M = Mg, X = 0.05	5.61	2.39
M = Ca, X = 0.10	5.55	1.73
(Hot-pressed)		
M = Ca, X= 0.02	5.272	1.67 ± 0.01 (3)
M = Ca, X= 0.05	5.532	1.61 ± 0.01 (2)

+ oxidation treatment - 1200°C in air for 6 hours

( ) number of samples tested when more than one

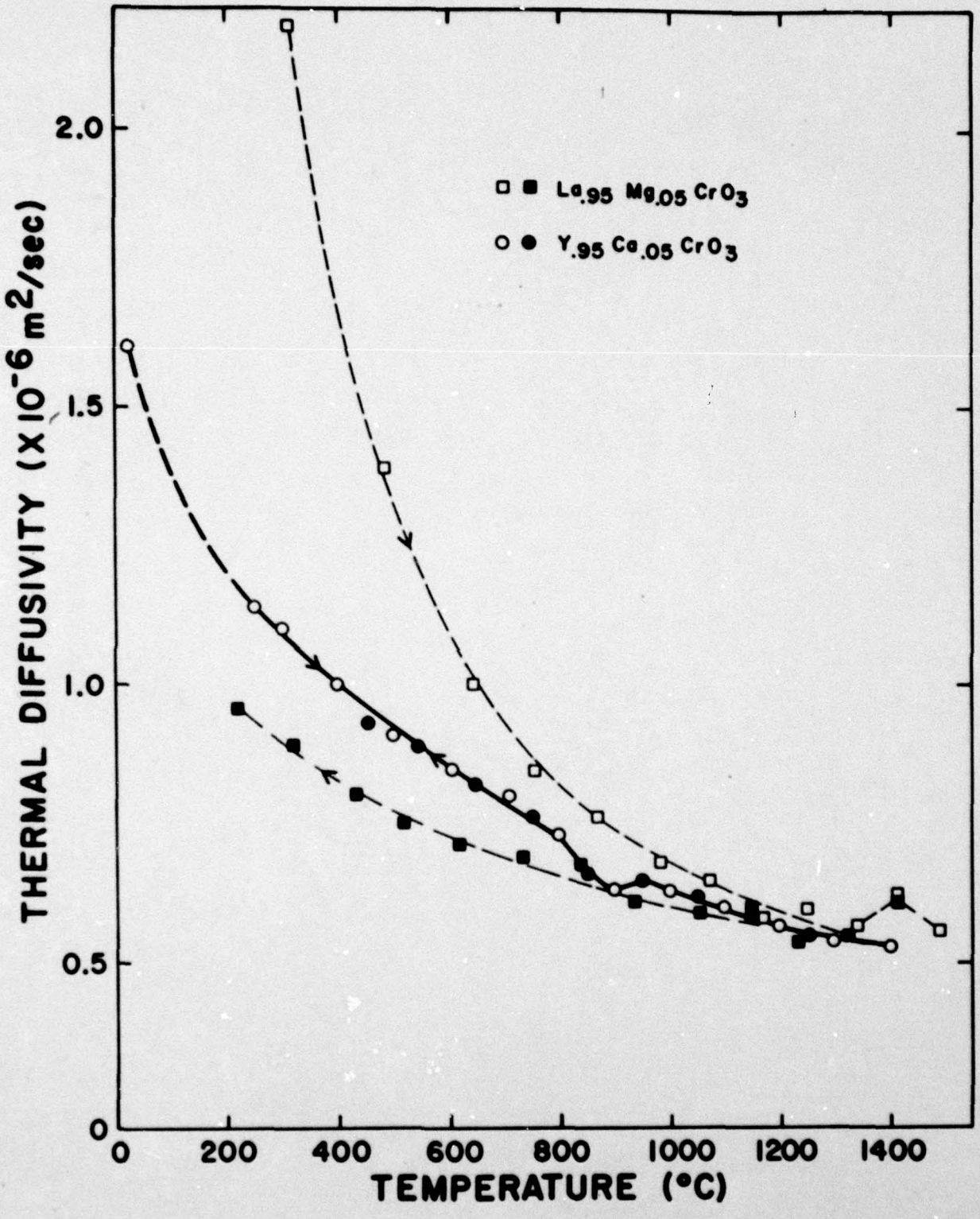


Figure 11.--Thermal diffusivity of $Y_{.95}Ca_{.05}CrO_3$ on heating and cooling from RT to 1400°C compared to values for $La_{.95}Mg_{.05}CrO_3$ after similar treatment.

V. TECHNICAL ARTICLES

The following are the six technical reports which set forth the results of research conducted during 1979. The reader is directed to the final reports for years 1975, 1976, and 1977 for complete copies of the other 17 technical articles listed in Appendix A.

ARTICLE IV-A

EFFECT OF CRYSTALLIZATION ON THERMAL DIFFUSIVITY OF A CORDIERITE GLASS-CERAMIC*

by

K. Chyung†

G. E. Youngblood⊖

D. P. H. Hasselman§

† Corning Glass Works, Corning, N.Y. 14830

⊖ Montana Energy and MHD Research and Development Institute, Inc., Butte, MT 59701

§ Virginia Polytechnic Institute and State University, Blacksburg, VA 24061

* Reprinted by permission from the American Ceramic Society

Reprinted from the Journal of The American Ceramic Society, Vol. 61, No. 11-12 November-December, 1978
Copyright 1978 by The American Ceramic Society

Effect of Crystallization on Thermal Diffusivity of a Cordierite Glass-Ceramic

K. CHYUNG,* G. E. YOUNGBLOOD,* and D. P. H. HASSELMAN*

THE magnitude of the thermal conductivity and diffusivity of solids is controlled by the specific heat and by transport properties of the carriers responsible for the heat transfer (e.g. electrons, phonons, and photons[1]). Dielectric glassy (noncrystalline) materials with low values of phonon mean free path at low and moderate temperatures (at which phonon transport is the primary mechanism for heat transport) are expected to exhibit much lower thermal conductivity and diffusivity than crystalline materials with much higher values of mean free path. For this reason, crystallization of a glass to form a glass-ceramic is expected to significantly increase the thermal conductivity and diffusivity, as confirmed by experimental data for the effect of crystallization on the thermal diffusivity of a mica glass-ceramic.[2]

In general, the relative effect of partial crystallization of a glass on the heat-transfer properties is expected to be a function of the relative amount of the crystalline phase, its crystal structure and nature of the atomic bonding, and other properties relevant to the transport of thermal energy. The phonon mean free path and velocity are expected to be much smaller in a mica crystalline phase, with Van der Waals bonding between the basal planes, than in a crystalline phase with primarily ionic and covalent atomic bonds. The latter type of crystalline phase is expected to have a greater relative effect on the thermal diffusivity of a glass-ceramic than does a mica crystalline phase. In the present note this hypothesis is verified by comparing experimental data for the thermal diffusivity of a cordierite glass-ceramic with corresponding data for a mica glass-ceramic reported previously.[2]

Several samples (1 in. high by ½ in. in diam.) of the original glass of a commercial glass-ceramic* were crystallized by heating to 820°C in ≈45 min and holding for 2 h for crystallite nucleation. The samples were then heated rapidly to, and held for 8 h at, several temperature levels to promote crystallite growth. The crystallite morphology was studied by replication transmission electron microscopy.† The nature of the crystalline phase was measured by X-ray analysis.† The thermal diffusivity was measured‡ from room temperature to ≈750°C by laser flash with the same equipment and procedures followed for the mica glass-ceramic.[2]

Figure 1 shows electron micrographs for two heat-treated samples. Table I lists the density for all samples and the nature and amount of crystalline phase for the samples shown in Fig. 1. Figure 2 shows the experimental data for the thermal diffusivity; no difference was noted between the data obtained on heating and cooling for two of the samples investigated.

Figure 2 indicates that near room temperature the crystallization increased the thermal diffusivity by a factor >3. At the higher temperature the relative increase is smaller. Qualitatively, these relative differences in thermal diffusivity may be attributed to the combined effect of the decrease in thermal conductivity due to increased phonon scattering in the crystalline phase with increasing temperature and the simultaneous increase in thermal conductivity due to photon transport in the glassy phase. The present data for the thermal diffusivity of the fully crystallized glass-ceramic (1260°C)

Received March 31, 1978.
K. Chyung is with the Corning Glass Works, Corning, New York 14830. G. E. Youngblood is with the Montana Energy and MHD Research and Development Institute, Butte, Montana 59701. D.P.H. Hasselman is with the Department of Materials Engineering, Virginia Polytechnic Institute and State University, Blacksburg, Virginia 24061.
*Member, the American Ceramic Society.

Table I. Heat Treatment, Type, and Amount of Crystalline Phases and Densities of Heat-Treated Cordierite Glass-Ceramics

Heat treatment (temp. and time)	Crystalline phases (vol%)	Density (g/cm³)
As-received glass		2.65
820°C, 2 h		2.66
820°C, 2 h; 905°C, 8 h		2.76
820°C,2 h; 1000°C, 8 h	β-quartz (85–90) Spinel (5–10) Enstatite (5) Glass (2–5)	2.92
820°C 2 h; 1100°C, 8 h		2.67
820°C, 2 h; 1150°C, 8 h		2.66
820°C, 2 h; 1260°C, 8 h	Cordierite (70–80) $MgTiO_5$ (10–15) α-cristobalite (10–15)	2.60

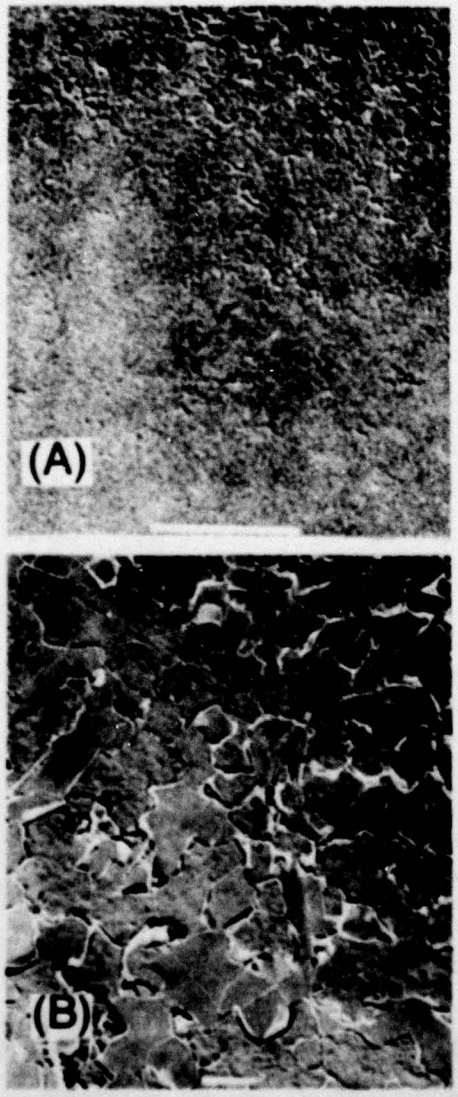


Fig. 1. Replica electron micrographs of partially crystallized cordierite glass-ceramics. Nucleation heat treatment: 2 h at 820°C followed by crystal growth for 8 h at (*A*) 1000° and (*B*) 1260°C (bar = 1 μm).

*C9606, Corning Glass Works, Corning, N.Y.
†Data obtained at Corning Glass Works.
‡Measured as part of a larger research program on the thermal properties of engineering ceramics supported by the Office of Naval Research.

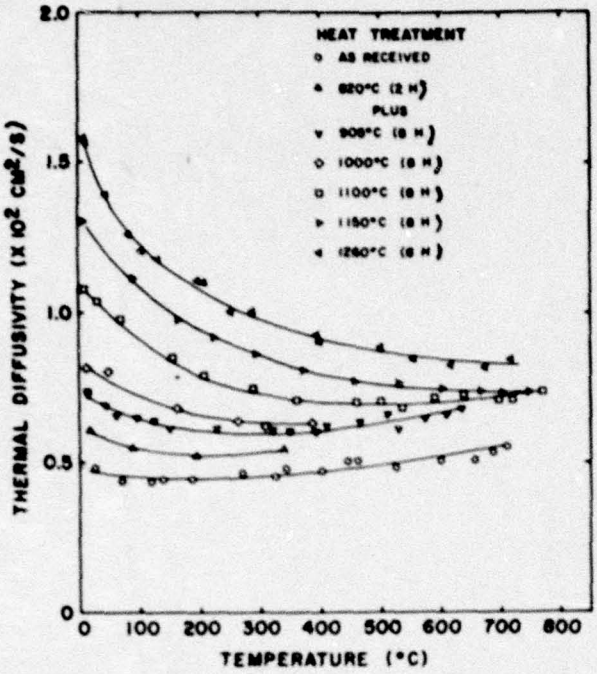


Fig. 2. Effect of crystallization on thermal diffusivity of cordierite glass-ceramic. *Open symbols* indicate measurements made during heating, *filled symbols* those made during cooling.

lie somewhat below the data collected for the commercial cordierite glass-ceramic.[3] This difference may be partially attributable to the difference in the heat schedule used for crystallizing the commercial material and the present samples, possibly resulting in differences in the relative amounts of the various crystalline phases.

Comparing the present data with those reported for the mica glass-ceramic shows that the original glasses for both studies have about the same thermal diffusivity value. On crystallization, however, the increases in the thermal diffusivity obtained for the cordierite glass-ceramic are far greater than for the mica glass-ceramic. This observation agrees qualitatively with the original hypothesis that for a glass-ceramic a crystalline phase without Van der Waals bonding is expected to be far more effective in increasing the thermal diffusivity of the glass-ceramic than a crystalline phase partially held together by such bonding. This conclusion is verified by the present data which show that at crystallization temperatures of ≥1000°C the increase in thermal diffusivity is governed primarily by the change in the nature and relative amounts of the various crystalline phases rather than by the decrease in the amount of glassy phase.

Exact quantitative estimates of this phenomenon in terms of lattice-dynamics theory are beyond the scope of the present study. In general, however, the present data and those obtained for the mica glass-ceramics strongly support the suggestion that the thermal diffusivity of glass-ceramics can be tailored to specific values by careful control over composition and heat treatment.

---

[1] C. Kittel, Introduction to Solid State Physics, 3d ed. Wiley & Sons, New York, 1966.

[2] H. J. Siebeneck, K. Chyung, D. P. H. Hasselman, and G. E. Youngblood, "Effect of Crystallization of the Thermal Diffusivity of a Mica Glass-Ceramic," *J. Am. Ceram. Soc.*, **60** [7–8] 375–76 (1977).

[3] Thermal Diffusivity (Thermophysical Properties of Matter, Vol. 10), p. 581. Edited by Y. S. Touloukian, R. W. Powell, C. Y. Ho, and M. C. Nicolaou. IFI/Plenum, New York, 1973.

ARTICLE IV-B

THERMAL DIFFUSIVITY OF BA-MICA/ALUMINA COMPOSITES*

by

G. E. Youngblood[†]
Larry D. Bentsen[†]
James W. McCauley[B]
D. P. H. Hasselman[ζ]

[†] Montana Energy and MHD Research and Development Institute, Inc., Butte, MT 59701

[B] Army Materials and Mechanics Research Center, Watertown, MA 02172

[ζ] Virginia Polytechnic Institute and State University, Blacksburg, VA 24061

* Reprinted by permission from the American Ceramic Society.

Reprinted from the American Ceramic Society Bulletin, Vol. 58, No. 6 June 1979.
Copyright 1979 by The American Ceramic Society

Thermal Diffusivity of Ba-Mica/Alumina Composites

**GERALD E. YOUNGBLOOD*
and LARRY D. BENTSEN**

Montana Energy R&D Institute, Butte

JAMES W. McCAULEY*

Army Materials & Mechanics Research Center, Watertown, Mass.

and

D. P. H. HASSELMAN*

Virginia Polytechnic Institute, Blacksburg

Particulate composites based on mica dispersions are excellent candidate materials for many engineering applications in view of their improved friction and wear behavior,[1] enhanced fracture toughness,[2] and thermal shock resistance,[3,4] as well as their enhanced machinability.[5] The mica phase of such composites can also have a profound effect on physical properties such as strength,[6] elastic behavior,[6] thermal expansion, and thermal conductivity.[7] The present note reports data for the effect of a Ba-mica–dispersed phase on the thermal diffusivity of polycrystalline alumina.

Samples of alumina containing up to 50 vol% of a dispersed phase of Ba mica, identical in composition to those studied previously,[6] were prepared by uniaxial hot pressing of mixed powders of nominally $BaMg_3Al_2Si_2O_{10}F_2$ mica* and γ-Al_2O_3† at 1250°C and 7000 psi. The mica was in the form of thin circular flakes[6] ≈10 μm thick by 30 μm in diameter. The γ-Al_2O_3 had an average particle diameter of 1.1 μm. The mica flakes were oriented with their long dimension and basal plane perpendicular to the hot-pressing direction. The densities of the samples at room temperature are given in Table I. In agreement[6] with previous data, the densities with increasing mica content showed an approximate linear negative deviation from the theoretical density calculated by the rule of mixtures, giving a total deviation of ≈6% at 50 vol% mica. The microstructures showed that their deviations in density cannot be attributed to an increase in pore phase with increasing mica content. Instead, these density variations are the result of the formation of a small amount of a glassy reaction product between the mica and the alumina phase. Possibly, the lower densities may also be attributable to microcracking by cleavage within the mica due to the internal stresses that develop on cooling as the result of the mismatch in the coefficients of thermal expansion of the mica and the alumina.

The thermal diffusivity parallel to the hot-pressing direction from 25°C to ≈800°C was measured by the laser-flash technique with equipment and procedures described elsewhere.[8] Figure 1 shows the experimental data for all compositions with the exception of the sample with 20 vol% mica, which exhibited an apparently anomalous behavior. To provide a basis of comparison of the relative temperature dependence, Fig. 1 includes experimental data for a pure dense polycrystalline alumina.[8] Figure 2 shows the compositional dependence for various temperatures obtained from the curves drawn through the data of Fig. 1. Figure 2 also includes the data for the sample containing 20 vol% mica.

The anomaly in the present data for the thermal diffusivity at 20 vol% mica was also found for the thermal conductivity,[7] with the exception that in the latter study the anomaly occurred at 15 vol% mica. This anomaly is attributable to the type and amount of reaction products formed between the mica and the alumina during hot pressing.[10] Preparation of full-density composites is accomplished within a narrow temperature range below which complete densification does not occur and above which undesirable reaction products are formed. This situation is particularly critical near 15–20% Ba mica. Below this amount an excess temperature results in the formation of a glass and a spinel, whereas above this amount only a glassy phase is formed. In support of this explanation, X-ray analysis of the present samples showed diffraction peak intensities, for the mica phase of the composite containing 20% mica, smaller than those for the other samples, as expected from initial amount of mica present. For the present data the anomalous value for the thermal diffusivity probably occurs because the reaction products have either a higher thermal conductivity or a lower specific heat than the corresponding value for the mica or the alumina.

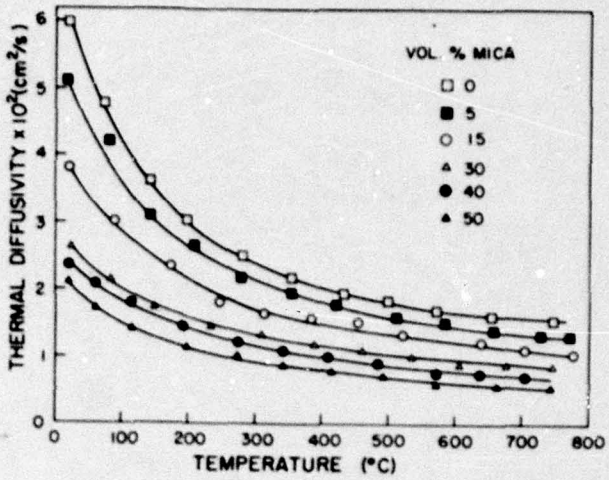


Fig. 1. Effect of temperature on thermal diffusivity of Ba-mica/alumina composites.

Table I. Composition and Density of Ba-Mica/Alumina Composites

Ba-mica content (vol%)	Density (g/cm³)
5	3.935
15	3.845
20	3.750
30	3.695
40	3.625
50	3.540

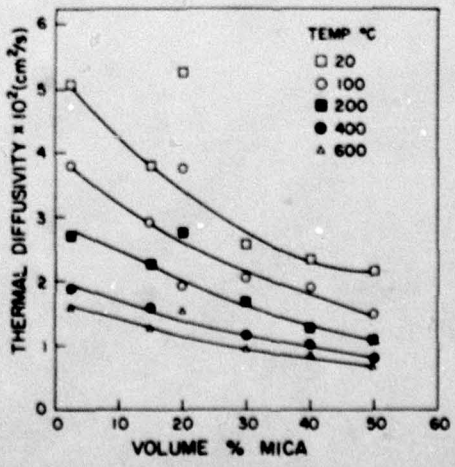


Fig. 2. Effect of composition on thermal diffusivity of Ba-mica/alumina composites.

*Member, the American Ceramic Society.
*Synthane-Taylor Corp., Myktroy Ceramics Div., Ledgewood, N.J.
†Cerac, Inc., Milwaukee, Wis.
‡SN60, Feldmühle, A.G., Plochingen, West Germany.

Received August 28, 1978; approved October 12, 1978.

The relative temperature dependence of the thermal diffusivity of the mica-alumina composites is similar to that for the pure alumina. In fact, a plot of α^{-1} vs T shows a straight line behavior with an intercept near zero at $T=0$ K for all compositions. It may be noted again that the present data are for the thermal diffusivity with heat flow through the mica occurring perpendicular to the weakly bonded basal planes. On the basis of experimental data for other micas,[11] boron nitride,[12,13] and pyrolytic graphite,[14,15] heat flow perpendicular to the basal plane is expected to result in a thermal conductivity at least an order of magnitude less than that of polycrystalline aluminum oxide and also to result in a temperature dependence less than T^{-1}, expected for phonon conduction over the range of temperature of the present data. The reason that the temperature dependence of the thermal conductivity/diffusivity of the mica has little or no influence on the temperature dependence of the Ba-mica/alumina composites is that the heat is conducted primarily by the continuous alumina phase. If, however, the mica had been the continuous phase, its temperature dependence would have had a significant effect on the temperature dependence of the thermal conductivity and diffusivity of the composite, especially at higher mica volume fractions. This latter conclusion is easily verified by expressions for the thermal conductivity of composites or, by analogy, by equivalent parallel or series electrical circuits. This suggests that the magnitude of thermal conductivity and its temperature dependence in composites can be controlled by the proper choice of components and their distribution within the composite.

Acknowledgments

Specimen preparation was performed at the Army Materials & Mechanics Research Center, Watertown, Mass. The measurement of the thermal diffusivity was performed as part of a larger program supported by the Office of Naval Research, Alexandria, Va.

References

[1] M. E. Belitskii and D. S. Yas, "Erosion Wear of Mica-Ceramic Materials," *Sov. Powder Metall. Met. Ceram. (Engl. Transl.)*, **1969**, No. 4, pp. 303–305.

[2] J. W. McCauley and S. J. Acquaviva, "Property Characterization of Ba-Mica/Al_2O_3 Composites"; for abstract see *Am. Ceram. Soc. Bull.*, **52** [4] 364 (1973).

[3] C. C. Seaton and J. W. McCauley, "Thermal Shock Characteristics of Ba-Mica/Al_2O_3 Composites"; for abstract see *ibid.*, [9] 708.

[4] K. Chyung, "Fracture Energy and Thermal Shock Resistance of Mica Glass-Ceramics"; pp. 495–508 in Fracture Mechanics of Ceramics, Vol. 2. Edited by R. C. Bradt, D. P. H. Hasselman, and F. F. Lange. Plenum, New York, N.Y., 1974.

[5] D. G. Grossman, "Machinable Glass-Ceramics Based on Tetrasilicic Mica," *J. Am. Ceram. Soc.*, **55** [9] 446–49 (1972).

[6] J. W. McCauley, "Structural and Chemical Characterization of Processed Crystalline Ceramic Materials"; Ch. 7 in Characterization of Materials in Research: Ceramics and Polymers. Edited by J. J. Burke and V. Weiss. Syracuse University Press, Syracuse, N.Y., 1975.

[7] R. P. Tye and J. W. McCauley, "The Thermal Conductivity and Linear Expansion of Ba-Mica/Alumina Composite Materials," *Rev. Int. Hautes Temp. Refract.*, **12** [2] 100–105 (1975) (in Engl.).

[8] J. W. McCauley, "Fabrication and Properties of Ba-Mica/Al_2O_3 Composites"; for abstract see *Am. Ceram. Soc. Bull.*, **51** [4] 434 (1972).

[9] H. J. Siebeneck, K. Chyung, D. P. H. Hasselman, and G. E. Youngblood, "Effect of Crystallization of the Thermal Diffusivity of a Mica Glass-Ceramic," *J. Am. Ceram. Soc.*, **60** [7-8] 375–76 (1977).

[10] J. W. McCauley; unpublished work.

[11] Y. S. Touloukian, R. W. Powell, C. Y. Ho, and P. G. Klemens, Thermal Conductivity: Nonmetallic Solids (Thermophysical Properties of Matter, Vol. 2). IFI/Plenum, New York, N.Y., 1970.

[12] A. Simpson and A. D. Stuckes, "The Thermal Conductivity of Highly Oriented Pyrolytic Boron Nitride," *J. Phys. C*, **4** [13] 1710–18 (1971).

[13] E. K. Sichel and R. E. Miller, "Thermal Conductivity of Highly Oriented Pyrolytic Boron Nitride"; pp. 11–17 in Thermal Conductivity 14. Edited by P. G. Klemens and T. K. Chen. Plenum, New York, N.Y., 1974.

[14] T. Tanaka and H. Suzuki, "The Thermal Diffusivity of Pyrolytic Graphite at High Temperatures," *Carbon*, **10** [3] 253–57 (1972).

[15] S. Nasu, T. Takahashi, and T. Kikuchi, "Anisotropy Ratio of Thermal Diffusivity in Pyrolytic Graphite over the Temperature Range 300 to 1600°C," *J. Nucl. Mater.*, **43** [1] 72–74 (1972).

ARTICLE IV-C

THERMAL DIFFUSIVITY OF Al_2O_3 WITH DISPERSED MONOCLINIC AND TETRAGONAL ZrO_2 PARTICLES

by

Larry D. Bentsen[+]

G. E. Youngblood[+]

Nils Claussen[*]

[+] Montana Energy and MHD Research and Development Institute, Inc., Butte, MT 59701

[*] Max-Planck-Institut, Stuttgart, West Germany

Presented at the 81st Annual Meeting of the American Ceramic Society, Cincinnati, Ohio, May 1, 1979 (Basic Science Division No. 42-B-79).

ABSTRACT

Thermal diffusivity values are reported for two types of hot-pressed Al_2O_3/ZrO_2 composites : one where many of the ZrO_2 particles exceed the critical size (≃ 3 μm) for tetragonal to monoclinic transformation and the other where most of the ZrO_2 particles are sub-critical. A high density of microcracks, induced in the alumina matrix during fabrication only in the former type, is responsible for a large reduction in values of thermal diffusivity (conductivity) at temperatures below the zirconia phase transformation. For successive temperature cycles to temperatures above the phase transformation, reproducible hysteresis occurs in the thermal diffusivity values. This indicates that the microcracks themselves close and partially heal on heating above the transformation temperature; on cooling below the transformation temperature (which is lower than on the heating part of the cycle), the microcracks reopen restoring their original morphology.

For this study the thermal diffusivity values and hysteresis effects are correlated to the microcracking characteristics of both types of composites for a range of 0 to 24 vol. % ZrO_2 content. Detailed analysis is carried out for the 16 vol. % case which has shown near optimum mechanical toughness and strength.

THERMAL DIFFUSIVITY OF Al_2O_3 WITH DISPERSED MONOCLINIC AND TETRAGONAL ZrO_2 PARTICLES

Larry D. Bentsen, Nils Claussen, and G. E. Youngblood

I. INTRODUCTION

It is well known that the fracture toughness of a ceramic may be increased by the addition of a second phase dispersion. The increase in fracture energy can be attributed to the interaction of the crack front with the second phase producing crack blunting or crack deviation,[1] or the strain energy may be released by microfracture in a process zone through nucleation and extension of microcracks.[2,3,4] Another mechanism which can improve the fracture toughness under certain conditions is the interaction of the crack front with pre-existing microcracks.[5]

Microcracks may be formed due to a phase formation with an accompanying volume change.[3,6] In a composite of unstabilized ZrO_2 dispersed in an Al_2O_3 matrix, microcracks can be formed in the alumina matrix when the composite is cooled from the fabrication temperature and the zirconia particles transform from the tetragonal to monoclinic phase with an increase in volume.[2] The fracture toughness and strength of such composites containing unstabilized zirconia particles of various sizes and concentrations has already been reported.[7] These materials had been prepared by ball-milling followed by hot pressing. An optimum effect, where the fracture toughness doubled compared to that of pure alumina while the strength was unchanged, was obtained for 15 v/o unstabilized ZrO_2 of particle size 1.25 μm. However, microcracking as a toughening mechanism where the microcracks pre-exist has usually been accompanied by a decrease in strength. The problem has been to derive

conditions for the inclusion of particles so that toughness is increased with little or no loss of strength.

By using attritor milling rather than ball milling it is possible to produce an alumina-zirconia composite where the zirconia particle size is much less than in the ball-milled materials.[8] In this case the zirconia particles are small enough so that even at room temperature nearly 100% of the zirconia remains in the tetragonal phase. Since transformation to the monoclinic phase has not taken place, microcracks do not pre-exist in the material as in the ball-milled materials; rather, microcracking occurs under an externally applied stress, such as in front of a major crack. This condition of stress-induced transformation can be even more energy absorbing (due to a higher density of microcracks) than in the ball-milled specimens.

Initially the presence of microcracks in the ball-milled alumina-zirconia composites was confirmed by measuring the thermal diffusivity.[9] For an Al_2O_3 / 16 v/o unstabilized ZrO_2 composite, the thermal diffusivity was lowered approximately by a factor of two below that of single phase Al_2O_3 . Similarly, an effective thermal conductivity λ, calculated from the thermal diffusivity α, heat capacity c, and density ρ by the relation $\lambda = \alpha\rho c$, was decreased by a factor of two since microcracks have little effect on heat capacity or density. Rule of mixtures could not account for such a large decrease in thermal conductivity; therefore, the decrease was attributed to the presence of microcracks. Significantly, the thermal diffusivity values determined during heating and cooling cycles between 100 and 800°C were reproducible. However, the maximum temperature attained (800°C) was below the zirconia phase transformation. The degree of microcracking

would be expected to be unaffected by subsequent temperature cycling as long as the temperature never exceeds the zirconia phase transformation temperature in these composites.

In contrast, considerable hysteresis was observed in the thermal diffusivity of Fe_2TiO_5,[10] $MgTi_2O_5$,[11] and $AlNbO_4$[12] on temperature cycling below 800°C. For these single-phase polycrystalline ceramics with anisotropic thermal expansion, the degree of microcracking (number, size, and separation width of cracks) is a function of the amount of cooling from the specimen preparation temperature as well as previous thermal history.[13] Crack closure and healing, reopening, and in some cases extension during temperature cycling give rise to the hysteresis effect which itself is typically non-reproducible with subsequent temperature cycling. In these materials hysteresis has been reported in strength[14,15] and elastic properties[14,15] as well as in thermal properties.

The degree of microcracking in these non-cubic materials also was shown to be dependent on grain size.[11,12] For instance, values of thermal diffusivity for microcracked $AlNbO_4$ of 3 μm average grain size were decreased by about 30% when compared to values for non-microcracked $AlNbO_4$. At the other extreme thermal diffusivity values for severely microcracked Fe_2TiO_5 of roughly 50 μm grain size were lowered by about 65%.

It is obvious from these results that microcracks are very effective thermal barriers. Even though fracture toughness is enhanced in a material with pre-existing microcracks, the lowering of the thermal diffusivity may offset this benefit in a thermal shock situation. On the other hand, very high strains-at-fracture in combination with a stable (non-catastrophic) mode of crack propagation may be expected to outweigh the requirement for a high thermal conductivity. As pointed

out by Siebeneck et al,[13] the lower thermal conductivity of microcracked materials is an advantage in applications requiring high thermal shock resistance in combination with good thermal insulating properties.

It is also obvious that the measurement of thermal diffusivity is a convenient method to study the degree and character of microcracking. It provides necessary engineering data characterizing microcracked materials for thermal shock or thermal fatigue studies as well; therefore, this method was used to extend the study of the effect of microcracking on the thermal diffusivity of alumina with a zirconia dispersed phase during temperature cycling to temperatures above the zirconia phase transformation. In addition, these results will be compared to thermal diffusivity measurements on a series of alumina-zirconia composites where the zirconia particles are less than critical size so that microcracks are not expected to pre-exist.

II. EXPERIMENTAL

A. Materials and Preparation

Following procedures described elsewhere,[2,8] samples of pure Al_2O_3* and Al_2O_3 with 4, 12, and 16 v/o unstabilized ZrO_2+ were ball milled (material BM) and with 4, 8, 12, 16, 20, and 24 v/o unstabilized ZrO_2 were attritor-milled (material AM). A single sample with 10 v/o of Y_2O_3-stabilized ZrO_2 also was prepared by ball milling. All specimens were hot-pressed in graphite dies under vacuum at a pressure of 40 MN/m^2

*99.5% pure, Alcoa A16, Aluminum Co. of America, Pittsburgh, PA

+No. 8914, E. Merck, Dumstadt, West Germany

for periods of 30 minutes to 1 hour at 1500°C. For both types of composites, the densities increased linearly with ZrO_2 content and were close (> 98%) to theoretically expected mixture values.

Although the zirconia used in the BM material was classified as 1.25 μm particle size, it was determined that agglomeration took place during milling and the actual average ZrO_2 particle size was roughly a factor of three larger.[2] X-ray diffraction revealed that 70 to 95% of the ZrO_2 particles were monoclinic at room temperature with the higher ZrO_2 concentration BM material having the higher concentration of monoclinic phase.[8]

Most of the ZrO_2 particles contained in the AM material were slightly less than 1 μm size. X-ray diffraction revealed that almost 100% of the ZrO_2 particles were tetragonal at room temperature.[8] The ZrO_2 particle size and distribution were examined in flat-polished samples by SEM using a solid-state backscatter electron detector[+] to enhance the atomic number contrast between alumina and zirconia.

The major portion of the analysis reported here applies to the composition with near optimum fracture toughness (K_{1c}) and strength (MOR) properties. Unless specified otherwise, this composition is 16 v/o ZrO_2. For the BM material K_{1c} and MOR were 7 $MN/m^{3/2}$ and 500 MN/m^2, respectively; while for the AM material K_{1c} and MOR were about 10 $MN/m^{3/2}$ and 700 MN/m^2, respectively.[16]

[+] Robinson Independent Backscatter Electron Detector System, International Scientific Instruments, Inc. Santa Clara, CA

B. Measurement of Thermal Diffusivity

The thermal diffusivity was measured by the laser-flash diffusivity technique over the temperature range 25°C to 1400°C.[17] In this experiment a single flash (∿ 1 msec) from a glass-Nd laser[+] irradiates the front face of the specimen (1/2-inch diameter by ∿ 2.0 mm thick disc) and either an intrinsic thermocouple[18] (25°C - 400°C range), an infrared detector[*] (250°C - 1000°C range), or a photodiode detector[**] (900°C - 1400°C range) was used to monitor the temperature transient from the back face. Glass plates were used to attenuate the laser pulse so that the typical steady-state temperature rise was kept below 3°C.

For low temperature measurements the specimen disc was held by three minimum contact alignment pins in air inside a wire-wound, temperature controlled, split-tube furnace. The specimen front face was coated with carbon[†] to ensure uniform absorptivity properties. A 1/4-inch diameter Ag-print spot was painted onto the specimen back face to average local heating effects and to provide electrical continuity for an intrinsic Type E thermocouple. It was spring-loaded to press up firmly against the back face to monitor the chamber temperature as well as the temperature transient.

For higher temperature measurements (250°C-1400°C) the specimens with each face carbon coated were held in a split-tube graphite holder in a carbon resistance furnace[++] with nitrogen atmosphere. Since the experiment required the transfer of the specimen from one holder to

---

[+] Korad K1, 70 Joules maximum per flash, Santa Monica, CA
[*] Barnes Engineering IT-7B (InSb) Stamford, CT
[**] Silicon-diffused PIN Photodiode EG&G SDO-100A
[†] Miracle DGF spray, Miracle Power Products Co., Cleveland, OH
[++] Astro Model 1000A, Santa Barbara, CA

another, a helium-neon laser mounted on the optical rail directly behind the glass-Nd laser rod was used to visually check alignment. In addition, Footprint paper,* cut and taped to the face of a dummy sample disc, was inserted to check beam uniformity and alignment. These are critical steps since simple analysis of the transient heating curve requires strict adherence to boundary conditions, in particular uniform heating of the front face of the sample.

The transient temperature response from either the thermocouple, infrared, or photodiode detector was fed into an oscilloscope† equipped with signal storage. The effective thermal diffusivity (α) of the composite sample was calculated from the expression

$$\alpha = 0.1388\ L^2/t_{\frac{1}{2}} \qquad (1)$$

where L is the specimen thickness and $t_{\frac{1}{2}}$ is the time required for the temperature of the back surface of the specimen to reach one half of its final value. The concept of an effective thermal diffusivity as a characteristic property of the composite is expected to be valid for the range of compositions examined here according to criteria recently reviewed by Lee and Taylor.[19]

Measured α's were corrected for heat loss in a manner described by Heckman.[20] These corrections amounted to only a few percent at low temperature and increased to about 13 % by 1400°C. No corrections for finite pulse width were necessary.

---

*Korad 920 Footprint paper, Santa Monica, CA
†Tektronix 5111 with plug-ins, Beaverton, OR

The response time of the thermocouple or the infrared detector and associated electronics was less than 50 msec for the present samples. With this experimental apparatus corrrelation with reference values of thermal diffusivity of Armco iron and a glass-ceramic* were obtained to better than ± 5% over a 25 to 1200°C temperature range.

C. Results

The distribution and relative size of the ZrO_2 particles in both the AM and BM materials with 16 v/o ZrO_2 can be seen in the SEM micrographs in Figures 1(A-B). The backscattered electron detector used to obtain these micrographs samples the surface layer to a depth of 2-3 microns, but sacrifices resolution. It is obvious from these photos that the zirconia particles in the AM material are numerous and mostly submicron with only a few particles in the 2-3 micron range. In comparison, the number of zirconia particles in the BM material are fewer than in the AM material, but many of the agglomerates are in the 3-5 micron range.

In Figure 2 the thermal diffusivity values determined during a single heating-cooling cycle to 1400°C (above the ZrO_2 tetragonal to monoclinic phase transition) for both BM and AM materials are compared with values similarly determined for pure Al_2O_3. The alumina was hot-pressed from the same high-purity powder as used for the composites and should show similar impurity effects, if any.

To study the reproducibility of the hysteresis loop observed in the thermal diffusivity values for the BM material, five successive heating-cooling cycles to 1400°C were run and the data are shown in

---

* Code C9606, Corning Glass Works, Corning, NY

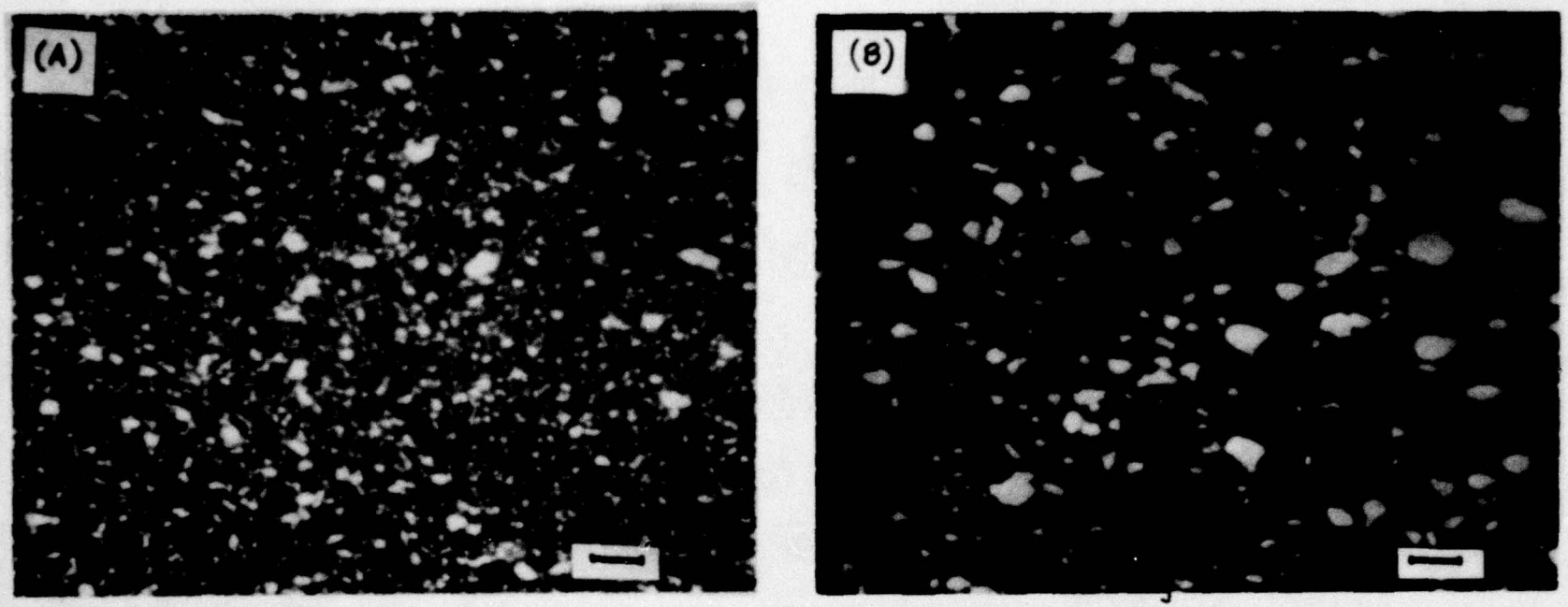


Figure.1.--Back-scatter electron SEM image (15 kV) of flat-polished Al_2O_3/ 16 v/o ZrO_2 composites: (A) attritor-milled and (B) ball-milled (bar = 3 μm).

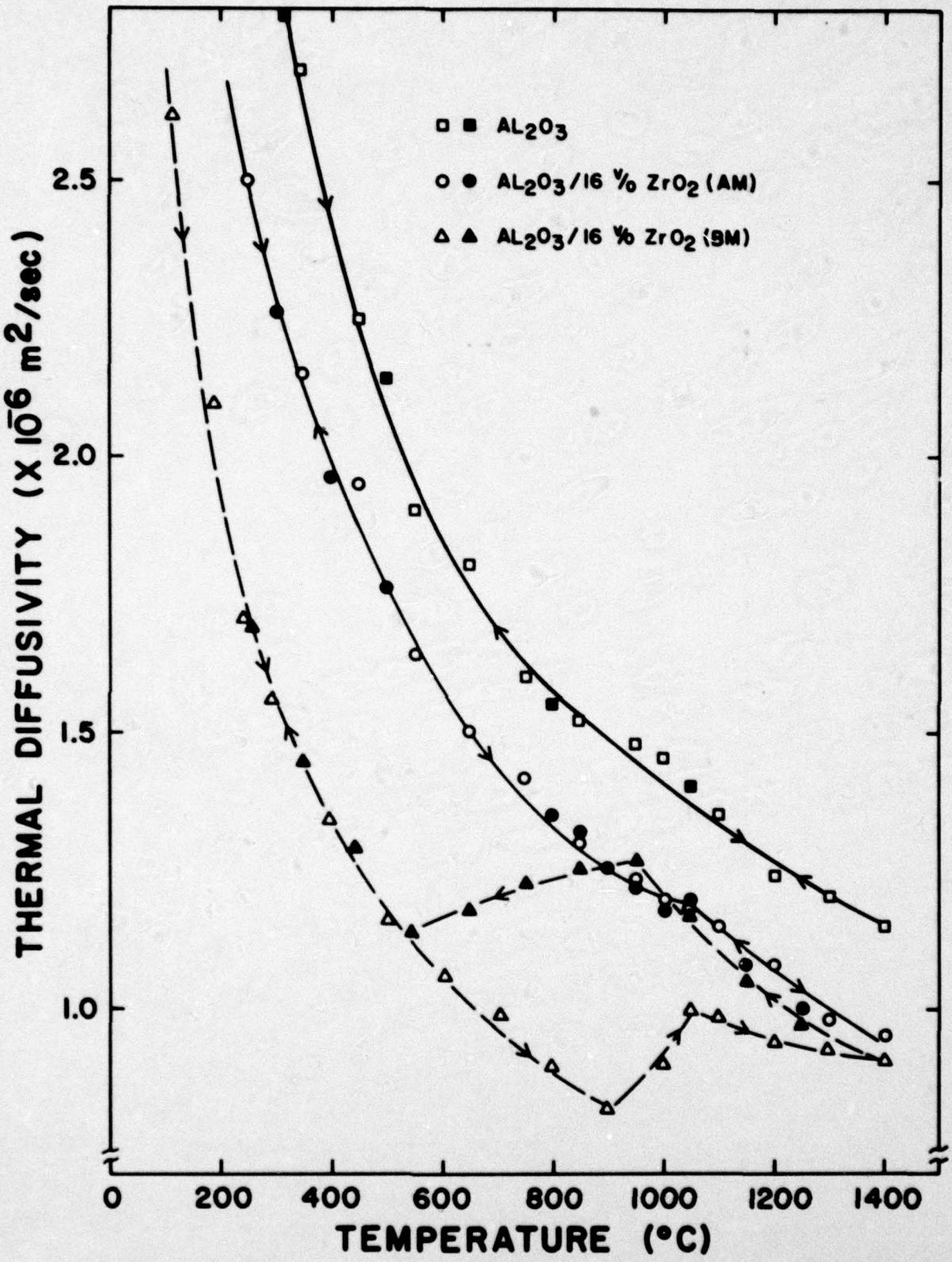


Figure 2.--Comparison of thermal cycling effect on the thermal diffusivity of attritor-milled (AM) and ball-milled (BM) Al_2O_3/ 16 v/o ZrO_2 as well as nominally pure Al_2O_3. Open (closed) symbols indicate data taken on heating (cooling).

Figure 3. Likewise, thermal diffusivity data were taken for the AM material during five successive cycles to 1400°C and also are shown in this Figure; the lines were transcribed from the data points shown for the first heating-cooling cycle in Figure 2. For clarity only the data points for cycles 2 and 5 are shown in Figure 3. Also for clarity, the vertical scales for the AM and BM data are shown offset; the thermal diffusivity values in the 900-1400°C range actually overlap for both materials.

Thermal diffusivity values at 200°C for both BM and AM materials as a function of ZrO_2 content are shown in Figure 4. In order to compare the thermal diffusivity values at a common temperature (200°C) for all compositions some of the data points were extrapolated from measurements at 250°C. In addition, α of an "ideal" alumina-zirconia composite was derived from the relation $\alpha = \lambda / \rho C$ where the effective thermal conductivity λ was estimated from the Maxwell-Eucken[21] relation.* The effective volume heat capacity ρC, in turn, was estimated by rule of mixtures using literature values of heat capacity[22] and density for alumina and zirconia.

In Figure 4 a single data point for an Al_2O_3 / 10 v/o ZrO_2 composite, where the ZrO_2 was stabilized in the cubic phase with 12 m/o Y_2O_3 prior to mixing with the alumina, also is shown. For this particular material, thermal diffusivity data taken during a single heating and cooling cycle to 1400°C were reproducible and agreed almost identically

---

* $\lambda = \lambda_c \left\{ \frac{2\lambda_c + \lambda_d - 2V_d (\lambda_c - \lambda_d)}{2\lambda_c + \lambda_d + V_d (\lambda_c - \lambda_d)} \right\}$ where $\lambda_c = 15.2$ and $\lambda_d = 1.5$ watts /mK, thermal conductivities of alumina and zirconia at 200°C, respectively, and $\rho C = \rho_c C_c V_c + \rho_d C_d V_d$ with $\rho_c C_c = 4.09$ and $\rho_d C_d = 2.96$ MJ/m^{3}K, volume heat capacities of alumina and zirconia at 200°C, respectively. V_c and V_d are volume fractions of the continuous or dispersed phases, respectively.

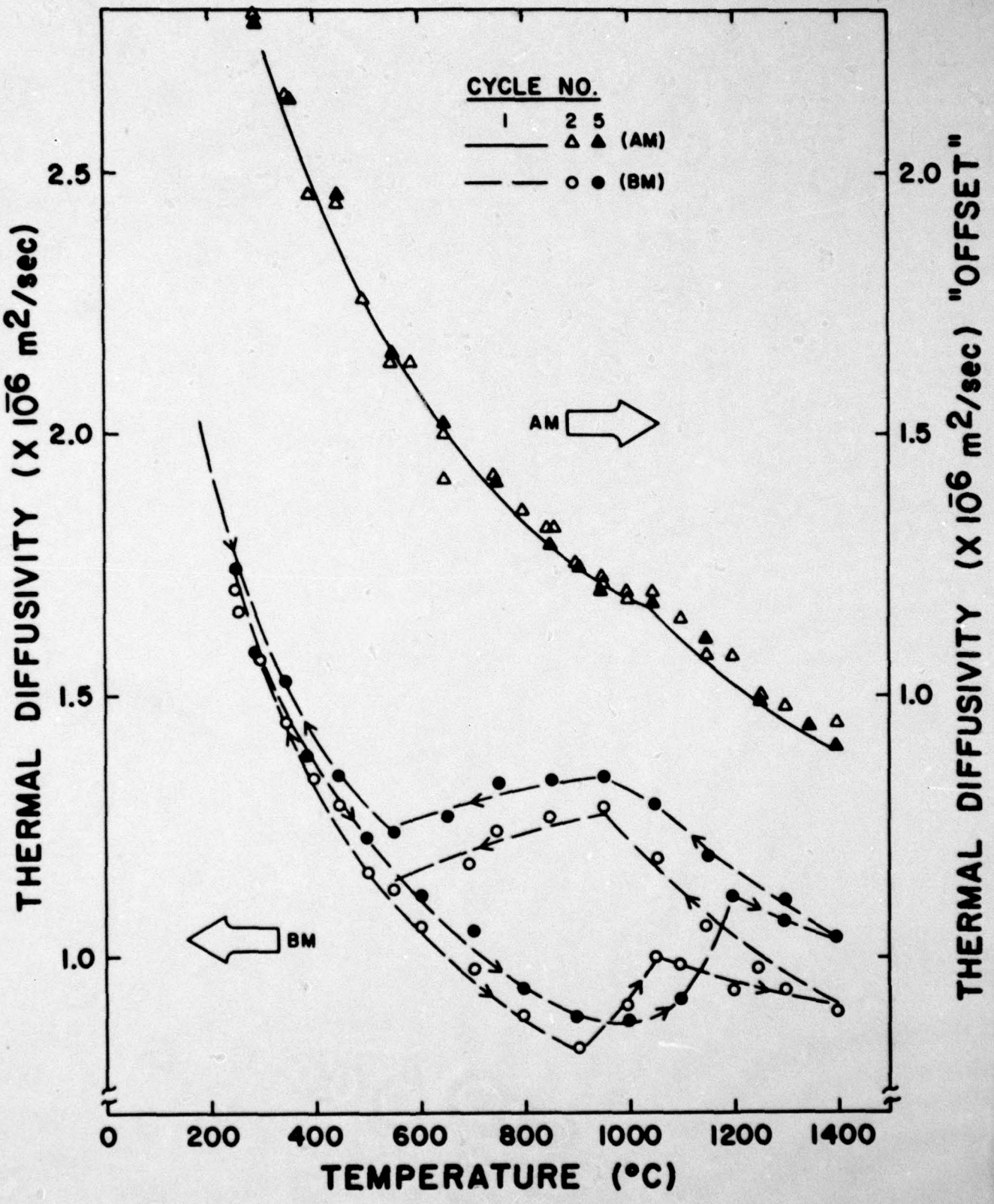


Figure 3.--Effect of five successive thermal cycles to 1400°C on the thermal diffusivity of attritor-milled (AM) and ball-milled (BM) Al_2O_3/ 16 v/o ZrO_2 composites.

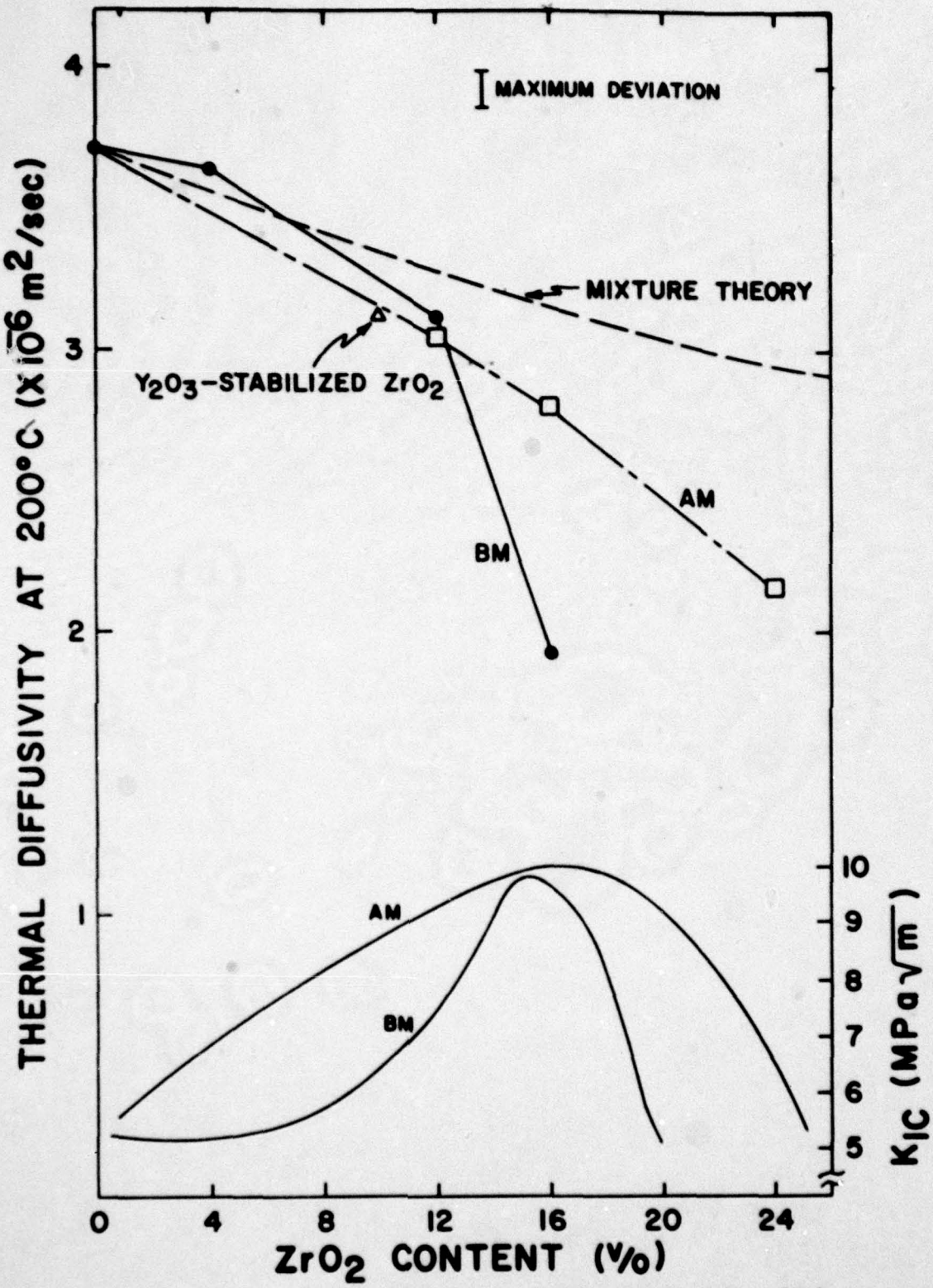


Figure 4.--Top: Thermal diffusivity at 200°C of ball-milled (BM) and attritor-milled (AM) Al_2O_3/ZrO_2 composites as a function of ZrO_2 concentration.

Bottom: Qualitative fracture toughness (K_{1c}) curves for AM and BM composites.

REV. 8/31/79 8-000-007-A

with similar data taken for AM material with 12 v/o ZrO_2. The thermal diffusivity values for both materials (not shown) were only about 3-4% higher than values for the 16 v/o ZrO_2 AM material in the 200-1400°C temperature range and indicated no hysteresis.

III. DISCUSSION

Using Lange's criterion[23] the critical zirconia particle size necessary for inducing microcracks in an alumina matrix was estimated by Claussen[2] to be $\sim$ 3 μm. As observed in Figures 1(A-B) most of the zirconia particles in the AM material are sub-critical, whereas many of the zirconia particles in the BM material exceed 3 μm. Upon cooling from fabrication temperature a minor amount of microcracking, if any, would be expected in the AM material, while a high density of microcracks would be expected in the BM material.

The effect of pre-existing microcracks in the BM material on the thermal diffusivity is readily observed in Figure 2. At temperatures above 200°C and below the zirconia phase transformation ($\sim$ 900°C for the 16 v/o ZrO_2 composition*) the thermal diffusivity values are about 55% of the values of nominally pure and dense alumina, and about 67% of the values of the "non-microcracked" AM material of the same zirconia content. Previous results,[9] where the temperature never exceeded 800°C, also indicated an average reduction about 55% of the α for alumina for the same composition BM material.

The hysteresis loop depicted in Figure 2 for the BM material is reproduced in Figure 5 where it is compared to a similar hysteresis

---

* In reference 7, measurements of linear expansion indicate that the transformation temperature depends on the zirconia content as well as whether the temperature is attained during the heating or cooling part of the cycle.

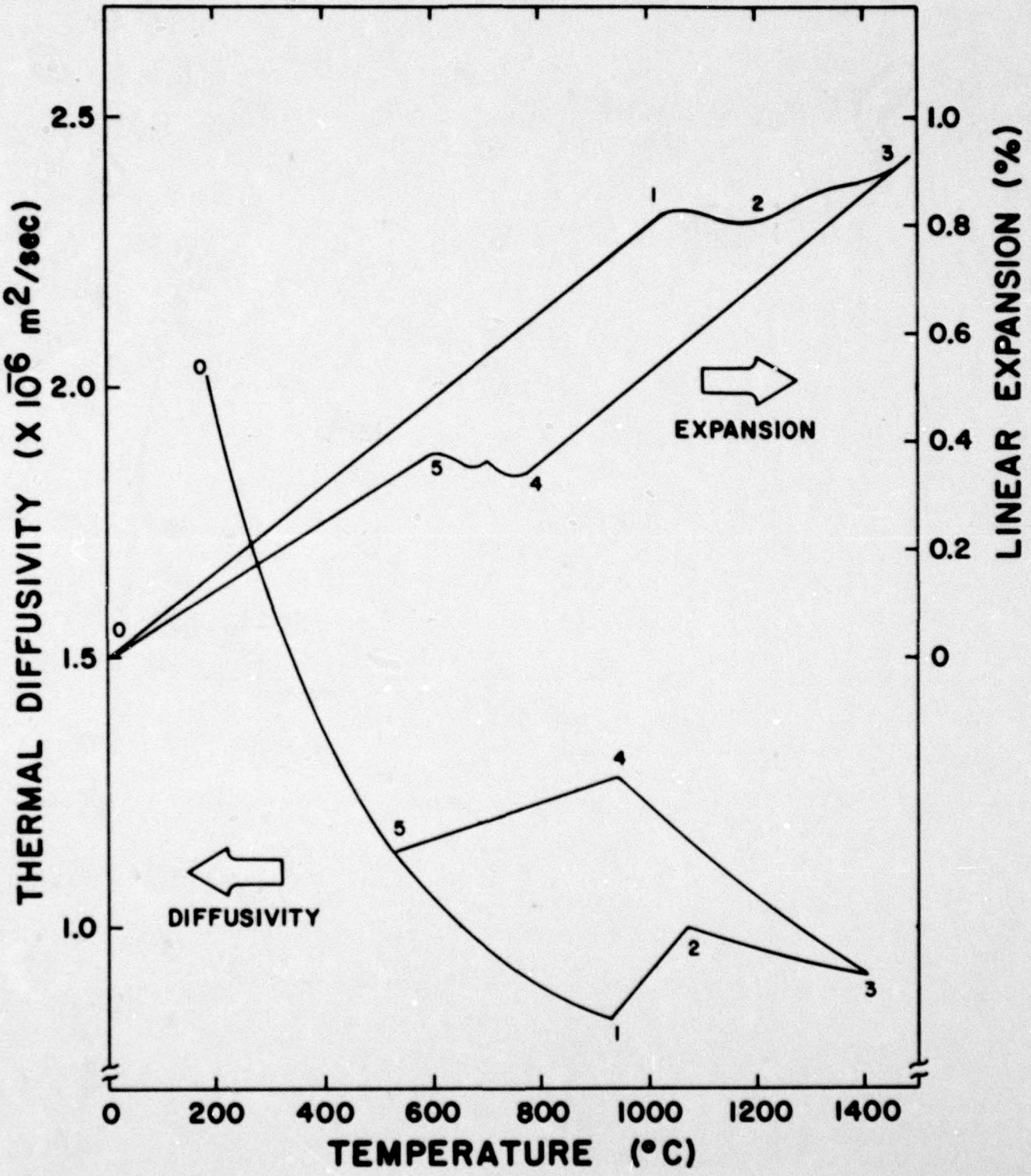


Figure 5.--Thermal diffusivity (bottom loop) and linear expansion (top loop) of ball-milled Al_2O_3/ 16 v/o ZrO_2 composite during a single thermal cycle to 1400°C.

loop in the thermal expansion reproduced from reference 7. Between points 0-1 the thermal diffusivity follows its usual $\sim 1/T$ dependence while the thermal expansion is linear with a coefficient that matches that of alumina. A rather abrupt change in both the expansion and diffusivity curves occurs between points 1-2 ($\sim$ 900 to 1150°C), the temperature range over which the zirconia transforms from monoclinic to tetragonal and the microcracks close. Between points 2-3 ($\sim$ 1150 to 1400°C) the diffusivity and expansion curves gradually approach their normal temperature dependence. Over this temperature range the microcracks may partially heal and actual values of thermal diffusivity or expansion would be expected to depend on the heating rates. On cooling from 1400°C (range 3-4) the thermal diffusivity resumes its normal 1/T dependence, the values now being higher and described approximately by the mixture of alumina and zirconia phases. Over approximately the same temperature range the thermal expansion is again linear with a coefficient matching that of alumina.

On further cooling between points 4-5 (750 to 600°C for expansion and 950 to 550°C for diffusivity) the pressure of the surrounding alumina matrix prevents the completion of the zirconia phase transformation until lower temperatures are reached. The zirconia particles then expand reinducing microcrack formation. This process continues until all the zirconia has been transformed and the diffusivity and expansion values approximately match those of the heating curve on further cooling. Exact temperature correspondence between expansion and diffusivity hysteresis loops probably depends on details of the heating/cooling rates and slight differences in the ZrO_2 particle size and distribution between individual samples.

The hysteresis loop was itself approximately reproduced five successive times in the BM material as depicted in Figure 3. The microcrack structure appears to retain its original morphology on repeated thermal cycling to 1400°C. In contrast, the microcrack morphology changes considerably during temperature cycling of several single-phase materials with anisotropic thermal expansion and over a much lower temperature range, i.e., 25-800°C (see Section I). Slight microcrack healing over the 1100-1400°C range could account for a general upward shift in the diffusivity hysteresis loop.* Annealing of residual stresses also may cause slight shifts in the zirconia transformation temperatures and the degree of microcracking. Nevertheless, the preexisting microcracks apparently close and then reform reproducibly on repeated temperature cycling. As previously noted, as long as the temperature never exceeds the zirconia transformation at Point 1, the thermal diffusivity values would be expected to be reproducible and exhibit no hysteresis with repeated thermal cycling in the BM-type material.

As depicted in Figures 2 and 3, the thermal diffusivity of the AM material was reproducible and no significant hysteresis was observed during temperature cycling for five cycles up to 1400°C. Furthermore, the thermal diffusivity values were about 85% of the values for nominally pure alumina. These values also are only about 10% lower than values predicted for a non-microcracked alumina-zirconia composite by the Maxwell-Eucken Rule of Mixtures Finally, there is overlap between the thermal diffusivity values over the 950-1400°C range during the

---

* A sixth temperature cycle to 600°C was attempted to try to enhance a microcrack healing effect. Instead, serious sample bloating occurred and the thermal diffusivity decreased ~ 20%.

cooling part of the cycle for both the non-microcracked AM material and the microcracked but healed BM material of the same ZrO_2 content.

There is a small change in slope in the 950-1000°C range of the AM diffusivity curves. This effect was hardly noticeable except that it was reproducible over all five cycles; it is probably due to the few larger zirconia agglomerates that exceed the critical size for phase transformation which remain after attritor-milling. In fact, X-ray analysis shows some monoclinic zirconia fraction with increasing zirconia content. In addition, slight hysteresis was observed in the thermal diffusivity values for a 24 v/o ZrO_2 AM material, where more larger size agglomerates occurred.

The maximum relative effect of the microcracking should be observed in the thermal diffusivity at lower temperatures where the phonon thermal conductivity is high. As observed in Figure 4, the thermal diffusivity values at 200°C of pure alumina, a series of AM materials with increasing ZrO_2 content, and a sample of alumina with Y_2O_3-stabilized ZrO_2 decreases approximately linearly with increasing ZrO_2 content. The thermal diffusivity values of BM materials decrease at 200°C with added ZrO_2 content up to 12 v/o ZrO_2 but a large change in slope occurs between 12 and 16 v/o ZrO_2. For all concentrations of ZrO_2, the thermal diffusivity values of both AM and BM materials fall below the mixture theory curve and the deviation increases with increasing ZrO_2 content. Qualitative fracture toughness (K_{1c}) curves that show dependence on ZrO_2 concentration have been reproduced from work by Claussen,[7,16] and are shown in Figure 4. The steeply increasing slope of the fracture toughness in the 12-16 v/o range for a BM material correlates well with the more abrupt change in the thermal diffusivity

in the same composition range and for the same ZrO_2 particle size. Obviously, the onset of microcrack generation occurs primarily over this range of ZrO_2 content for the BM material as described in more detail in Reference 7. Since there are some ZrO_2 particles that exceed critical size in the AM material, some microcrack generation may account for the slight decrease in slope with increasing ZrO_2 content observed for the AM material.

It also was observed that below ~ 200°C the measured thermal diffusivity values for the AM material were much lower than predicted by simple composite mixture theory; i.e., where the effective diffusivity (conductivity) depends only on the component diffusivity values and volume fraction of dispersed phase. For instance, the thermal diffusivity of the non-microcracked Al_2O_3 / 16 v/o ZrO_2 AM material was 57% of the value for pure Al_2O_3 at 50°C compared to 85% above 200°C.

At this time it is thought that a significant amount of phonon scattering occurs at temperatures below ~ 200°C in the AM material. Examination of a typical AM material microstructure (as in Figure 1) indicates a mean spacing between the small ZrO_2 particles of about one-half micron. Although this is still much larger than the estimated phonon mean free path at this temperature (~ 10^{-2} micron), it is plausible that strain fields surrounding the particles increase the phonon scattering effectiveness at lower temperatures. Analysis of low temperature (RT to 200°C) thermal diffusivity data for composites with dispersed phases of sub-micron particles will be the subject of a subsequent paper.

IV. SUMMARY

In alumina with a dispersed phase of unstabilized zironia, microcracking in the alumina matrix is induced during cool-down from fabrication temperatures by the tetragonal to monoclinic phase transformation

with attendant volume expansion of the zirconia particles if the zirconia particles exceed a critical size of approximately three microns. In this manner extensive microcracking was induced in hot-pressed alumina-zirconia composites where the raw powders were ball-milled prior to pressing. The thermal diffusivity (conductivity) values of a composite with 16 v/o ZrO_2 were reduced to about 67% of the values for a non-microcracked alumina-zirconia composite of the same composition as long as the temperature remained below the zirconia phase transformation temperature. For temperatures that exceed this point, hysteresis occurs in the thermal diffusivity values on heating and cooling wi h one-to-one correspondence with hysteresis in thermal expansion. Reproducibility of the thermal diffusivity values below the zirconia phase transformation or of the hysteresis loops themselves for successive heating-cooling cycles to 1400°C indicate that the microcrack morphology is retained through several heating/cooling cycles. At temperatures near $\sim$ 1400°C, where the microcracks close and partially heal, the thermal diffusivity values match those of non-microcracked material of the same composition.

It is possible to prepare non-microcracked alumina-zirconia composites where the dispersed zirconia particles are sub-critical in size and remain tetragonal throughout successive temperature cycling from RT to 1400°C. From 200 to 1400°C the measured thermal diffusivity values of these materials are only slightly lower than those expected by simple mixture theory. Below $\sim$ 200°C the smaller sized ZrO_2 particles begin to scatter phonons effectively and the thermal diffusivity values are again lowered below values predicted by mixture theories that only consider volume fractions of the dispersed and matrix phases.

The thermal transport properties presented herein are expected to be combined with mechanical properties in order to assess overall thermal shock or fatigue resistance in either type of alumina-zirconia composite. The combination of high toughness and good thermal diffusivity (conductivity) should produce excellent thermal shock resistance in AM-type material.

Acknowledgement

This study was carried out as part of a larger research program on the thermal conductivity and diffusivity of engineering ceramics supported by the Office of Naval Research nder Agreement No. N000014-78-C-0726.

REFERENCES

1. F. F. Lange, "Interaction of a Crack Front with a Second-Phase Dispersion," Philos. Mag., 22 [179], 983-92 (1970).

2. N. Claussen, "Fracture Toughness of Al_2O_3 with an Unstabilized ZrO_2 Dispersed Phase," J. Am. Ceram. Soc., 59 [1-2], 49-51 (1976).

3. D. J. Green, P. S. Nicholson, and J. D. Embury, "Fracture Toughness of a Partially Stabilized ZrO_2 in the System $CaO-ZrO_2$," J. Am. Ceram. Soc., 56 [12], 619-23 (1973).

4. F. E. Buresch, pp. 383-98 and 475-90 in Science of Ceramics 7 (Proceedings of the Seventh International Conference, September 1973.) Societe´ Francaise de Ceramique, Paris, 1973.

5. R. F. Pabst, J. Steeb, and N. Claussen; pp. 821-833 in Fracture Mechanics of Ceramics, Vol. 4. Edited by R. C. Bradt, D. P. H. Hasselman, and F. F. Lange, Plenum Press, New York, 1978.

6. R. C. Garvie and P. S. Nicholson, "Structure and Thermomechanical Properties of Partially Stabilized Zirconia in the $CaO-ZrO_2$ System," J. Am. Ceram. Soc., 55 [2], 152-57 (1972).

7. N. Claussen, J. Steeb, and R. Pabst, "Effect of Induced Microcracking on the Fracture Toughness of Ceramics," Am. Ceram. Soc. Bull., 56 [6], 559-562 (1977).

8. N. Claussen, "Stress-Induced Transformation of Tetragonal ZrO_2 Particles in Ceramic Matrices," J. Am. Ceram. Soc., 61 [1-2], 85-86 (1978).

9. D. Greve, N. Claussen, D. P. H. Hasselman, and G. E. Youngblood, "Thermal Diffusivity/Conductivity of Alumina with a Zirconia Dispersed Phase," J. Am. Ceram. Soc., 56 [5], 514-515 (1977).

10. H. J. Siebeneck, D. P. H. Hasselman, J. J. Cleveland and R.C. Bradt, "Effect of Microcracking on the Thermal Diffusivity of Fe_2TiO_5," J. Am. Ceram. Soc., 59 [5-6], 241-44 (1976).

11. H. J. Siebeneck, J. J. Cleveland, D. P. H. Hasselman and R. C. Bradt, "Effects of Grain Size and Microcracking on the Thermal Diffusivity of $MgTi_2O_5$," J. Am. Ceram. Soc., 60 [7-8], 336-338 (1977).

12. W. R. Manning, G. E. Youngblood, and D. P. H. Hasselman, "Effect of Microcracking on the Thermal Diffusivity of Polycrystalline Aluminum Niobate," J. Am. Ceram. Soc., 60 [9-10], 469-470 (1977).

13. H. J. Siebeneck, J. J. Cleveland, D. P. H. Hasselman, and R. C. Bradt; pp. 753-762 in Ceramic Microstructures '76, (Proceedings of Sixth International Materials Symposium held at University of California, Berkeley). Edited by Richard M. Fulrath and Joseph A. Pask, Westview Press, Boulder, Colorado, 1977.

14. E. A. Bush and F. A. Hummel, "High Temperature Mechanical Properties of Ceramic Materials: I, Magnesium Dititanate," J. Am. Ceram. Soc., 41 [6], 189-95 (1958).

15. E. A. Bush and F. A. Hummel, "High Temperature Mechanical Properties of Ceramic Materials: II, Beta-Eucryptite," Ibid, 42 [8], 388-91 (1959).

16. Nils Claussen, private communication.

17. W. J. Parker, R. J. Jenkins, C. P. Butler, and G. L. Abbott, "Flash Method of Determinfng Thermal Diffusivity, Heat Capacity, and Thermal Conductivity," J. Appl. Phys., 32 [9], 1679-81 (1961).

18. K. O. Maglic and B. S. Marsicanin, "Factors Affecting the Accuracy of Transient Response of Intrinsic Thermocouples in Thermal Diffusivity Measurement," High Temperatures-High Pressures, 5, 105-110 (1973).

19. T. Y. R. Lee and R. E. Taylor, "Thermal Diffusivity of Dispersed Materials," Journal of Heat Transfer, 100 (Nov.), 720-724 (1978).

20. R. C. Heckman, "Finite Pulse-time and Heat-Loss Effects in Pulse Thermal Diffusivity Measurements," Journal of Applied Physics, 44 [4], 1455-1460 (1973).

21. A. E. Powers, "Conductivity in Aggregates," Knolls Atomic Power Report KAPL 2145, General Electric Co., March 6, 1961.

22. Y. S. Touloukian and E. H. Buyco, Specific Heat : Nonmetallic Solids (Thermophysical Properties of Matter, Vol. 5). IFI/Plenum, New York, NY, 1970.

23. F. F. Lange; pp. 599-609 in Fracture Mechanics of Ceramics, Vol. 2. Edited by R. C. Bradt, D. P. H. Hasselman, and F. F. Lange, Plenum Press, New York, 1974.

ARTICLE IV-D

EFFECT OF THERMAL EXPANSION MISMATCH ON THE THERMAL DIFFUSIVITY OF GLASS-NI COMPOSITES

by

G. E. Youngblood [*]

Larry D. Bentsen [*]

R. R. Powell, Jr. [†]

D. P. H. Hasselman [+]

[*]Montana Energy and MHD Research and Development Institute, Butte, Montana 59701

[†]Department of Material Science and Engineering University of California, Berkeley, CA 94720

[+]Department of Materials Engineering, Virginia Polytechnic Institute and State University Blacksburg, VA 24061

ABSTRACT

The effect of interfacial de-cohesion, due to thermal expansion mismatch, on the thermal diffusivity of a hot-pressed glass matrix with a dispersed phase of nickel was investigated by the laser-flash technique over the temperature range of 25 to 600°C. The interfacial gap formed on cooling acts as a barrier to heat flow and lowers the thermal diffusivity to values below those predicted from composite theory. However, the temperature dependence of the thermal diffusivity is strongly positive. Preoxidation of the Ni spheres promotes interfacial bonding to yield values of thermal diffusivity higher than those for non-oxidized spheres and a thermal diffusivity which is relatively temperature independent. At temperatures near the fabrication temperature where effects due to thermal expansion mismatch are negligible, the concept of an effective thermal diffusivity for composites is demonstrated.

EFFECT OF THERMAL EXPANSION MISMATCH ON THE THERMAL DIFFUSIVITY OF GLASS-NI COMPOSITES

G. E. Youngblood, Larry D. Bentsen, R. R. Powell, Jr., and D. P. H. Hasselman

I. INTRODUCTION

Numerous composite materials have been developed to meet special requirements for many engineering applications. Such composites frequently exhibit favorable properties not found in the individual components. The science of "composite theory" for the calculation of the properties of composites from the properties of the components represents a very active field.

Many expressions for the calculation of the thermal conductivity of composites for a wide variety of phase composites and distributions are available from the literature.[1,2,3] These theories, however, generally assume that perfect bonding exists between the components; the interfacial boundaries are assumed to offer no resistance to the transport of heat through the composite. In practice, however, many composites will exhibit less than perfect bonding between the components as the direct result of poor wettability or the absence of good mechanical adhesion. This problem is expected to be especially severe for composites with a large mismatch in the coefficients of thermal expansion of the components. Changes in temperature of such composites can lead to the formation of "internal" stress of high magnitude. Such stresses can lead to "microcracking" in the composites, normally by interfacial separation, depending on the direction of the mismatch. Such microcracking also can

occur in single phase polycrystalline materials which exhibit a high degree of thermal expansion anisotropy of the individual grains. In these latter materials microcracking has been shown to lead to major decreases in the thermal diffusivity [5,6] in accordance with analytical results for the effect of cracks on thermal conductivity.[7] Similar effects would be expected for composites with a large mismatch in thermal expansion between components as was observed by Kingery[7] in magnesia-spinel and alumina-mullite composites and recently by Buykx[9] in UO_2-U_4O_9.

The purpose of the present study was to investigate the effect of the mismatch in thermal expansion on the thermal diffusivity of a bonded and non-bonded composite consisting of a low thermal expansion, low thermal conductivity matrix containing a high thermal expansion, high thermal conductivity dispersed phase. On cooling of such a composite, de-cohesion between the phases results in the formation of an interfacial gap which, in analogy to microcracks, is expected to have a large effect on the transport of heat through the composite. The choice of low thermal conductivity matrix and high thermal conductivity dispersed phase increases the relative magnitude of the effect of de-cohesion or cohesion between the phases on the overall thermal transport.

II. EXPERIMENTAL

A. Materials, Preparation and Characterization

D-glass of the same composition (16% Na_2O, 14% B_2O_3 and 70% SiO_2) as used in previous investigations[10,11,12] was chosen as a suitable matrix phase. The dispersed phase consisted of near spherical particles of Ni with a diameter $45 < D < 53$ μm. Composites contained nickel in the "raw" (non-oxidized) form or nickel particles with an oxide coating produced by oxidation in air to a weight gain of one percent. As found in an earlier

study,[12] the presence of an oxide coating promoted the adherence of the glass and nickel phases. The composites were prepared by vacuum hot-pressing mixtures of the Ni and glass in powder form in graphite dies at a pressure of 14 MPa at 700°C for 10 min. The initial heating rate was ∿ 9°C/min. After hot-pressing the specimens were permitted to cool naturally within the hot-pressing chamber maintained at vacuum.

The densities of the composites were determined for the individual thermal diffusivity specimens using the Archimedes method with H_2O as the fluid medium. The experimental and theoretical densities are compared in Table I. The sample nominally containing 45 vol. % Ni (raw) exhibits a density greater than theoretical. This may be attributable to a Ni concentration somewhat higher than 45% or to uncertainties in the density of the glass. For the samples with oxidized Ni a density somewhat less than theoretical is attributable to the existence of a pore phase created during cooling from the hot-pressing temperature as the direct result of the expansion mismatch.

Figure 1 shows optical micrographs of the glass with 15, 30 and 45% Ni. Direct Ni particle-to-particle contact is evident especially at 45% Ni. Although most particles are very close to being spherical, some are tear-shaped or ellipsoidal in shape. As indicated by the theoretical results of Bruggeman[13] and Niesel,[14] a deviation from perfectly spherical shape should have no effect on the thermal conductivity and thermal diffusivity as long as the dispersed particles are oriented randomly.

Figures 2 (A-B) and 3 (A-B) show scanning electron fractographs at two magnifications for the glass containing raw and oxidized Ni dispersions, respectively. It is evident in Figure 2A that the raw Ni particles were easily pulled from the glass matrix during fracture which is indicative

Table I.--Composition and density of glass-nickel composites.

Sample	ρ Bulk*	ρ Theory**	% Theoretical
D-glass	2.476	2.48	100
+ 15 v/o Ni (raw)	3.44	3.44	100
+ 30 v/o Ni (raw)	4.29	4.41	97.3
+ 45 v/o Ni (raw)	5.45	5.37	101.5
+ 15 v/o Ni (ox.)	3.24	3.43	94.5
+ 30 v/o Ni (ox.)	4.24	4.38	96.8
+ 45 v/o Ni (ox.)	5.21	5.32	97.9

* Density determined in H_2O

** Estimate made using 8.9 and 8.8 gm/cc for raw and oxidized Ni, respectively.

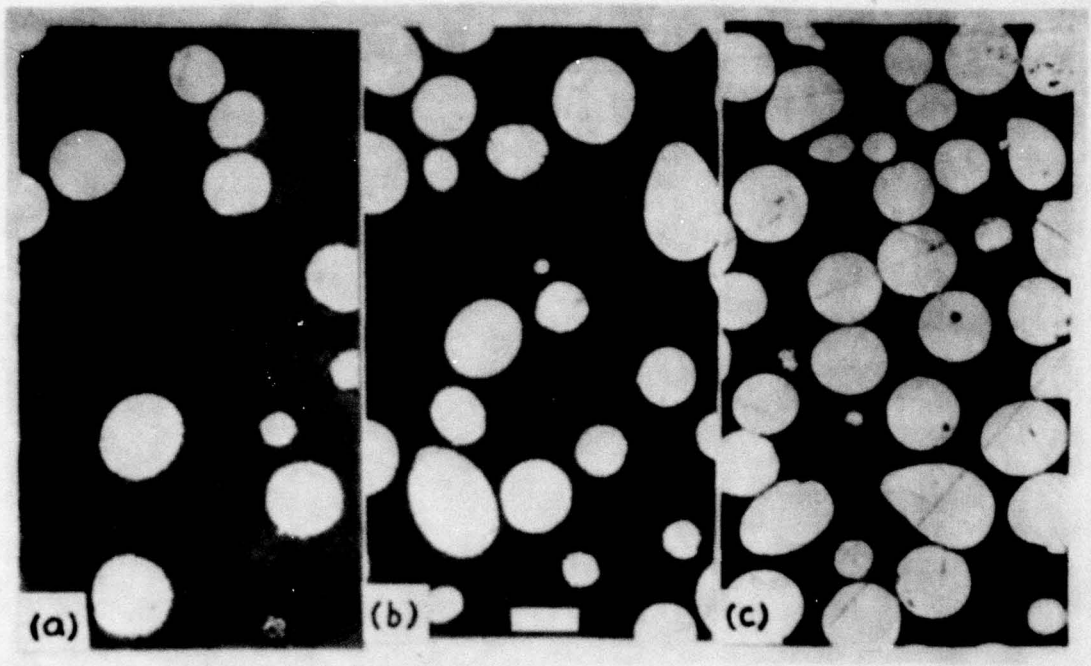


Figure 1.--Micrographs of polished surfaces of glass-nickel composites: (A) 15, (B) 30, and (C) 45 vol. % Ni. The bar = 50 microns.

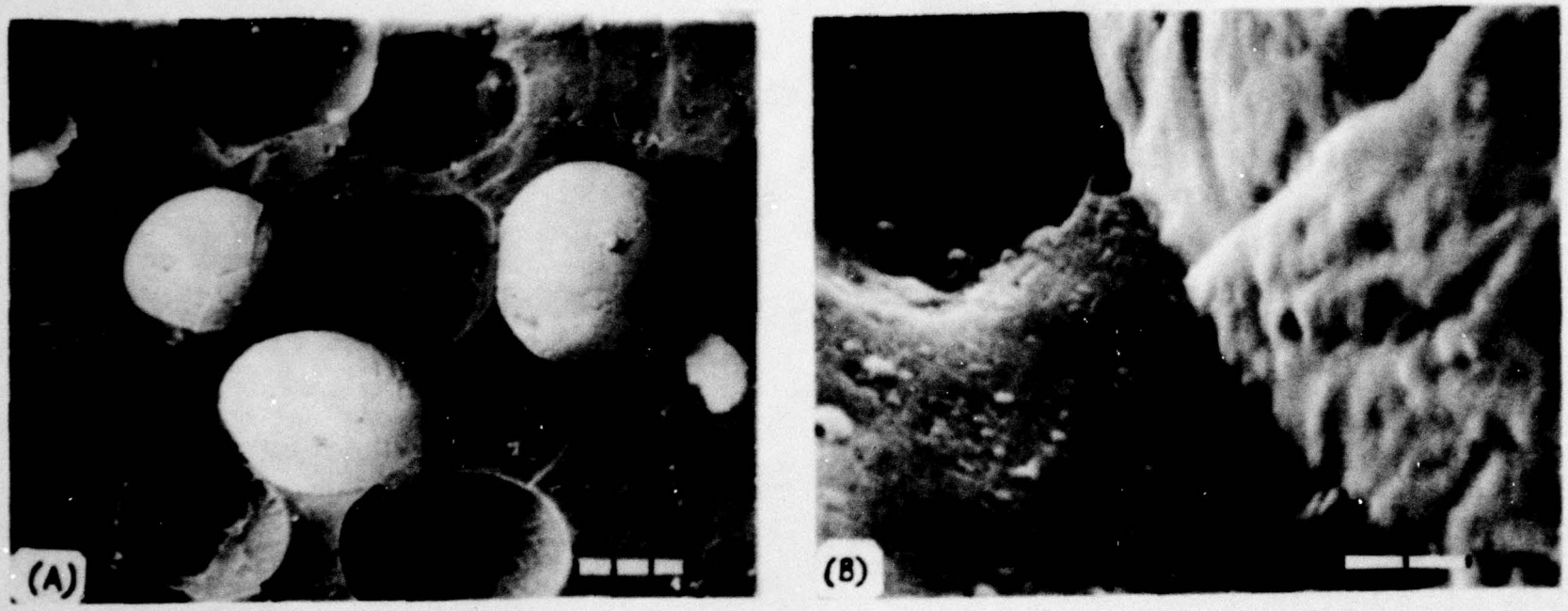


Figure 2.--Scanning electron micrographs of freshly fractured surface of 45 vol. % raw Ni/glass composite: (A) non-bonded nickel spheres and cavities (bar segments = 10 μm) and (B) detailed view of interfacial gap at Ni/glass interface (bar segments = 1 μm).

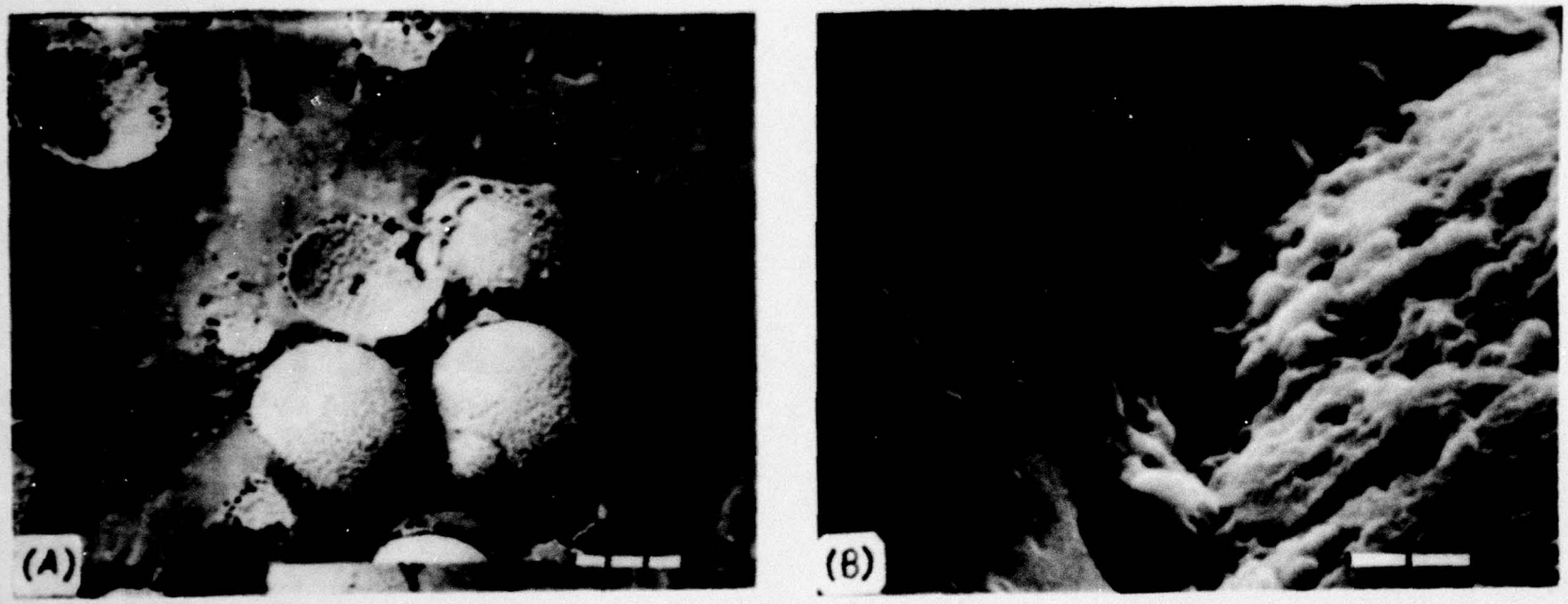


Figure 3.--Scanning electron micrographs of freshly fractured surface of 45 vol. % oxidized Ni/glass composite: (A) bonded nickel spheres or cavities (bar segments = 10μm) and (B) detailed view of glass/nickel interface and induced porosity (bar segments = 1 μm).

of a lack of adhesion. The detailed view of the glass-Ni interface (Fig. 2B) indicates a submicron gap with no evidence of induced porosity. For the oxidized Ni-glass composites the fractographs (Figs. 3A-B) indicate that the Ni and glass show good adherence through the NiO coating. In these composites the thermal expansion mismatch appears to be accommodated by visco-elastic deformation of the glass, which resulted in the formation of a highly porous fibrous glass phase in the immediate vicinity of the Ni-glass interface as depicted in Figure 3B. Such a fibrous glass phase most likely occurred at temperatures immediately below the hot-pressing temperatures where such visco-elastic deformation is expected to occur.

B. Measurement of Thermal Diffusivity

The thermal diffusivity was measured over the temperature range 25°C to 600°C by the laser-flash technique.[15] A single flash (∿ 1 msec) from a glass-Nd laser[+] irradiates the front face of the disc-shaped specimen (1/2-inch diameter by 2.0 mm thick). An intrinsic thermocouple[16] (low temperature) or an infrared detector[*] (high temperature) was used to monitor the temperature transient at the back face. The typical steady-state temperature rise of the specimen was kept below 3°C.

For low temperature measurements (25°C-400°C) a specimen was held by three alignment pins inside a wire-wound temperature controlled split-tube furnace with air atmosphere. The specimen front face was coated with carbon[**] to ensure uniform absorptivity. A 1/4-inch diameter Ag-print

---

[+] Korad K-1, 70 Joules maximum per flash, Santa Monica, CA
[*] Barnes Engineering IT-7B (InSb) Stamford, CT
[**] Miracle DGF spray, Miracle Power Products Co., Cleveland, OH

spot was painted onto the specimen backface to average local heating effects and to provide electrical continuity for a chromel-alumel intrinsic thermocouple. The thermocouple was spring-loaded to press up firmly against the backface to monitor the chamber temperature as well as the transient temperature of the sample.

For higher temperature measurements (200°C-600°C), where the infrared detector was used for monitoring specimen temperature, a specimen with each face coated with carbon was held in a split-tube graphite holder in a carbon resistance furnace[++] with nitrogen atmosphere.

The transient temperature response from either the thermocouple or infrared detector was fed into an oscilloscope[*] equipped with signal storage. The thermal diffusivity (α) of the composite sample was calculated using the expression

$$\alpha = 0.1388\ L^2/t_{1/2} \qquad (1)$$

where L is the specimen thickness and $t_{1/2}$ is the time required for the temperature of the back surface of the specimen to reach one-half of its final value. The measured values of the thermal diffusivity were corrected for heat losses in a manner described by Heckman.[17] These corrections amounted to only a few percent at low temperature and increased to about five percent by 1000°C. No corrections for finite pulse width were necessary. The equipment was calibrated against Armco iron which resulted in agreement to within three percent with standard values[18] for the infrared detector and within 11% for the thermocouple measurements. This latter discrepancy could be due to less than perfect thermal contact between the sample and/or non-uniformity in the laser pulse.

[++] Astro Model 1000A, Santa Barbara, CA
[*] Tektronix 5111 with plug-ins, Beaverton, OR

In order to establish whether the value of thermal diffusivity obtained by the laser-flash method represents the effective thermal diffusivity, the ratios of thermal properties and micro-structural parameters of the present composites were compared with the limits of non-homogeneity extablished by Lee and Taylor.[19] Briefly, Lee and Taylor showed that the concept of an effective or "homogeneous" thermal diffusivity of a composite is valid for ratios of 0.48-1137 for α_d/α_m; 0.02-1.16 for $(\rho_d C_d V_d)/(\rho_m C_m V_m)$; 3.8-2857 for L/D; 0.23-0.88 for nD/L, and 0.012-0.34 for V_d, where α is the thermal diffusivity, ρ is the density, C is the specific heat, V is the volume fraction, L is the sample thickness, D is the particle diameter, $n = [V_d L^3/1.33\pi(D/2)^3]^{1/3}$ is the total number of particles in the sample thickness direction, and the subscripts d and m refer to dispersed and continuous (matrix) phases, respectively. Table II lists the room temperature thermal properties of the Ni and glass, respectively. *Table III lists the values of the above ratios for the composites studied.*

It is noted that all of the various ratios fall within the experimental bounds established by Lee and Taylor except nD/L for the 45 vol.% Ni sample. Thus, for all practical purposes the measured values of thermal diffusivity would represent homogeneous thermal diffusivity of the composites except possibly for the effects of the interfacial separations between the glass and Ni phases.

III. RESULTS AND DISCUSSION

The experimentally determined values of the effective thermal diffusivity for D-glass and D-glass with 15, 30, and 45 vol. % dispersed Ni spheres are shown in Figures 4 and 5 for the glass with raw and with

Table II.--Thermophysical properties of glass and nickel at 27°C.

Property	Nickel*	D-glass
Density (Kg/m^3)	8900	2476
Specific Heat (J/KgK)	450	840**
Thermal Diffusivity ($x10^{-6} m^2/sec$)	22.9	0.52
Thermal Conductivity (W/m K)	91	1.1
Thermal Expansion ($x10^{-6}\ K^{-1}$)	13.4	7.0+**

*Literature values
+Data for Corning 8370 (70% SiO_2, 11.5% B_2O_3, 3% BaO, 9% Na_2O, and 7% K_2O)

Table III.--Ratios of various properties considered for glass-Ni composite diffusivity samples.

	V_d (vol. % Ni)		
	15	30	45
α_d/α_m (27°C)	44	44	44
α_d/α_m (358°C)	21	21	21
λ_d/λ_m (27°C)	83	83	83
$(\rho_d\ C_d\ V_d)\ /\ (\rho_m\ C_m\ V_m)$	0.37	1.02	164
L/D	41	41	41
nD / L	0.66	0.83	0.95

oxidized Ni spheres, respectively. The dashed curves in each figure show the thermal diffusivity values (α_c) calculated from the Bruggeman[13] variable-dispersion (BVD) relation for the conductivity of a composite (λ_c):

$$\frac{\lambda_c - \lambda_d}{\lambda_m - \lambda_c}\left[\frac{\lambda_m}{\lambda_c}\right]^{1/3} = 1 - V_d \qquad (2)$$

the volumetric heat capacity:

$$\rho_c C_c = \rho_m C_m V_m + \rho_d C_d V_d \qquad (3)$$

and the relation:

$$\alpha_c = \lambda_c / \rho_c C_c \qquad (4)$$

The implicit assumption in the derivation of Eq. (2) is that the components are perfectly bonded with no thermal resistance at the interface.

Referring to Figure 4, the α-values for the 15 and 30 vol. % raw Ni-glass composites match the α-values of D-glass alone from room temperature to $\sim$ 300°C. Above 300°C, the α-values have positive temperature dependence. Values of α for the 15 and 30 vol. % raw Ni composites increase with increasing temperature until they show excellent agreement with values calculated by the BVD relation at 600°C, near the fabrication temperature of 700°C. For the 45 vol. % raw Ni composite, the thermal diffusivity increases to values above that predicted by the BVD theory for temperatures above 500°C. The effect of the Curie point transition (at 358°C in nickel) on thermal diffusivity is readily observable in the Ni-glass composites, although the minimum in α appears displaced to slightly lower temperatures.

For the oxidized Ni/glass composites measured α values are lower than those calculated by the BVD relation for all temperatures, as shown in

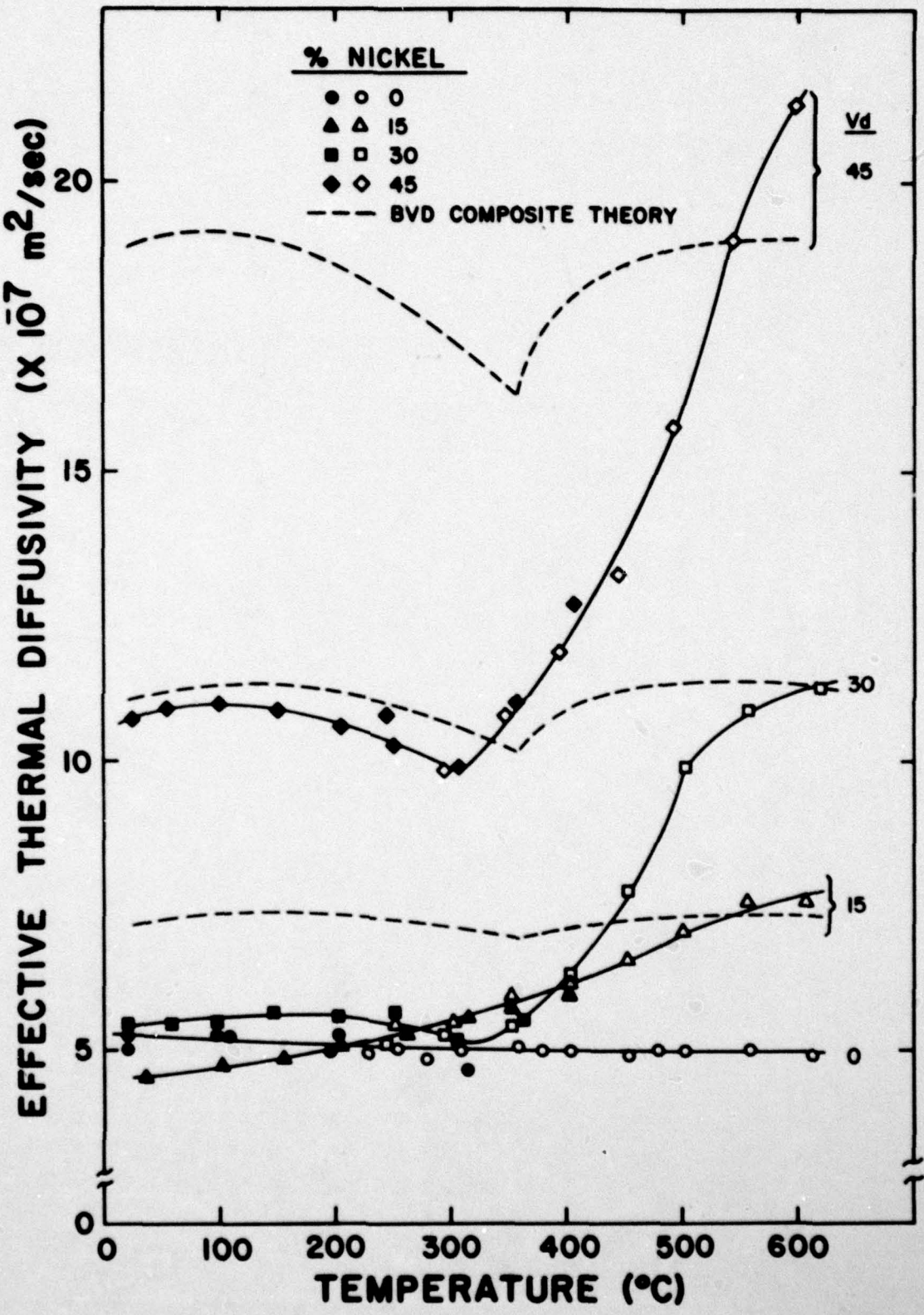


Figure 4.--Measured effective thermal diffusivity of D-glass with 15, 30, and 45 vol. % raw nickel spheres compared to calculated thermal diffusivity for Ni/glass composite. Closed (open) symbols indicate data taken by thermocouple (infrared) detector.

Figure 5. However, at room temperature α-values for the composites with oxidized nickel spheres are higher than α-values for composites with raw nickel spheres of corresponding concentration. The positive temperature dependence of α for these composites is much less than those with non-oxidized spheres. Again, the effect on thermal diffusivity of the Curie transition in the Ni is observable at temperatures slightly below 358°C for all three nickel concentrations.

At least qualitatively the deviations of α from α_c can be explained on the basis of the mismatch in the coefficients of thermal expansion of the glass and Ni phases and the resulting differences in the interfacial bonding.

For the glass with raw Ni spheres, the lack of bonding is clearly evident from the SEM fractographs shown in Fig. 2. The lack of adhesion at the interface between the glass and Ni also can be justified from the magnitude of the internal stress which would have arisen for perfect bonding. After Selsing,[7] the magnitude of the radial stress (σ_r) perpendicular to the interface of a single spherical particle contained in an infinite matrix is:

$$\sigma_r = \frac{\Delta\beta\Delta T E_d}{(1+\nu_m)(E_d/2E_m)+(1-2\nu_d)} \qquad (5)$$

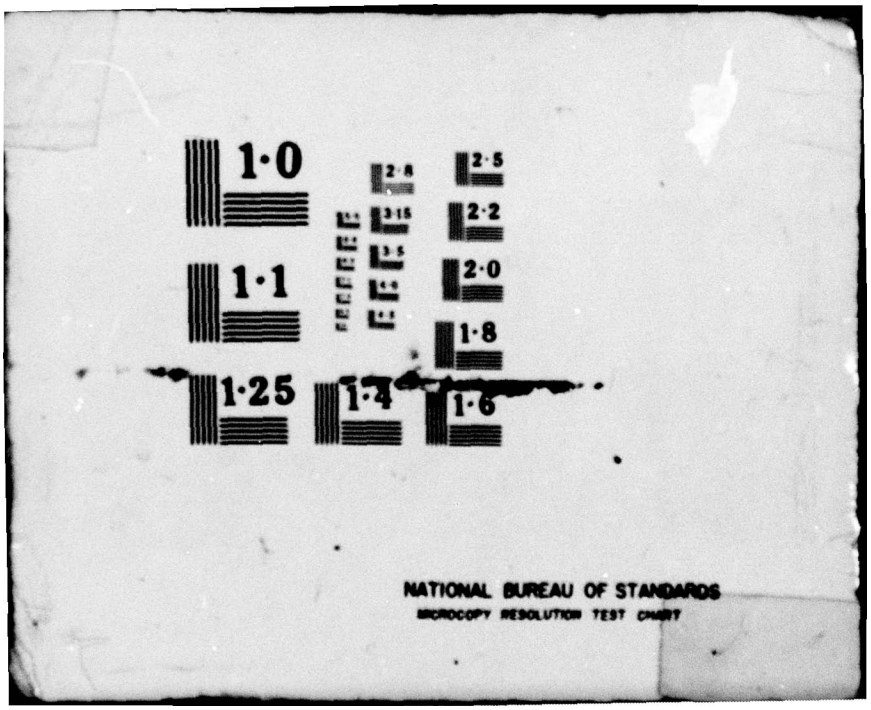
where $\Delta\beta$ is the mismatch in the coefficients of linear thermal expansion, ΔT is the temperature difference over which the composite is cooled and over which no stress relaxation can occur, E is Young's modulus, ν is Poisson's ratio and, as before, subscripts d and m refer to the dispersed and matrix phases, respectively. With $\Delta\beta = 6.7\times10^{-6}K^{-1}$, $\Delta T = 600°C$,

AD-A078 540 MONTANA ENERGY AND MHD RESEARCH AND DEVELOPMENT INST --ETC F/G 11/4
THERMAL CONDUCTIVITY AND DIFFUSIVITY OF ENGINEERING CERAMICS.(U)
NOV 79 G R YOUNGBLOOD , L D BENTSEN N00014-78-C-0726
UNCLASSIFIED 4TC-NAVY-F/79 NL

2 OF 2
AD-
A078540



END
DATE
FILMED
1-80
DDC


1·0
1·1
1·25
1·4
1·6
1·8
2·0
2·2
2·5
NATIONAL BUREAU OF STANDARDS
MICROCOPY RESOLUTION TEST CHART

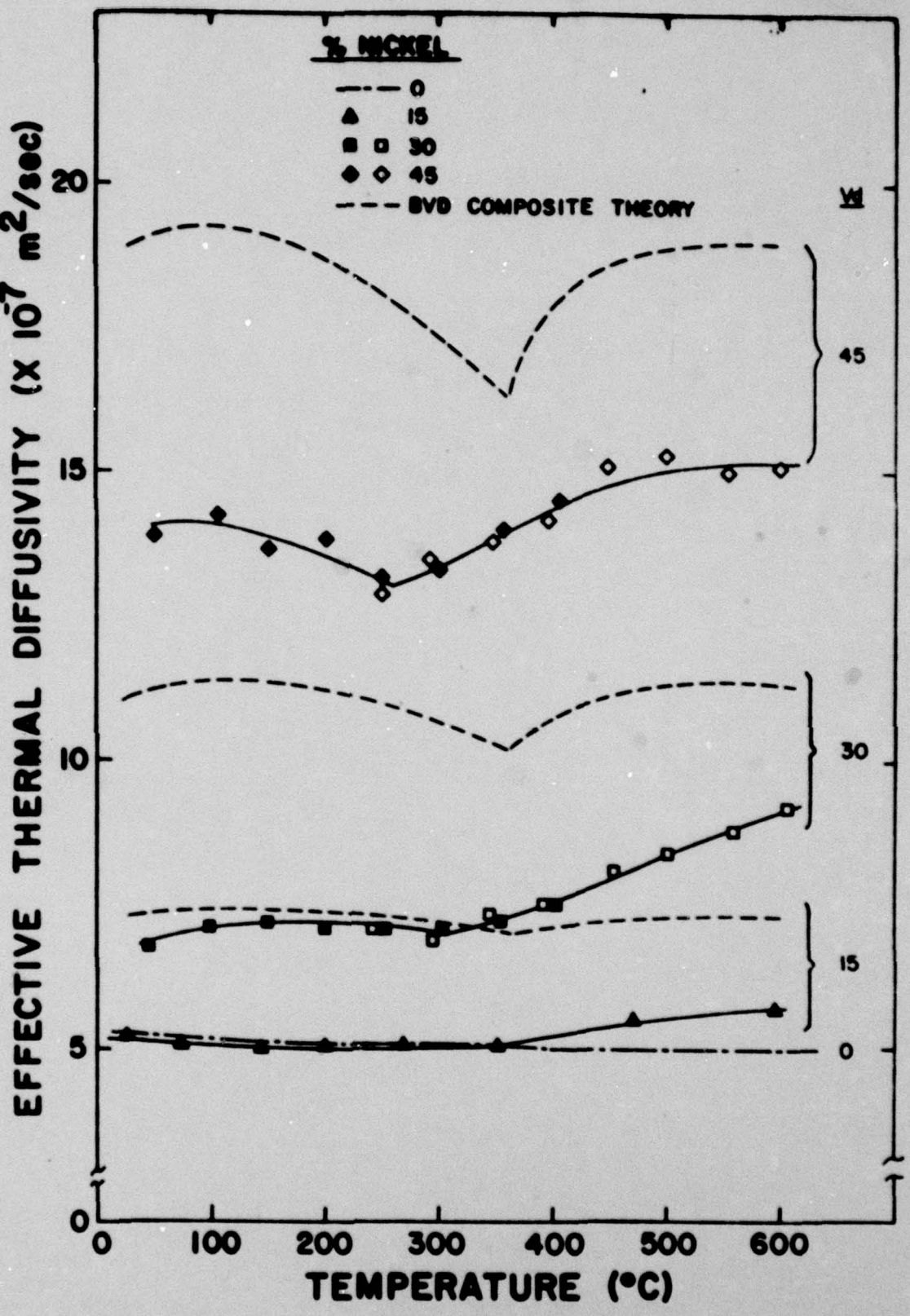


Figure 5.--Measured effective thermal diffusivity of D-glass with 15, 30, and 45 vol. % oxide-coated nickel spheres compared to calculated thermal diffusivity for Ni/glass composite. Closed (open) symbols indicate data taken by thermocouple (infrared) detector.

6/9/78 8-000-003-A

E_d = 210 GPa MPa, E_m = 70 GP_a MPa, ν_m = 0.3, and ν_d = 0.18, Eq. (5) yields

$$\sigma_r = 326 \text{ MPa}(46{,}600 \text{ psi}).$$

This magnitude of stress quite likely exceeds the strength of the interfacial bond of a non-wetting metal-glass system such as the present case for raw Ni-glass. Separation of the glass-Ni interface probably occurs during the cooling phase immediately following hot-pressing. It is calculated that for a 50 μm spherical inclusion and 600°C temperature range of cooling, an interfacial gap of ≈0.2 μm will result due to thermal expansion mismatch. Such a gap is expected to act as a significant barrier to the flow of heat. It is for this reason that over the temperature range from RT to about 300°C the α-values for the composites with 15 and 30 vol. % raw Ni approach the values for the D-glass. In the glass in which at the lower temperatures heat conduction occurs primarily by phonon transport, the thermal diffusivity is directly proportional to the product of the phonon velocity and mean free path in the direction of the temperature gradient. The presence of the gaps increases the total distance required for phonon transport and accordingly decreases the thermal diffusivity below values predicted by BVD composite theory.

Despite the presence of the gaps, the nickel metal still makes a contribution to the thermal diffusivity as indicated by the unique temperature dependence which reflects the presence of the Curie point in the nickel. Also, the α-values of the glass-raw Ni composites do not fall below the α-values of the D-glass, which would have been expected if the Ni-phase made no contribution to the conduction of heat. Furthermore, if the Ni did not contribute to the conduction of heat the thermal diffusivity would be expected to decrease with increasing

Ni content, i.e., increasing number of interfacial gaps. The contribution of the Ni to the conduction of heat can occur by means of Ni particle-to-particle contact, especially expected for the glass with 45 vol. % Ni. Even isolated particles, however, can contribute to the thermal transport since contact with the glass can occur at multiple points, particularly for the non-spherical particles.

With increases in temperature back to the hot-pressing temperature the contact between the glass and Ni inclusions will improve. At higher temperatures, therefore, the Ni particles can make a greater contribution to the thermal transport than at the lower temperatures. This results in a positive temperature dependence of the thermal diffusivity, in agreement with observations. For the highest temperatures (600°C) excellent agreement exists between the experimental α-values and those calculated by the BVD composite theory for the glass with 15 and 30% Ni. This is indicative of the absence of an interfacial barrier to heat flow at 600°C. This agreement reconfirms the validity of the criteria for the thermal diffusivity established by Lee and Taylor[18] when no significant interfacial effects are present. For the composite with 45% Ni, the observed α-values exceed those predicted by the BVD theory, probably as the result of parallel high conductivity paths through the nickel due to many direct particle-to-particle contacts which is not taken into account in the BVD theory.

The magnitude and temperature dependence of the thermal diffusivity values of the glass with the oxidized Ni dispersion is expected to show different behavior. Since the fibrous glass phase at the interface provides physical contact between the glass matrix and the nickel,

at least at the lower temperatures, the nickel can make a much larger contribution to the thermal diffusivity than the non-oxidized (raw) Ni dispersions. This should result in relatively higher α-values, in agreement with observations (depicted in Figure 5). Because of the presence of a thermally insulating porosity layer at the interface, the measured α-values are expected to fall below those predicted by composite theory over the entire temperature range, as is observed.

The fibrous phase at the interface will form only at those temperatures at which visco-elastic deformation can take place. Below these temperatures on further cooling the thermal expansion mismatch will place the fibrous phase in tension without further changes in fiber and pore morphology nor significant alteration of the glass-Ni interfacial bonding. For this reason the temperature dependence of the α-values for the glass with oxidized Ni particles is expected to be less than for the glass with raw Ni dispersions, again in agreement with observations.

The thermal diffusivity values determined during thermal cycling, i.e. heating followed by cooling, of both types of composites (glass with raw or oxidized Ni dispersed phase) are shown in Figure 6. For the glass with oxidized Ni spheres the α-values determined during heating and cooling over one cycle were observed to be reproducible. This suggests that the interfacial bond is permanent, at least over the temperature range examined.

For the glass with raw Ni dispersions, however, the α-values determined on the cooling part of the cycle lie well above the α-values obtained on heating. This suggests that near 600°C the glass and nickel form a bond of some sort which requires some degree of cooling before rupture occurs. This results in a discontinuity in the slope of the thermal

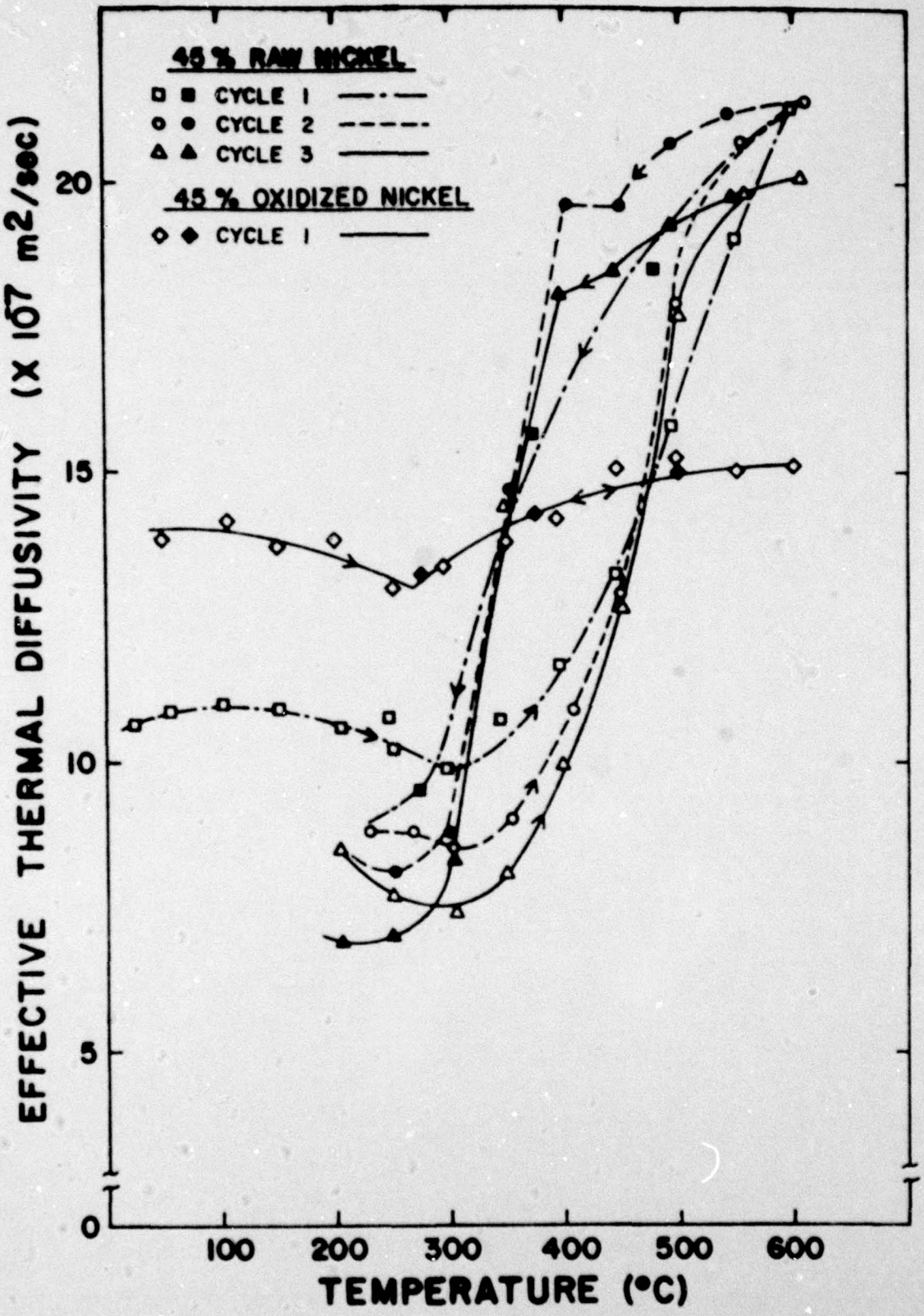


Figure 6.--Measured effective thermal diffusivity of 45 v/o raw Ni/glass and 45 v/o oxide-coated Ni/glass composites on heating (open symbols) and cooling (closed symbols).

diffusivity as a function of temperature at ≈400°C. It is of interest to note that a similar hysteresis was observed by Siebeneck et. al.[5] for the effect of microcracking on the thermal diffusivity of iron titanate. The general reproducibility of the shape of the hysteresis loop for the glass-raw Ni composites in repeated thermal cycling is expected to be characteristic of a composite of dissimilar materials, i.e., a metal and a glass, where the dispersed phase forms only a weak interfacial bond with the matrix phase.

In summary, the results of the present study indicate that the nature of the interfacial bond between the individual components of a composite can have a profound effect on the thermal transport properties if the components have a thermal expansion mismatch.

In a composite with non-bonded phases and a thermal expansion mismatch $\beta_d > \beta_m$, α can be reduced to that of the continuous phase alone at temperatures sufficiently far below fabrication temperatures. For a composite with $\alpha_d > \alpha_m$ as well, this combination of physical properties offers the unique possibility of making a material that is a good thermal insulator at low temperatures while being a good thermal conductor at higher temperatures.

Even though there is a thermal expansion mismatch $\beta_d > \beta_m$, in a composite with sufficiently strong bonds between phases or with an intervening phase to neutralize residual stresses due to thermal expansion mismatch, contributions to the overall thermal diffusivity (or conductivity) from both phases can be retained. The additional effects of the introduction of enhanced porosity regions or of secondary phases during fabrication must be considered, however.

Acknowledgements

This study was conducted as part of research program sponsored by the Office of Naval Research under Contracts N-00014-78-C-0726 and N-00014-78-C-0431. The specimens were prepared in the Department of Materials Science and Engineering at the University of California in Berkeley. The authors are indebted to C. Wood for assistance in sample characterization.

REFERENCES

1. A. E. Powers, "Conductivity in Aggregates," Knolls Atomic Power Report KAPL 2145, General Electric Company, March 6, 1961.

2. Z. Hashin, "Assessment of the Self Consistent Scheme Approximation: Conductivity of Particulate Composites," J. Comp. Mat., 2 (3), 284-300 (1968).

3. S. C. Cheng and R. I. Vachon, "The Prediction of the Thermal Conductivity of Two and Three Phase Solid Heterogeneous Mixtures." Int. J. Heat Mass. Transfer, 12, 249-64 (1969).

4. A. Nir and A. Acrivos, "The Effective Thermal Conductivity of Sheared Suspensions," J. Fluid Mech. 78 (1), 33-48 (1976).

5. H. J. Siebeneck, J. J. Cleveland, D. P. H. Hasselman and R. C. Bradt, "Effect of Microcracking on the Thermal Diffusivity of Fe_2TiO_5," J. Amer. Ceram. Soc., 59 (5-6), 241-44 (1976)

6. H. J. Siebeneck, J. J. Cleveland, D. P. H. Hasselman and R. C. Bradt, "Grain Size Microcracking Effects on the Thermal Diffusivity of $MgTi_2O_5$," J. Am. Ceram. Soc., 60 (7-8), 336-38 (1977).

7. D. P. H. Hasselman, "Effects of Cracks on Thermal Conductivity," J. Comp. Mat., 12, 403-07 (1978).

8. W. D. Kingery, "Thermal Conductivity : XIV, Conductivity of Multicomponent Systems," J. Amer. Ceram. Soc., 42 (12), 617-27 (1959).

9. W. J. Buykx, "The Effect of Microstructure and Microcracking on the Thermal Conductivity of UO_2-U_4O_9," J. Amer. Ceram. Soc., 62 (7-8), 326-32 (1979).

10. D. P. H. Hasselman and R. M. Fulrath, "Proposed Fracture Theory of a Dispersion Strengthened Glass Matrix," J. Amer. Ceram. Soc., 49, 68-71 (1966).

11. D. P. H. Hasselman and R. M. Fulrath, "Micromechanical Stress Concentrations in Two-Phase Brittle Matrix Ceramic Composites," J. Amer. Ceram. Soc., 50, 399-404 (1967).

12. D. P. Nason, "Effect of Interfacial Bonding on Strength of a Model Two-Phase System," M. S. Thesis, University of California, Berkeley (1962).

13. D. A. G. Bruggeman, "Dielectric Constant and Conductivity of Mixtures of Isotropic Materials," Annalen Physik, 24, 636-79 (1935).

REFERENCES (Cont.)

14. W. Niesel, "The Dielectric Constants of Heterogeneous Mixtures of Isotropic and Anisotropic Substances," Annalen Physik, 10, 336-48 (1952).

15. W. J. Parker, R. J. Jenkins, C. P. Butler and G. L. Abbott, "Flash Method of Determining Thermal Diffusivity, Heat Capacity, and Thermal Conductivity," J. Appl. Phys., 32 (9), 1679-84 (1961).

16. K. D. Maglic and B. S. Marsicanin, "Factors Affecting the Accuracy of Transient Response of Intrinsic Thermocouples in Thermal Diffusivity Measurement," High Temperatures-High Pressures, 5, 105-110 (1973).

17. R. C. Heckman, "Finite Pulse-Time and Heat-Loss Effects on Pulse Diffusivity Measurements," J. Appl. Phys. 44 (4), 1455-60 (1973).

18. H. R. Shanks, A. H. Klein and G. S. Danielson, "Thermal Properties of Armco Iron, " J. Appl. Phys., 38 (7), 2885-92 (1967).

19. T. Y. R. Lee and R. E. Taylor, "Thermal Diffusivity of Dispersed Materials," J. Heat Transfer, 100, 720-24 (1978).

20. J. Selsing, "Internal Stresses in Ceramics," J. Amer. Ceram. Soc., 44 (8), 419 (1961).

ARTICLE IV-E

SIMPLE LASER PULSE CALORIMETER

by

R. S. Parker* and G. E. Youngblood*

*Montana Energy and MHD Research and Development Institute, Inc.
Butte, Montana 59701

ABSTRACT

A simple and sensitive relative energy calorimeter that will allow the simultaneous determination of the energy of a short laser pulse and, in this application, the operation of a laser-flash diffusivity experiment is described. The use of a silicon diode thermometer on the back face of a graphite disc infrared absorber increases the calorimeter sensitivity from about 100 μV/J, which is typical for a standard calorimeter based on thermopile thermometry, to 10 mV/J.

SIMPLE LASER PULSE CALORIMETER

by

R. S. Parker and G. E. Youngblood

In pulsed laser thermal analysis experiments it is frequently desirable to have available a measurement of the energy of an individual laser pulse.[1] Such laser calorimeters are commercially available but typically are costly, slow to use and relatively insensitive.[1] Additionally, commercial calorimeters are built with sufficient thermal inertia to prevent even qualitative indication of beam homogeneity.

A simple infrared absorber is described which allows the determination of laser pulse energy. In this design standard thermopile thermometry is replaced with a silicon diode thermometer.[2] This change increases the calorimeter sensitivity from about 100 μV/J to nearly 10 mV/J. A beam splitter is used to divert only ≈ 5% of the laser energy to the calorimeter so this sensitivity increase is of great importance. The remainder of the beam energy is thus available to simultaneously carry out an experiment.

The device consists of a 5/8" diameter high-purity graphite disc (mass ∿ 0.5g) absorber with a silicon diode thermometer on its rear face. (See Figure 1). This disc is slightly larger than the beam diameter in order to intercept the entire pulse. The silicon diode used is an unencapsulated zener diode chip* approximately 0.5 mm on a side with a mass of ≈ 0.3 mg. It is operated with a constant forward bias current of about 100 μa and exhibits a linear voltage versus T shape of about a 3 mV/K.

*Motorola MCZ 2.4 A10, Motorola Semiconductor Products, Inc. Phoenix, AZ

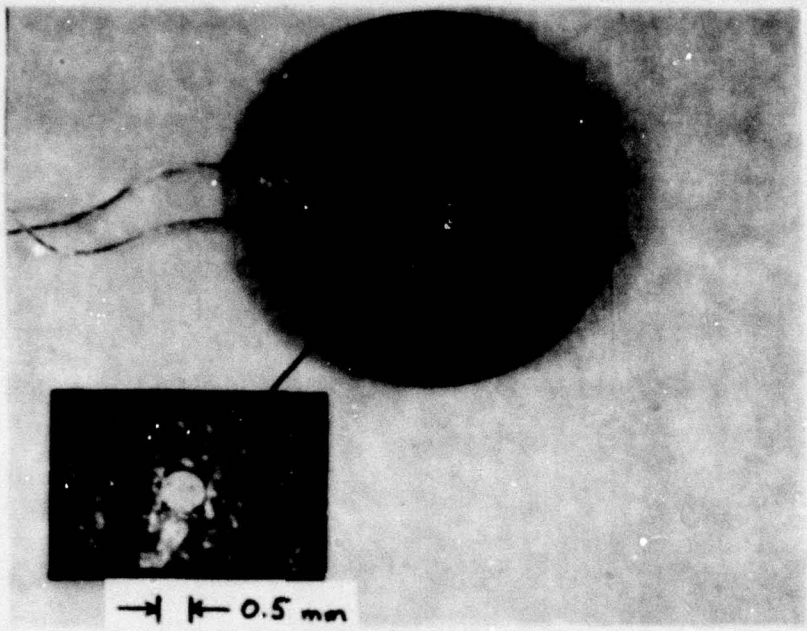


Figure 1.--Photograph of back face of the graphite disc absorber showing diode thermometer and lead attachments.

The diode chip is bonded to the back surface of the graphite disc using a conductive epoxy. A ribbon of this conducting epoxy is used to provide electrical contact to the chip block (cathode) and to bond a copper lead wire to the graphite. The anode side of the chip is ultrasonically bonded to a gold wire and masked by a small drop of opaque epoxy to avoid light sensitivity effects. The gold lead is, in turn, joined to an internal copper lead by an epoxy bond on an alumina standoff (0.05" x 0.02"). The total mass added to the absorber back face is $\sim$ 5 mg. which is about 1% of the total absorber mass. An alternative arrangement is available using any commercial diode of suitably small mass. One in particular is available commercially and is designed as a silicon diode thermometer.[+] These alternatives both use sensors which are more massive than ours and care must be taken to avoid calibration errors because of this mass.

The circuitry associated with the absorber is shown in Figure 2. It consists of a constant current generator and op-amp interface which allows the independent zeroing and scale adjustment of the thermometer. Overall thermometer sensitivity is set at 4.75 mV/K which yields a 10 mV signal for an input pulse of about 1 J. This is 10 to 100 times the sensitivity normally quoted for thermopile-based calorimeters and allows the use of a meter (or oscilloscope) with millivolt rather than microvolt sensitivity.

Ultimately, this device will be used to measure the relative amount of energy deposited on the front face of a disc-shaped sample used for the determination of thermal diffusivity by the laser-flash diffusivity

[+]Model DT-520FP-HRC Silicon Diode, Lake Shore Cryotronics, Inc.

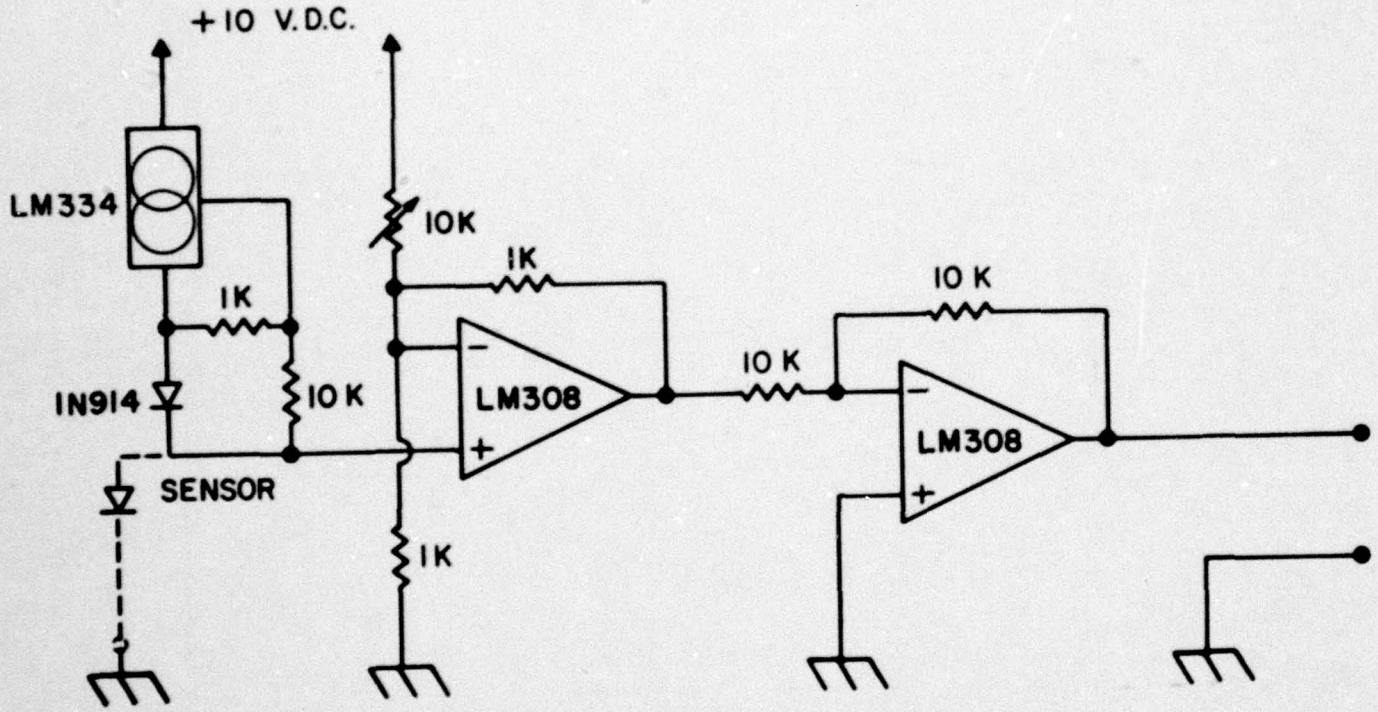


Figure 2.--Schematic diagram of circuitry used to control and display calorimeter output.

technique.[3] In this experiment the goal is to simultaneously determine the heat capacity and thermal diffusivity, and by back-calculation to determine the thermal conductivity as well. This will require calibration with a reference sample of known heat capacity.

In operation the transient heating signals from both the calorimeter and the diffusivity test sample are displayed simultaneously on a dual-trace storage oscilloscope.* A photograph of such a display is shown in Figure 3. The calorimeter temperature transient (Curve a) rises to a maximum and then decreases to a plateau in a time of ≈ 350 ms., which is somewhat longer than the characteristic rise time of the test sample temperature transient (Curve b). The calorimeter temperature change represented by the difference in the plateau and equilibrium signals (Curve a - Curve d) is proportional to the fraction of the pulse energy diverted to the calorimeter.

The overshoot (Curve a) is due to the fact that the disc is larger than the beam diameter and thus depends on the ratio of diameter to thickness of the absorber. In the course of testing the calorimeter it was discovered that changes in beam uniformity and alignment resulted in observable changes in the amount and shape of the overshoot. It is anticipated that this feature can be quantified to allow simultaneous confirmation of acceptable beam homogeneity and alignment requirements for laser-flash diffusivity determinations.

---

* Tektronix 5111 with two 5A22N vertical amplifier and a 5B10N time base plug-in. Tektronix, Inc. Beaverton, OR

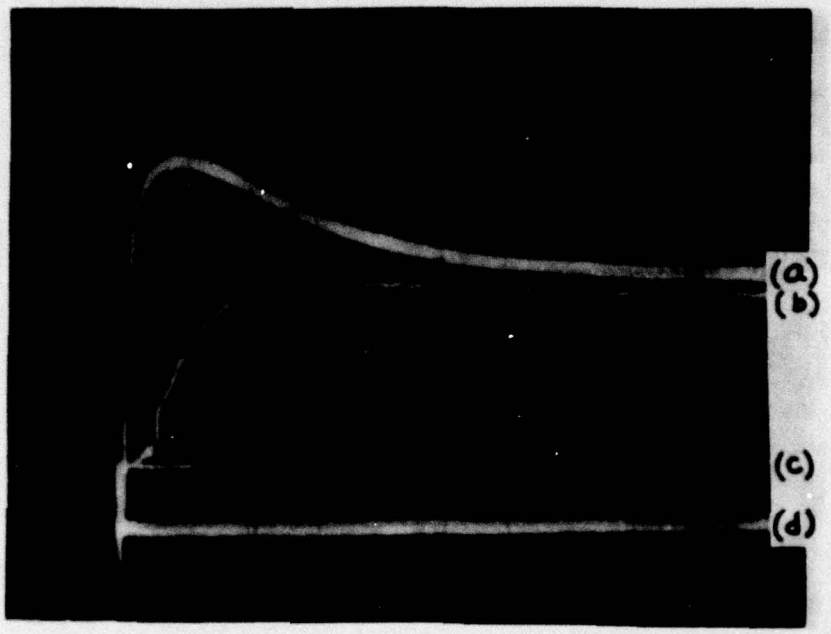


Figure 3.--Photograph showing oscilloscope presentation of (a) the calorimeter temperature transient, (b) the thermal diffusivity test sample temperature transient, (c) the test sample equilibrium temperature, and (d) the calorimeter equilibrium temperature.

Acknowledgments

This work was supported by the Office of Naval Research under Contract No. N00014-78-C-07L6. We also wish to thank Mr. Dale Lawrence of the University of Washington Department of Electrical Engineering for assistance in mounting the diode chips and Mr. Larry D. Bentsen for experimental assistance.

REFERENCES

1. Arthur L. Smirl, R. L. Shoemaker, J. B. Hambenne, and J. C. Matter, "Simple Laser Pulse Energy Monitor," Rev. Sci. Instruments, 49 (5), 672-73 (1978).

2. D. L. Swartz and J. H. Swartz, Proc. of ISA-76 Int'l. Conf. and Exhibit, Houston, Oct. 1976 (Instrum. Soc. Am. New York, 1976), pp. 1-15.

3. W. J. Parker, R. J. Jenkins, C. P. Butler, and G. L. Abbott, "Flash Method of Determining Thermal Diffusivity, Heat Capacity, and Thermal Conductivity, Journal of Applied Physics, 32 (9), 1679-89 (1961).

ARTICLE IV-F

THERMAL DIFFUSIVITY/CONDUCTIVITY OF DENSE MAGNESIA/MAGNESIA-ALUMINA SPINEL CERAMIC

BY

Louis P. Domingues,[+] Larry D. Bentsen,[*x] and G. E. Youngblood[*]

+ Trans-Tech, Inc., Gaithersburg, Maryland

* Montana Energy and MHD Research and Development Institute, Inc., Butte, Montana

x New Address - Virginia Polytechnic Institute and State University, Blacksburg, Virginia

THERMAL DIFFUSIVITY/CONDUCTIVITY OF DENSE MAGNESIA/MAGNESIA-ALUMINA SPINEL CERAMIC

Louis P. Domingues, Larry D. Bentsen, and G. E. Youngblood

In many cases the properties of a composite material can be estimated from the properties of the individual components. For instance, methods and equations for calculating the thermal conductivity of composites with specific geometries have been reviewed in detail by Powers.[1] Unfortunately, the microstructures of real engineering composite materials rarely satisfy the idealized models necessary for mathematical treatment, so it is necessary to determine the thermal conductivity directly in order to estimate heat flow and temperature distributions for these materials.

The present note reports effective thermal diffusivity values over a temperature range 25 to 1400°C for a series of dense, polycrystalline $MgO/MgAl_2O_4$ spinel composites where the content of the relatively high-conductivity MgO phase varies from 0 to 100%. These materials have commercial application as extremely low loss dielectrics with a thermal expansion adjustable by composition control. They are mechanically stable and generally corrosion resistant to high temperatures.

The materials were prepared by conventional mixing of high-purity MgO* and $MgAl_2O_4$† powders, isostatic pressing, and sintering in air at 1600°C. Table I lists resulting densities and pertinent microstructural characteristics for the compositions studied.

---

* Meller 99.98% pure, Providence, Rhode Island
† Trans-Tech, Inc., Gaithersburg, Maryland

TABLE I.--Composition, density, and grain-size of $MgO/MgAl_2O_4$ ceramic.

MgO Content (mole %)[a]	(wgt.%)[b]	~(vol.%)[b]	Density[c] (gm/cm^3)	Grain-size[d] (μm)	Comments
50.0	0.0	0.0	3.51	10-25	bimodal
56.6	7.9	7.8	3.48	5-15	bimodal
72.0	30.8	30.4	3.51	5-20	bimodal
84.3	55.3	54.8	3.52	5-12	equiaxed grains
92.5	76.3	75.9	3.52	5-10	equiaxed grains
100.0	100.0	100.0	3.50	30-60	equiaxed grains

a) Balance in Al_2O_3 by difference from 100%.
b) Balance in $MgAl_2O_4$ by difference from 100%.
c) Determined by water displacement.
d) Estimated from optical micrographs and SEM fractographs.

The theoretical densities for MgO and $MgAl_2O_4$ are 3.576 and 3.59 gm/cm^3, respectively. All of the sintered products were 98 ± 1% of theoretical density and had similar low amounts of porosity. The fact that both MgO and $MgAl_2O_4$ have almost the same densities means that wgt. % and vol. % are essentially equivalent for the composites.

Since the original compact was formed from stable oxide powders, the final product consisted of a two-phase mixture of MgO and $MgAl_2O_4$ except for the end members. Of course, some solid solution alloying is expected during sintering, but the amount was kept below a few percent by sintering at 1600°C, as ascertained by reference to the MgO-$MgAl_2O_4$ phase diagram.[2]

Figure 1 is a micrograph of a polished and thermally etched sample of the 55.4 vol. % MgO material. This structure is typical of the other two-phase materials. The larger grains are primarily the spinel phase surrounded by the smaller grained MgO phase as confirmed by SEM/EDX analysis (not shown here). Although the single-phase MgO and $MgAl_2O_4$ materials exhibited a larger grain-size than the mixed-phase materials, no direct grain-size effect on thermal transport properties is expected.

The laser-flash technique[3] was used to measure thermal diffusivity as a function of temperature during heating and cooling for one cycle from 25 to 1400°C. The details are described elsewhere.[4]

Figure 2 shows measured thermal diffusivity values as a function of temperature for sintered single-phase MgO and $MgAl_2O_4$ and several two-phase mixtures. Although only values measured on heating are indicated, it is significant that reproducible values were measured during cooling, i.e., no hysteresis effects were observed.

The thermal diffusivity values were determined for a large-grained (∿ 100 μm), dense (99.9% theoretical), hot-pressed MgO sample and also are shown in Figure 1 for comparison. The slightly lower values of thermal

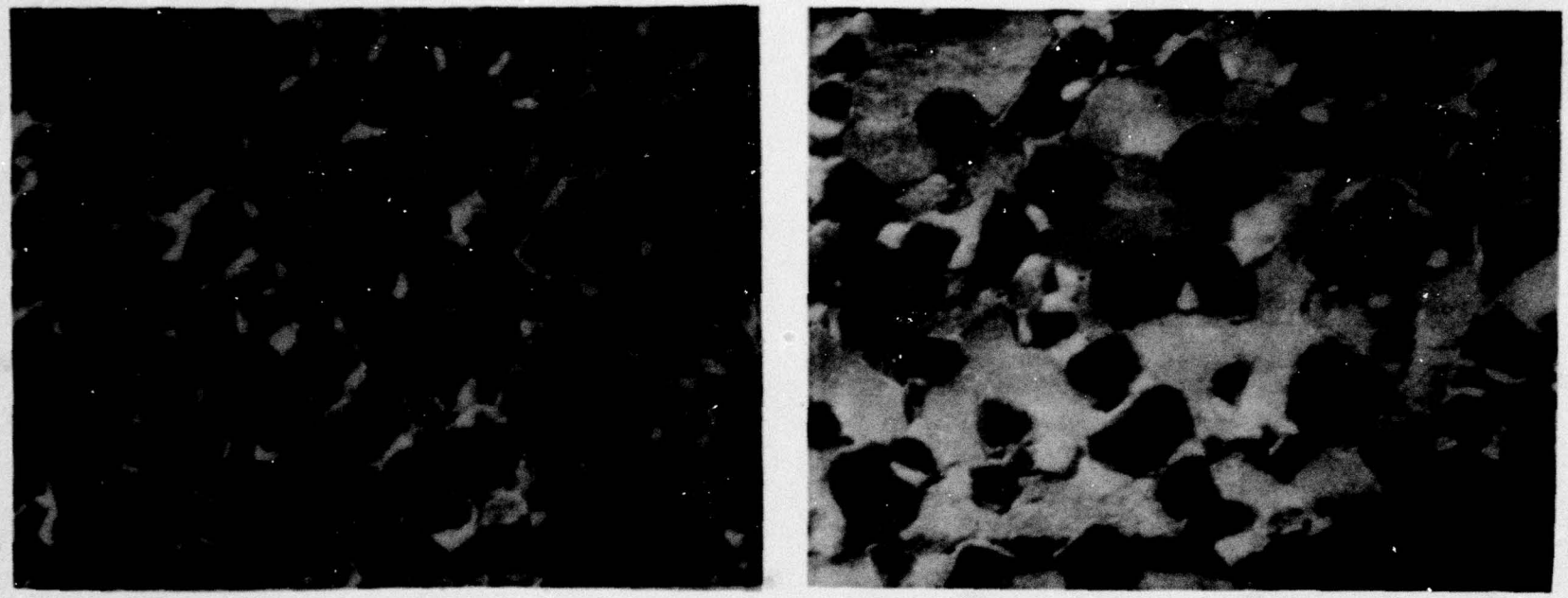


Figure 1.--Scanning electron microscope image of flat-polished and thermal etched 55.4% MgO/44.6% $MgAl_2O_4$. No conductive coating was applied. (A) Secondary electron image showing grain size; (B) back scatter electron image (15 kV, 30° tilt) of the same area showing MgO (dark phase) and $MgAl_2O_4$ (light phase) distribution. The black bar = 3 μm.

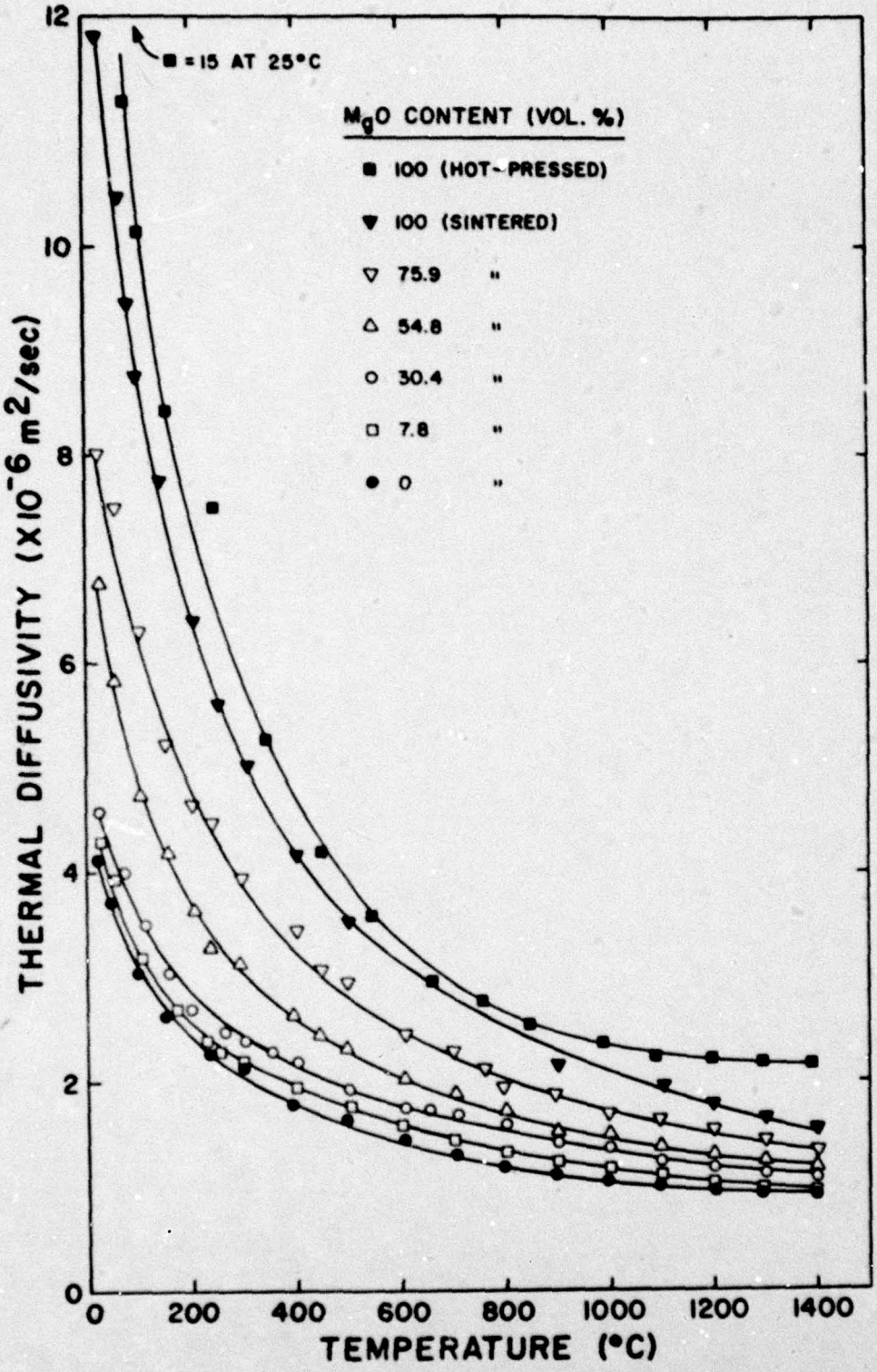


Figure 2.--Thermal diffusivity as a function of temperature for the magnesia-spinel system.

10/24/79 S-GQO-05-A

diffusivity are probably caused by the small amount of porosity for the sintered MgO. The porosity effects are expected to be small for the other materials as well so no corrections for porosity were made.

Because of the inherent difficulty in making steady-state thermal conductivity measurements over a large temperature range, it is easier to derive the thermal conductivity (λ) from the experimentally determined values of thermal diffusivity (α), density (ρ), and specific heat at constant pressure (c) by the relation

$$\lambda = \alpha \rho c \tag{1}$$

For the case of a composite material each of the terms are understood to represent effective or "homogeneous" values.

Using heat capacity values calculated by use of the Kopp-Neuman Mixture Law,[5] measured room temperature densities corrected for thermal expansion at higher temperatures, and measured thermal diffusivity values, thermal conductivity values were calculated by Equation (1) for the magnesia-spinel system. Isothermal values are shown in Figure 3 for four different temperatures--27, 200, 600, and 1400°C.

Also shown in Figure 3 are values predicted by various mixture rules for the lower three temperatures. In an ideal binary system with no intervening, high thermal resistance phases (or microcracks), limiting values of thermal conductivity are represented by the parallel (upper curve) and series cases (lower curve).[6] The Bruggeman Mixture Equation [1,7]

$$V_1\left\{\frac{\lambda_1 - \lambda}{\lambda_1 + 2\lambda}\right\} + V_2\left\{\frac{\lambda_2 - \lambda}{\lambda_2 + 2\lambda}\right\} = 0 \tag{2}$$

where V_1 and V_2 are volume fractions and λ_1 and λ_2 are thermal conductivity values of the respective phases and λ is the effective thermal

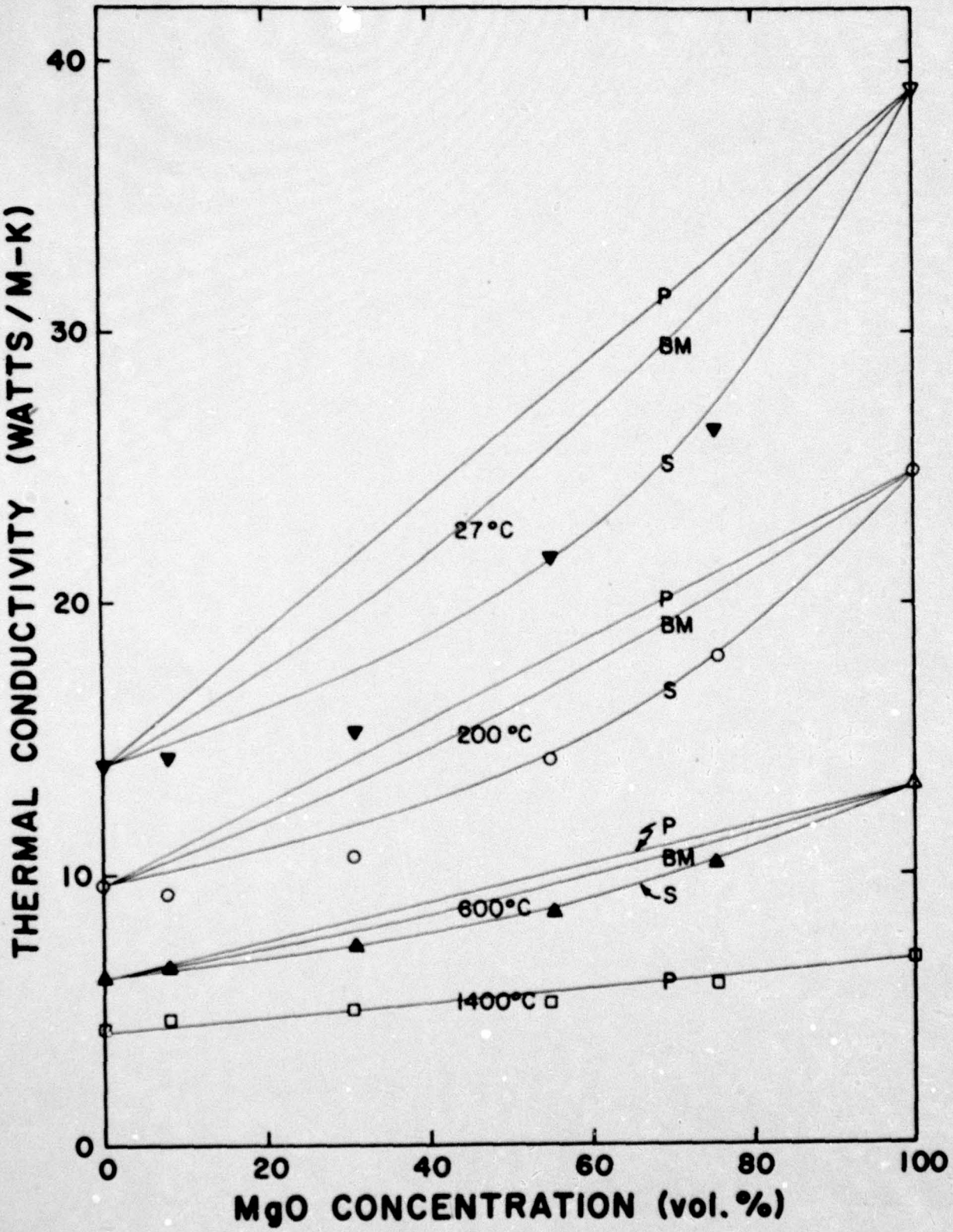


Figure 3.--Calculated thermal conductivity at 27, 200, 600, and 1400°C by Equation (1) for the magnesia-spinel system. Light-weight lines represent values calculated by the parallel (upper), Bruggeman Mixture (middle), and series (lower) models at each temperature.

10/24/79 8-000-092-A

conductivity, was used to calculate the values represented by the middle curves. Since microstructural examination indicated both phases more or less continuous except for V_{MgO} = 7.8%, Equation (2) should be the most representative of the various mixture rules for the materials examined here.

For all compositions the calculated thermal conductivity values are equal to or lower than the series case limit and the values are much lower than the Bruggeman mixture prediction up to 600°C.

There are two possible explanations for these results. One, microcracking at grain boundaries between the two phases with thermal expansion mismatch was used previously by Kingery[8] to explain similar results for the MgO-$MgAl_2O_4$ system. As in Kingery's results, the deviations from predicted mixture values are larger for smaller concentrations of MgO and are more noticeable at lower temperatures. This would indicate that the microcrack density or the crack sizes are larger when the MgO phase is more or less discontinuous as expected for lower MgO concentrations and when the degree of cooling from fabrication temperatures is larger. However, hysteresis effects were <u>not</u> observed for these MgO-$MgAl_2O_4$ mixtures. Large hysteresis effects, attributed to microcracking in single-phase ceramics with anisotropic thermal expansion, have been observed in thermal diffusivity,[9,10] thermal expansion,[11,12] and elastic moduli.[13] In analyzing the microcracking dependence on grain size in $MgTi_2O_5$, Fe_2TiO_5, and Al_2TiO_5, Cleveland and Bradt[14] show that a critical grain size for microcracking is related to the inverse square of the maximum difference in single-crystal thermal expansion coefficients, $\Delta\alpha_{max}$. A similar relation was derived by Evans for single-phase materials,[15] and when modified for differences in elastic properties between components, should also apply for

composites. Thermal expansion hysteresis, attributed to microcracking in an alumina mullite composite where $\Delta\alpha_{max}$ is about $3.3 \times 10^{-6} °C^{-1}$, has been reported by Kingery. For the MgO-$MgAl_2O_4$ system, $\Delta\alpha_{max}$ is 5.2×10^{-6} $°C^{-1}$; certainly large enough to cause microcracking if grain-size and elastic property effects are disregarded.

When considering the degree of thermal expansion mismatch and the observed degree of thermal conductivity, microcracks are expected to be present in MgO-$MgAl_2O_4$ mixtures. Once introduced, however, these microcracks may not thermally heal or extend during subsequent heating-cooling cycles. In contrast to hysteresis effects observed in the microcracked single-phase materials, no hysteresis in the thermal diffusivity would occur in these mixtures.

The other possible explanation is that there are no microcracks in these MgO-$MgAl_2O_4$ samples with moderate grain-size. The lower diffusivity values are due, instead, to a combination of solid solution alloying and a resulting nonstoichiometry. This is particularly possible in $MgAl_2O_4$ which has a wide phase field.[2] In a study of the effect on thermal diffusivity of nonstoichiometric TiO_2,[16] it was shown that oxygen vacancies lowered thermal diffusivity far more effectively than solid-solution atoms. For instance, for TiO_2 with one percent deviation from stoichiometry, the thermal diffusivity was lowered about 30% at 200°C and 20% at 800°C. A similarly large decrease in the thermal conductivity of a nonstoichiometric $MgAl_2O_4$ phase would substantially lower thermal conductivity values in the MgO/$MgAl_2O_4$ mixtures (by any of the mixture models). In fact, lower limit values predicted by a series model with the thermal conductivity of $MgAl_2O_4$ reduced by 30% would be below the thermal conductivity values calculated from experimental thermal diffusivities reported here.

Although the second explanation is plausible, the first explanation is favored. That is, microcracks probably are present in these $MgO\text{-}MgAl_2O_4$ mixtures but are not subject to crack healing or extension on temperature cycling, thus precluding hysteresis effects. From Figure 3 it is observed that the deviation from predicted thermal conductivity values has nearly vanished by 600°C and is totally absent by 1400°C. Although the relative effect of the presence of point defects on thermal conductivity (diffusivity) decreases with increasing temperature, it does not vanish as would the effect of microcracks induced by thermal expansion mismatch.

The final proof for the presence or lack of microcracks in the $MgO\text{-}MgAl_2O_4$ system awaits corroboration with other microcrack sensitive properties such as thermal expansion or elastic moduli. Careful analysis of such bulk properties (including examination for hysteresis effects) for other composites also should be carried out when the presence of microcracks is suspected.

Acknowledgments

The present study was sponsored jointly by the Office of Naval Research (as part of a larger research program on the thermal transport properties of engineering ceramics) and the MHD division of the U. S. Department of Energy.

REFERENCES

1. A. E. Powers, "Conductivity in Aggregates," Knolls Atomic Power Report KAPL 2145, General Electric Company, March 6, (1951).

2. A. M. Alper, R. N. McNally, P. H. Ribbs, and R. C. Doran, "The System MgO-$MgAl_2O_4$," J. Amer. Ceram. Soc., 45 (6), 263-68 (1962).

3. W. J. Parker, R. J. Jenkins, C. P. Butler, and G. L. Abbott, "Flash Method of Determining Thermal Diffusivity, Heat Capacity, and Thermal Conductivity, Journal of Applied Physics, 32 (9), 1679-84 (1961).

4. J. E. Matta and D. P. H. Hasselman, "Thermal Diffusivity of Al_2O_3-Cr_2O_3 Solid Solutions," J. Amer. Ceram. Soc., 58 (9-10), 458 (1975).

5. Y. S. Touloukian and E. H. Buyco, "Specific Heat, Nonmetallic Solids," p. 4a, *Thermophysical Properties of Matter Series*, Vol. 5. IFI/Plenum, New York (1970).

6. W. D. Kingery, H. K. Bowen, D. R. Uhlman, Introduction to Ceramics, 2nd edition, p. 636. John Wiley & Sons, New York, (1976).

7. D. A. G. Bruggeman, "Dielectric Constant and Conductivity of Mixtures of Isotropic Materials," Annalen Physik, 24, 636-79 (1935).

8. W. D. Kingery, "Thermal Conductivity : XIV, *Conductivity of* Multicomponent Systems," J. Amer. Ceram. Soc., 42 (12), 617-27 (1959).

9. H. J. Siebeneck, D. P. H. Hasselman, J. J. Cleveland, and R. C. Bradt, "Effect of Microcracking on the Thermal Diffusivity of Fe_2TiO_5," J. Amer. Ceram. Soc., 58 (5-6), 241-44 (1976).

10. H. J. Siebeneck, J. J. Cleveland, D. P. H. Hasselman, and R. C. Bradt, "Effects of Grain Size and Microcracking on the Thermal Diffusivity of $MgTi_2O_5$," J. Amer. Ceram. Soc., 60 (7-8), 336-38 (1977).

11. W. R. Buessem, H. R. Thielke, and R. V. Sarakauskas, "Thermal Expansion Hysteresis of *Aluminum Titanate*," Ceram. Age, 60 (5), 38-40 (1952).

12. J. A. Kuszyk and R. C. Bradt, "Influence of Grain Size on Effects of Thermal Expansion Anisotropy in $MgTi_2O_5$, J. Amer. Ceram. Soc., 56 (8), 420-23 (1973).

13. E. A. Bush and F. A. Hummel, "High-Temperature Mechanical Properties of Ceramic Materials : I," J. Amer. Ceram. Soc., 41 (6), 189-95 (1958).

14. J. J. Cleveland and R. C. Bradt, "Grain Size/Microcracking Relations for Pseudobrookite Oxides," J. Amer. Ceram. Soc., 61 (11-12), 478-81 (1978).

15. A. G. Evans, "Microfracture from Thermal Expansion Anisotropy - I. Single Phase Systems," Acta Metallurgica, 26, 1845-53 (1978).

16. H. J. Siebeneck, W. R. Minnear, R. C. Bradt, and D. P. H. Hasselman, "Thermal Diffusivity of Non-Stoichiometric Titanium Dioxide," J. Amer. Cer. Soc., 59 (1-2), 84 (1976).

November 1979

VI. BASIC DISTRIBUTION LIST

Technical and Summary Reports

Organization	No. of Copies
Scientific Officer Director Metallurgy and Ceramics Programs Material Sciences Division Office of Naval Research 300 North Quincy St. Arlington, VA 22217 Attn: Dr. S. W. Freiman Ref: Contract No. N00014-78-C-0726	(1)
Defense Contract Administration Services Management Area (DCASMA) Seattle SCD-C Building 5D Naval Support Activity 7500 Sand Point Way, N.E. Seattle, WA 98115	(1)
Director, Naval Research Laboratory Attn: Code 2627 Washington, D. C. 20375	(6)
Defense Documentation Center Bldg. 5 Cameron Station Alexandria, VA 22314	(12)
Office of Naval Research Branch Office Branch Office 1030 East Green Street Pasadena, CA 91106	(1)
Army Research Office Box CM, Duke Station Durham, North Carolina 27706 Attn: Metallurgy & Ceramics Div.	(1)
Army Materials and Mechanics Research Center Watertown, Massachusetts 02172 Attn: Res. Programs Office (AMXMR-P)	(1)

Air Force
Office of Scientific Research
Bldg. 410
Bolling Air Force Base
Washington, D.C. 20332
Attn: Chemical Science Directorate (1)
Electronics and Solid State
Science Directorate (1)

Air Force Materials Lab (LA) (1)
Wright-Patterson AFB
Dayton, Ohio 45433

NASA Headquarters (1)
Washington, D.C. 20546
Attn: Code RRM

NASA
Lewis Research Center (1)
21000 Brookpark Road
Cleveland, Ohio 44135
Attn: Library

National Bureau of Standards
Washington, D.C. 20234
Attn: Metallurgy Division (1)
Inorganic Materials Division (1)

Defense Metals and Ceramics (1)
Information Center
Battelle Memorial Institute
505 King Avenue
Columbus, Ohio 43201

Director (1)
Ordnance Research Laboratory
P.O. Box 30
State College, Pennsylvania 16801

Director Applied Physics Laboratory (1)
University of Washington
1013 Northeast Fortieth Street
Seattle, Washington 98105

Metals and Ceramics Division (1)
Oak Ridge National Laboratory
P.O. Box X
Oak Ridge, Tennessee 37380

Los Alamos Scientific Laboratory (1)
P.O. Box 1663
Los Alamos, New Mexico 87544
Attn: Report Librarian

Argonne National Laboratory (1)
Metallurgy Division
P.O. Box 229
Lemont, Illinois 60439

Brookhaven National Laboratory (1)
Technical Information Division
Upton, Long Island
New York 11973
Attn: Research Library

Library (1)
Building 50 Room 134
Lawrence Radiation Laboratory
Berkeley, California

SUPPLEMENTAL DISTRIBUTION LIST
Technical and Summary Reports

Advanced Research Project Agency
Materials Science Director
400 Willison Boulevard
Arlington, Virginia 22209

Dr. Clifford Astill
Solid Mechanics Program
National Science Foundation
Washington, DC 20550

Dr. N. N. Ault
Norton Company
1 New Bond St.
Worcester, Massachusetts 01606

Dr. E. K. Beauchamp, Div. 5846
Sandia Laboratories
Albuquerque, NM 87185

Dr. P. F. Becher
Code 6362
U.S. Naval Research Laboratory
Washington, DC 20375

Mr. Larry D. Bentsen
Dept. of Materials Engineering
Virginia Polytechnic Institute
& State University
Blacksburg, VA 24061

Dr. M. Berg
AC Spark Plug Division
General Motors Corp
1601 N. Averill Ave.
Flint, MI 48556

Dr. R. C. Bradt
Materials Science Dept.
Pennsylvania State University
University Park, PA 16802

Dr. R. J. Bratton
R&D Center
Westinghouse Electric Corp.
Pittsburgh, PA 15235

Dr. E. A. Bush
Ceramics Research
Corning Glass Works
Corning, NY 14830

Dr. B. Butler, Chief
Materials Branch
Solar Energy Research Institute
1536 Cole Blvd
Golden, CO 80401

Dr. R. J. Charles
General Electric Company
Research and Development Center
Schenectady, NY 12301

Dr. T. D. Chikalla
Battelle Northwest
Ceramics and Graphite Section
P.O. Box 999
Richland, WA 99352

Dr. K. Chyung
Research and Development
Corning Glass Works
Corning, NY 14830

Dr. Nils Claussen
Max-Planck Institute for
Metallforschung
D-7000 Stuggart 80
Buxauer Str. 75
West Germany

Dr. J. A. Coppola
The Carborundum Company
P.O. Box 1054
Niagara Falls, NY 14302

Dr. R. J. Cottschall
U.S. Dept. of Energy
Div. of Matls. Science
Mail Stop J309
Washington, DC 20545

Mr. W. B. Crandall
Alfred University
Alfred, New York 14802

Dr. D. DeCoursin
Fluidyne Engineering
5900 Olson Memorial Hway.
Minneapolis, MN 55422

Dr. J. E. Doherty
Materials Engineering and
Research Laboratory
Pratt & Whitney Aircraft Corp.
Middletown Plant
Middletown, CT 06457

Professor R. H. Doremus
Rensselaer Polytechnical Ins.
Troy, New York 12181

Dr. Louis P. Domingues
TransTech, Inc.
Box 457
Gaithersburg, Maryland 20761

Dr. S. Dutta
NASA-Lewis Research Center
Mail Stop 49-3
21000 Brookpark Rd.
Cleveland, OH 44135

Dr. R. E. Engdahl
Deposits and Composites, Inc.
318 Victory Dr.
Herndon, VA 22070

Dr. A. G. Evans
Department Materials Science &
Engineering
Hearst Mining Building
University of California
Berkeley CA 94720

Dr. S. W. Freiman
Deformation and Fracture Group
Physical Properties Section, Bldg 223
National Bureau of Standards
Washington, DC 20234

Professor P. J. Gielisse
Department of Chemical Engineering
University of Rhode Island
Kingston, Rhode Island 02881

Globe-Union, Inc.
5757 North Green Bay Avenue
Milwaukee, WI 53201
Attn: G. Goodman

Professor R. W. Gould
Department of Metallurgical &
Materials Engineering
University of Florida
Gainesville, Florida 32601

Ms. M. E. Gulden
Solar
Division of International Harvester
Company
P. O. Box 951
2200 Pacific Highway
San Diego, California 92112

Dr. R. H. Haag
Space Systems Division
AVCO Corporation
Lowell Industrial Park
Lowell, Massachusetts 01851

Dr. Jack Hansen
General Electric Company
Space Sciences Laboratory
P.O. Box 8555
Philadelphia, PA 19101

Mr. Doug H. Harris, President
APS - Materials, Inc.
153 Walbrook Ave.
Dayton, Ohio 45405

Mr. W. B. Harrison
Honeywell Ceramics Center
1885 Douglas Drive
Golden Valley, MN 55422

Dr. Marvin Hass
Naval Research Laboratory
Code 6408
Washington, DC 20375

Dr. D. P. H. Hasselman
Materials Engineering Dept.
Virginia Polytechnic Institute
& State University
Blacksburg, VA 24061

Dr. L. L. Hench
Department of Metallurgy
University of Florida
Gainesville, FL 32603

Professor A. H. Heuer
Case Western Reserve University
University Circle
Cleveland, Ohio 44106

Dr. C. O. Hulse
United Aircraft Research Labs
United Aircraft Corporation
East Hartford, CT 06108

Dr. Paul Jorgensen
Stanford Research Institute
333 Ravenswood Avenue
Menlo Park, CA 94025

Dr. R. N. Katz
Army Mechanics and Materials
Research Center
Watertown, MA 02172

Professor W. D. Kingery
Ceramics Div. Rm. 13-4090
MIT
77 Mass. Ave.
Cambridge, MA 02139

Dr. H. Kirchner
Ceramic Finishing Company
P.O. Box 498
State College, PA 16801

Dr. B. G. Koepke
Honeywell Corporate Research Center
10701 Lyndale Avenue
Bloomington, MN 55420

Dr. F. A. Kroger
University of Southern California
University Park
Los Angeles, CA 90007

Dr. F. F. Lange
Rockwell International
P.O. Box 1085
1049 Camino Dos Rios
Thousand Oaks, CA 91360

Dr. James Lankford, Jr.
Southwest Research Institute
8500 Culebra Road
San Antonio, Texas 78284

Dr. D. C. Larson
IIT Research Inst.
10 W. 35th Str.
Chicago, IL 60616

Dr. Charles L. LeBlanc
Naval Underwater Systems Center
Newport, Rhode Island 02840

Dr. Ronald E. Loehman
University of Florida
Ceramics Division
Gainesville, Florida 32601

Dr. E. D. Lynch
Lynchburg Research Center
Babcock and Wilcox Co.
Box 1260
Lynchburg, VA 24505

Professor P. M. Macedo
The Catholic University of America
Washington, DC 20017

Dr. W. R. Manning
Champion Spark Plug Company
20000 Conner Ave.
Detroit, Michigan 48234

Dr. M. O. Marlowe
General Electric Company
1900 South Tenth St.
San Jose, CA 95125

Dr. M. I. Mendelson
Government Products Division
Pratt and Whitney Aircraft Gr.
P.O. Box 2691
West Palm Beach, FL 33402

Dr. G. R. Miller
Dept. of Materials Engineering
University of Utah
Salt Lake City, Utah 84112

Dr. I. K. Naik
Airesearch Casting Corp.
Garrett Corp.
2525 W. 190th Str.
Torrance, CA 90509

Dr. Ram Natesh
Materials Research, Inc.
1380 East South Temple St.
Salt Lake City, Utah 84102

Dr. E. E. Niesz
Battelle Memorial Institute
505 King Avenue
Columbus, Ohio 43201

Mr. John Norbutas
Civil Engineering Laboratory
Naval Construction Battalion Center
Port Hueneme, CA 93043

Professor J. A. Pask
University of California
Department of Mineral Technology
Berkeley, CA 94720

Mr. R. Palicka
CERADYNE Inc.
P.O. Box 11030
3030 South Red Hill Ave.
Santa Ana, CA 92705

Dr. Hayne Palmour III
Engineering Research Division
N.C. State University
P.O. Box 5995
Raleigh, NC 27650

Dr. R. A. Penty
Hagne International
3 Adams Str.
South Portland, Maine 04106

Dr. H. A. Perry
Naval Ordnance Laboratory
Code 230
Silver Spring, Maryland 20910

Dr. W. Plummer
Research and Development
Corning Glass Works
Corning, New York 14830

Dr. Roy Rice
Naval Research Laboratory
Code 6360
Washington, DC 20375

Dr. D. W. Richerson
Airesearch Man. Comp. Code 503-44
Garrett Corp.
111 S. 34th Str., Box 5217
Phoenix, Arizona 85034

Dr. J. T. A. Roberts
Electric Power Research Institute
3412 Hillview Ave.
P.O. Box 10412
Palo Alto, CA 94304

Dr. J. H. Rosolowski
General Electric Company
Research and Development Center
P.O. Box 8
Schenectady, NY 02301

Dr. R. C. Rossi
Materials Sciences Division
Aerospace Corporation
P.O. Box 95085
Los Angeles, California 90045

Dr. B. Rossing
Westinghouse Research Laboratories
Beaulah Road
Pittsburgh, PA 15235

Dr. J. A. Rubin
Kyocera International, Inc.
8611 Balboa Avenue
San Diego, CA 92123

Dr. Robert Ruh
AFML/LLM
Wright-Patterson AFB
OH 45433

Dr. Paul Smith
Naval Research Laboratory
Code 6361
Washington, DC 20375

Professor V. S. Stubican
Department of Materials Science
Ceramic Science Section
Pennsylvania State University
University Park, Pennsylvania 16802

The Library
Attention: Assistant Librarian
(Technical Reference)
State University of New York
College of Ceramics at Alfred Univ.
Alfred, New York 14802

Dr. J. C. Swearengen
Materials Science Division
Sandia Laboratories
Livermore, CA 94550

Dr. V. J. Tennery
Oak Ridge Nat. Lab.
Oak Ridge, TN 38730

Dr. W. D. Tuohig
Bendix Research Laboratories
Southfield, MI 48076

Dr. T. Vasilos
AVCO Corporation
Research and Advanced Development Div.
201 Lowell St.
Wilmington, MA 01887

Dr. A. R. C. Westwood
Martin-Marietta Laboratories
1450 South Rolling Road
Baltimore, Maryland 21227

Professor D. H. Whitmore
Northwestern University
Department of Metallurgy
Evanston, IL 60201

Dr. T. J. Whalen
Process Research Department
Ford Motor Company
20000 Rotunda Drive
Dearborn, Michigan 48121

Dr. S. M. Wiederhorn
Physical Properties Section
Bldg. 223, Rm. A355
National Bureau of Standards
Washington, DC 20234

Dr. B. A. Wilcox
Ceramics Program, Room 336
National Science Foundation
Washington, DC 20550

Dr. P. D. Wilcox
Division 2521
Sandia Laboratories
Albuquerque, NM 85115

APPENDIX A

List of publications which have resulted from technical effort to date.

(5/15/74 to 7/1/77)

1. B. K. Ganguly, K. R. McKinney and D. P. H. Hasselman, "Thermal Stress Analysis of Flat Plate with Temperature Dependent Thermal Conductivity," Journal American Ceramic Society, 58, 455-56 (1975).

2. J. E. Matta and D. P. H. Hasselman, "The Thermal Diffusivity of Al_2O_3-Cr_2O_3 Solid Solutions," Journal American Ceramic Society, 58, 458, (1975)

3. J. E. Matta, H. J. Siebeneck and D. P. H. Hasselman, "The Effect of Microstructure and Composition on the Thermal Diffusivity of Structural Ceramics," Proceedings 1975 Conference on Laser-Hardening of Materials and Structures, NASA-Ames Research Center, Moffat Field, California.

4. B. K. Ganguly and D. P. H. Hasselman, "Effect of Conductivity on the Radiation Heat Transfer Across Spherical Pores," Journal American Ceramic Society, 59 (1-2), 83 (1976).

5. H. J. Siebeneck, W. P. Minnear, R. C. Bradt and D. P. H. Hasselman, "Thermal Diffusivity of Non-Stoichiometric Titanium Dioxide," Journal American Ceramic Society, 59 (1-2), 84 (1976).

6. H. J. Siebeneck, J. J. Cleveland, D. P. H. Hasselman and R. C. Bradt, "Effect of Micro-Cracking on the Thermal Diffusivity of Fe_2TiO_5," Journal American Ceramic Society, 58 (5-6) 241-44 (1976).

7. F. F. Lange, J. J. Siebeneck and D. P. H. Hasselman, "Thermal Diffusivity of Four Si-Al-O-N Compositions," Journal American Ceramic Society, 59 (9-10), 454-55 (1976).

8. J. E. Matta, W. L. Roper, D. P. H. Hasselman and G. E. Kane, "The Role of Thermal Diffusivity in the Machining Performance of Oxide Ceramic Cutting Tool Materials," Wear, 31, 323-32 (1976).

9. D. P. H. Hasselman, "Microcracking as a Mechanism for Improving Thermal Shock Resistance and Thermal Insulating Properties of Ceramic Materials," High Temperature - High Pressure. Also presented at the 5th European Conference on Thermophysical Properties of Solids at High Temperature, Moscow, May 18-21, 1976.

10. H. J. Siebeneck, J. J. Cleveland, D. P. H. Hasselman and R. C. Bradt, "Thermal Diffusivity of Microcracked Ceramic Materials," pp. 753-62 in Ceramic Microstructures '76, ed. by Richard M. Fulrath and Joseph A. Park, Westview Pres. Boulder (1977).

11. H. J. Siebeneck, J. J. Cleveland, D. P. H. Hasselman and R. C. Bradt, "Effect of Microcracking on the Thermal Diffusivity of $MgTi_2O_5$," Journal American Ceramic Society, 56 (8), 420-23 (1973).

List of publications (Continued)

12. H. J. Siebeneck, R. A. Penty, D. P. H. Hasselman and G. E. Youngblood, "Thermal Diffusivity and Thermal Conductivity of a Fibrous Alumina," Ceramic Bulletin, 5 (6), 572 (1977).

13. D. Greve, N. Claussen, D. P. H. Hasselman and G. E. Youngblood, "Thermal Diffusivity/Conductivity and Alumina with a Zirconia Dispersed Phase," Ceramic Bulletin, 56 (5), 414 (1977).

14. H. J. Siebeneck, E. J. Minford, P. A. Urick, D. P. H. Hasselman and R. C. Bradt, "Thermal Diffusivities of Glassy Carbon," Carbon (in press).

15. H. J. Siebeneck, K. Chyung, D. P. H. Hasselman and G. E. Youngblood, "Effect of Crystallization on the Thermal Diffusivity of a Mica Glass-Ceramic," Journal American Ceramic Society, 60 (7-8), 375-76 (1977).

16. G. E. Youngblood, W. R. Manning and D. P. H. Hasselman, "Effect of Microcracking on the Thermal Diffusivity of Polycrystalline Aluminum Niobate," Journal American Ceramic Society, 60 (9-10), 469-7) (1977).

17. D. P. H. Hasselman and G. E. Youngblood, "Enhanced Thermal Stress Resistance of Brittle Ceramics with Thermal Conductivity Gradient," Journal American Ceramic Society, 61)1-2), 49-52 (1978).

(8/15/78 to 8/14/79)

18. G. E. Youngblood, K. Chyung and D. P. H. Hasselman, "Effect of Crystallization on the Thermal Diffusivity of a Cordierite Glass-Ceramic," Journal American Ceramic Society, 61 (11-12), 530-31 (1978).

19. G. E. Youngblood, Larry D. Bentsen, James W. McCauley, and D. P. H. Hasselman, "Thermal Diffusivity of Ba-Mica/Alumina Composites," Ceramic Bulletin, 58 (6), 620-21 (1979).

20. Larry D. Bentsen, Nils Claussen, and G. E. Youngblood, "Thermal Diffusivity of Al_2O_3 with Dispersed Monoclinic and Tetragonal ZrO_2 Particles," (in review).

21. R. R. Powell, Jr., G. E. Youngblood, D. P. H. Hasselman, and Larry D. Bentsen, "Effect of Thermal Expansion Mismatch on the Thermal Diffusivity of Glass-Ni Composites," (in review).

22. Louis P. Domingues, Larry D. Bentsen, and G. E. Youngblood, "Thermal Diffusivity/Conductivity of Dense Magnesia/Magnesia-Alumina Spinel Ceramic," (in review).

23. R. S. Parker and G. E. Youngblood, "Simple Laser Pulse Calorimeter," (in review).